Combining remote sensing data at different spatial, temporal and spectral resolutions to characterise semi-natural grassland habitats for large herbivores in a heterogeneous landscape

Dissertation
to attain the doctoral degree (Dr. rer. nat.)
of the Faculty of Agricultural Sciences
Georg-August-Universität Göttingen

Submitted by
Christoph Benjamin Raab
born on the 18th March 1987 in Göttingen

Göttingen, May 2019

Members of the graduate committee

Prof. Dr. Johannes Isselstein	Grassland Science Faculty of Agricultural Science Georg-August-Universität Göttingen
Prof. Dr. Niko Balkenhol	Wildlife Sciences Faculty of Forest Sciences and Forest Ecology Georg-August-Universität Göttingen
Dr. Bettina Tonn	Grassland Science Faculty of Agricultural Science Georg-August-Universität Göttingen

Members of the examination committee

1. Referee:
Prof. Dr. Johannes Isselstein

2. Referee:
Prof. Dr. Niko Balkenhol

Co-referee: Prof. Dr. Hannes Feilhauer	Remote Sensing and Geoinformatics Department of Earth Sciences Freie Universität Berlin

Date of oral examination: 4th July 2019

‘‘Wherever we have been forced by the dictates of binary logic to draw artificially sharp boundaries in ecology, we can now draw more realistic distinctions in terms of fuzzy sets.’’

— Li and Rykiel (1996)

TABLE OF CONTENTS

SUMMARY

Semi-natural grasslands are ecosystems with high biodiversity. In Europe, such open and half-open areas are a fundamental characteristic of the cultural landscape, originating from and depending on management activities. The possibilities that grazing with wildlife can provide for sustaining these open-land ecosystems are subject to current research activities, because only a small proportion of grasslands protected under the EU Habitats Directive has a favourable conservation status. For an active grazing management, spatial information about the landscape structure and forage quality and quantity is required, as they can affect the spatial distribution and activities of free-ranging herbivores and thus their influence on the ecosystem e.g. by grazing. The collection of field data, however, is labour-intensive, time-consuming and often limited to a particular location. Therefore, this thesis is concerned with techniques and concepts offered by satellite remote sensing technology to characterise a heterogeneous landscape dominated by semi-natural grassland.

After a general introduction to the wider research context in **Chapter 1**, **Chapter 2** illustrates how Tasselled-Cap-transformed multi-temporal RapidEye remote sensing data can be successfully used to derive a classification map for a heterogeneous landscape. The results suggest that the RapidEye Tasselled Cap Transformation, which was designed for agricultural applications, can be an effective data compression tool, suitable

to map heterogeneous landscapes with no measurable negative impact on classification accuracy.

Chapter 3 presents a framework on mapping semi-natural grasslands at community level using multi-temporal RapidEye remote sensing imagery. For this, an automated training data selection was successfully implemented based on the Random Forest proximity measure. This strategy can support the reporting obligations under Art.-17 of the EU Habitats Directive in the future.

Chapter 4 discusses how semi-natural grassland forage quantity and quality indicators can be predicted using combined optical and radar satellite remote sensing data. A permutation-based variable importance measure indicated a strong contribution of simple-ratio-based optical indices to the model performance.

The final **Chapter 5** summarises and discusses the results of this work with reference to the current research context. The findings of this thesis can help to understand and manage the grazing behaviour of free-ranging large herbivores and thus, support the conservation of semi-natural grassland in the future.

ZUSAMMENFASSUNG

Naturnahes Grünland gehört zu den Ökosystemen mit höchster Biodiversität. In Europa sind solche offenen und halboffenen Gebiete ein grundlegendes Merkmal der Kulturlandschaft. Ihre Entstehungsgeschichte und Erhaltung hängen von einer aktiven Bewirtschaftung ab. Die Möglichkeiten, die eine Beweidung mit Wildtieren zum Erhalt dieser Offenlandökosysteme bieten, sind Gegenstand aktueller Forschung, denn nur ein geringer Teil des unter der EU-Habitat-Richtlinie geschützten Grünlands befindet sich in einem günstigen Erhaltungszustand. Für ein aktives Beweidungsmanagement werden räumliche Informationen zur Landschaftsstruktur und Futterqualität benötigt, da diese Parameter die räumliche Verteilung und Aktivitäten von freilebenden Herbivoren und somit deren Einfluss, z.B. durch die Futteraufnahme, auf das Ökosystem beeinflussen. Das Sammeln von Felddaten ist jedoch arbeitsintensiv, zeitaufwändig und räumlich oft nur in einem begrenzten Gebiet möglich. Daher befasst sich diese Arbeit mit Methoden der Satellitenfernerkundung, um eine von naturnahem Grünland dominierte, heterogene Landschaft zu charakterisieren.

Nach einer allgemeinen Einführung in den umfassenderen Forschungskontext (**Kapitel 1**) zeigt **Kapitel 2**, wie multi-temporale Tasseled-Cap-transformierte RapidEye-Fernerkundungsdaten erfolgreich angewendet werden können, um eine Landbedeckungskarte für eine

heterogene Landschaft abzuleiten. Die Ergebnisse deuten darauf hin, dass die RapidEye Tasselled Cap Transformation, die für landwirtschaftliche Anwendungen entwickelt wurde, ein effektives Datenkomprimierungs-werkzeug sein kann. Diese ist dazu geeignet, heterogene Landschaften ohne messbare negative Auswirkungen auf die Klassifizierungsgenauigkeit abzubilden.

In **Kapitel 3** wird ein Konzept für die Kartierung von naturnahen Grünlandgesellschaften unter Verwendung von RapidEye-Fernerkundungszeitreihen vorgestellt. Hierfür wurde eine automatisierte Auswahl der Trainingsdaten basierend auf der Random Forest Proximity erfolgreich implementiert. Diese Strategie könnte künftig die Berichterstattungspflichten gemäß Artikel 17 der EU-Habitat-Richtlinie unterstützen.

In **Kapitel 4** wird erörtert, wie Biomasse und Futterqualität naturnaher Grünlandaufwüchse mit kombinierten optischen und Radar-Fernerkundungsdaten vorhergesagt werden können. Ein auf Permutationen basierendes Maß für die Wichtigkeit einer Variable zeigt einen starken Beitrag optischer Indizes durch die Verhältnisse einzelner spektraler Kanäle zur Modellqualität.

Im abschließenden **Kapitel 5** werden die Ergebnisse dieser Arbeit zusammenfassend mit Bezug auf den aktuellen Forschungskontext diskutiert. Die Erkenntnisse dieser Forschungsarbeit können helfen, das

Beweidungsverhalten großer wildlebender Herbivoren zu verstehen und somit die Erhaltung von naturnahem Grünland in Zukunft zu unterstützen.

1

CHAPTER 1 – GENERAL INTRODUCTION

The conservation of semi-natural grassland in Europe

Semi-natural grasslands are ecosystems with high biodiversity (Dengler et al., 2014; Wilson et al., 2012). In Central Europe, such open and half-open areas are a fundamental characteristic of the cultural landscape and their origin and conservation depend on active management (Isselstein et al., 2005; Isselstein, 2018; Peeters et al., 2014). After the second half of the 20th century, most of the semi-natural grasslands were transformed into more productive pastures or meadows, e.g. by fertilisation. This agricultural intensification and the related eutrophication have been directly linked to a decrease in grassland species richness (Harpole and Tilman, 2007; Stevens et al., 2004; Tang et al., 2017), mainly due to light competition (Hautier et al., 2009). In addition to nitrogen, other soil chemical parameters such as phosphorus are related to the composition and species richness of semi-natural grasslands (Riesch et al., 2018). As biomass removal is required for the preservation of semi-natural grassland ecosystems, land abandonment was identified as a major challenge for the preservation of open habitats (Terres et al., 2015; Valkó et al., 2018). Without management, light limitation increases, which promotes the dominance of few, competitive species. Eventually, open and half-open landscapes are lost in favour of shrub- and finally woodland (Peco et al., 2006; Ruprecht et al., 2010). Climate change puts further pressure on grassland ecosystems and the ecosystems services they provide (Dangal et al., 2016;

Lamarque et al., 2014). Currently, only 12.3% of grasslands protected under the EU Habitats Directive have a favourable conservation status (European Environment Agency, 2015). Extensive grazing with livestock has become an established tool for the conservation of semi-natural grassland ecosystems in Europe (Borer et al., 2014; Bunzel-Drüke, 2008; Rosenthal et al., 2012; Van Wieren, 1995).

However, for inaccessible or remote areas, livestock grazing can not be established, because a regular monitoring of the animals and, in most cases, fencing is required. This is particularly the case for military training areas. The potential of wild herbivores, such as red deer (*Cervus elaphus*), as a management option for open habitats under such landscape conditions has recently been acknowledged (Pausas and Bond, 2018; Riesch et al., 2019; Schulze et al., 2018). The spatial distribution of wild herbivores is guided by a trade-off between a potential predation risk (Godvik et al., 2009; Lima and Dill, 1990) and the need to utilise foraging areas (Fryxell, 1991; Merkle et al., 2016). In this context, grazing decisions are made by the animal at varying spatial scales, in order to utilise potential foraging areas (Dupke et al., 2017; Felton et al., 2018). Their impacts on the ecosystem e.g. by grazing, trampling and seed dispersal also depend on the quality of forage resources (Fløjgaard et al., 2017). Therefore, spatially-explicit information about forage quality and landscape configuration is of pivotal importance for an active grazing management. However, the collection of field data is a

labour-intensive and time-consuming task (Catchpole and Wheeler, 1992), in particular for large areas with limited accessibility.

Remote sensing

According to Jensen (2009), remote sensing is defined as "[...] the art and science of obtaining information about an object without being in direct physical contact with the object". In the field of optical earth observation, satellites are equipped with sensors sensitive for specific parts of the electromagnetic spectrum (Figure 1). Hence, they depend on the radiation emitted by the sun, reflected to the sensor by the Earth's surface. These satellites have fixed orbits and therefore retrieve information over the same area with the same view angle in defined repeated cycles at defined spatial units, i.e. pixels. Exceptions are sensors that are able to tilt the view angle. Most optical sensors record radiation for a defined spectral range of the electromagnetic spectrum, which is often referred to as bands. From a combination of different bands, a remote sensing image can be composed. These bands or images can be used to relate the recorded reflectance intensity to observations made on the ground or to known biophysical principles. The most important biophysical principle is the absorption of radiation by the photosynthesis. Vegetation vitality, for example, can be approximated by the relationship of an absorption by chloroplasts in the red part of the electromagnetic spectrum and a strong reflectance in the near-infrared part due to cell structural components (Figure 1) (Sims and Gamon, 2002; Tong and

He, 2017). Optical satellite remote sensing is often challenged by cloud contamination and depends on illumination conditions. Microwave satellite remote sensing systems use an active sensing mechanism, where energy is emitted and the echoed intensity as well as the time lag is recorded (Woodhouse, 2017).

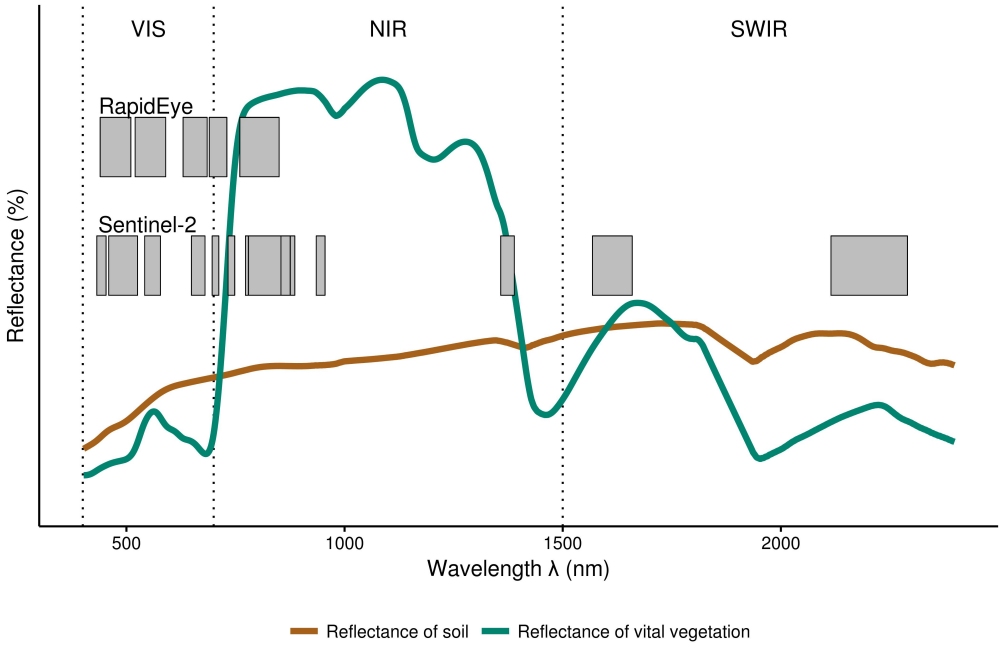

Figure 1: Typical reflectance curves of vegetated and soil surfaces in comparison to band location of two optical satellites depicted as grey boxes. VIS = visible, NIR = near infrared, SWIR = shortwave infrared part of the electromagnetic spectrum. The reflectance data is based on Herold et al. (2004).

Synthetic aperture radar (SAR) systems transmit microwave radiation and record the backscatter echo. The microwave radiation is able to penetrate through clouds and is independent from illumination conditions by the sun. SAR data can provide, for example, valuable information about vegetation structure and moisture conditions (Barrett et al., 2014; Ali et al.,

2016; Wachendorf et al., 2017). However, no information about other biophysical parameters, such as chlorophyll concentration, can be obtained using SAR data.

Optical and radar remote sensing have the advantage of collecting information about the Earth's surface at potentially every spatial and temporal scale. In addition, they can cover very large areas at repeated intervals and the processing of the data can be automated. This in turn can be considered as less prone to errors compared to non-automated processes. These benefits make the use of satellite remote sensing products and the potential contributions of such data to the conservation of semi-natural grassland particularly attractive.

Remote sensing land cover classification

The exemplary reflectance curves in Figure 1 can be related to soil and vegetation surfaces on the ground. These observations can be used to derive spectral patterns, from which each pixel of a satellite remote sensing image can be assigned to a respective land cover class. Land cover classification can be seen as a key element to quantify and monitor changes of the Earth's surface (Gómez et al., 2016). Applications range from global land cover mapping for climate modelling purposes (Houghton et al., 2012) to land cover mapping at fine scales (Schuster et al., 2012). As single images only capture information from one point in time, multi-temporal mapping approaches are able to integrate vegetation dynamics into the classification

model (Pettorelli et al., 2005). This can increase the predictive power of such models (Schmidt et al., 2014) and could be particularly beneficial for mapping and monitoring heterogeneous landscapes. However, multi-temporal classification approaches increase the amount of data which needs to be considered by a potential classification algorithm. Machine learning algorithms, such as Random Forest or Support Vector Machines, are able to cope with high-dimensional spectral data (Belgiu and Drăguţ, 2016; Schuster et al., 2012). In contrast to Support Vector Machines, only few parameters have to be adjusted for the non-parametric Random Forest algorithm (Belgiu and Drăguţ, 2016). This could make high-dimensional land cover classification tasks more applicable for nature conservation, compared to other machine learning approaches.

Comparable to a principal component analysis the Tasselled Cap Transformation (TCT) provides a potential data compression approach for spectral remote sensing data (Kauth and Thomas, 1976). By the application of empirically derived weighting factors, the original spectral bands are transformed to new bands with defined interpretations. Application of the TCT include the estimation of windthrow in forests (Einzmann et al., 2017), the prediction of biophysical crop parameters (Dahms et al., 2016; Schönert et al., 2015) and mapping of abandoned agricultural land (Löw et al., 2015). The TCT reduces the dimension of the input data and the correlation among the transformed bands is decreased. Thus, the TCT provides an attractive approach for multi-temporal land cover mapping. As the TCT is derived

from top of atmosphere reflectance data, potential influences by the atmosphere, due to absorption and scattering (Song et al., 2001) are not considered. As the atmospheric composition can be highly variable over space and time (Wilson et al., 2014), this could impact the result of a Tasselled-Cap-transformed multi-temporal land cover classification. This in turn would offset the advantages of a reduced correlation and data intensity of a TCT-based multi-temporal land cover classification.

Remote-sensing-based mapping of semi-natural grassland

Grassland ecosystems are typically mapped and monitored through field surveys, such as botanical mapping. However, these field mapping results can be biased by subjective interpretation in the field and might also depend on climatic conditions and the phenological phase at the time of the survey (Rocchini et al., 2013). Moreover, they are not easy to reproduce, can be time- and labour-intensive and, in some cases, not practically feasible. Satellite remote sensing has been recognised as a valuable resource for the monitoring of grassland ecosystems (Borre et al., 2011; Buck et al., 2013; Corbane et al., 2015; Nagendra et al., 2013). Remote-sensing-based mapping approaches for semi-natural grassland in Europe include: the assessment of image acquisition timing and number (Schmidt et al., 2014), the use of high resolution SAR data (Schuster et al., 2015), the identification of scattered Natura 2000 habitats (Stenzel et al., 2014) or mapping the floristic continuum instead of plant communities (Schmidtlein et al., 2007).

However, studies aiming at mapping semi-natural grasslands at plant community level to meet the requirements for reporting obligations under the EU Habitats Directive are limited (Rapinel et al., 2018). This can be attributed to the structural and botanical heterogeneity at very fine scales (Ali et al., 2016; Wachendorf et al., 2017) and the related floristic and spectral uncertainties of semi-natural grassland ecosystems (Feilhauer et al., 2013).

Remote sensing of semi-natural grassland biophysical properties

Biophysical properties of vegetated land cover include parameters such as organic acid detergent fibre concentration, crude protein concentration, compressed sward height or standing biomass. These parameters are known to influence grazing patterns of large herbivores (Felton et al., 2018; Merkle et al., 2016) and can vary in semi-natural grasslands at very fine spatial scales. This can be related to interactions between individual plants and changes in soil moisture and nutritional concentrations as well as grazing impacts at fine scales. Hence, remote-sensing-based information about biophysical properties across different phenological phases can help to interpret and understand grazing patterns of large herbivores, thus supporting the conservation management of grazed semi-natural grassland. For this, empirical relationships between field observations and the remote sensing signal are established using simple linear or machine learning regression techniques to derive spatial maps of

biophysical parameters (Ali et al., 2016; Wachendorf et al., 2017). The recent advances of the Sentinel satellite constellation by the European Commission provide optical and radar remote sensing data at very high temporal, spatial and spectral resolutions (Drusch et al., 2012). However, the combined use of these two satellite remote sensing techniques for the prediction of semi-natural grassland properties remains widely unexplored.

Study site

The Grafenwoehr military training area (GTA) is located in the south-east of Germany (Figure 2) and extends over about 230 km². Roughly 85% are part of the Natura 2000 network and contain numerous rare and highly protected habitat types, forming a refuge for many endangered species (Warren and Büttner, 2008b, 2008a; Warren et al., 2014; Riesch et al., 2018). Approximately 40% of the GTA are covered with open habitats, such as semi-natural grassland, while forest covers the majority of the area (about 60%). Since 1947, the GTA is used as a United States Army Garrison. This means that the land management aims at preserving the open landscape areas, primarily for military use, but also for maintaining the nature conservation status. Fire and wildlife grazing (Figure 3), especially by red deer, also play a role in some of these areas (Meißner et al., 2012).

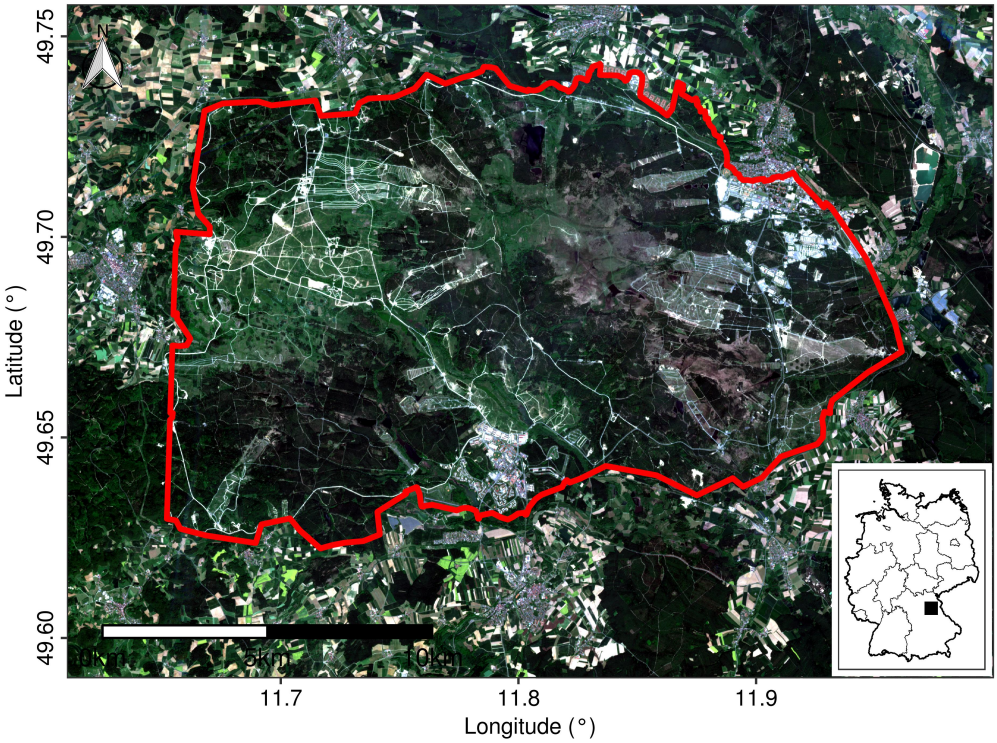

Figure 2: Area of the study site Grafenwoehr military training area outlined in red. The location of the study site in Germany is marked with a black square in the small map. The background map is based on modified Copernicus Sentinel-2 data (acquisition date: 22 May 2016).

The study area can be considered as a particular challenge to remote sensing applications. The GTA consists of a relatively fine-scale mosaic of open, semi-open, successional and forested areas. All kinds of transitions between managed and unmanaged grassland as well as shrub and forest are present, because of a heterogeneous management regime taking both military use and nature conservation requirements into account.

Figure 3: Red deer grazing on the Grafenwoehr military training area. Photograph taken by M. Meißner.

Aim of this thesis

The overall aim of this thesis is to evaluate different remote sensing sources at different spatial, spectral and temporal resolutions to characterise the heterogeneous landscape of the GTA. A particular focus is on semi-natural grassland as there is an urgent need for conservation activities across Europe to preserve these hot-spots of biodiversity for future generations.

Structure of this thesis

This thesis is subdivided into three main chapters, each with an individual focus on one specific research challenge discussed here with a spatial focus on the GTA.

Chapter 2 illustrates how Tasselled-Cap-transformed multi-temporal RapidEye remote sensing data can be successfully used to derive a classification map for a heterogeneous landscape. The results suggest that the RapidEye Tasselled Cap Transformation, which was designed for

agricultural applications, can be an effective data compression tool, suitable to map heterogeneous landscapes with no measurable negative impact on classification accuracy.

Chapter 3 presents a framework for mapping semi-natural grassland at the plant community level using multi-temporal RapidEye remote sensing data. For this, an automated training data selection was successfully implemented based on the Random Forest proximity measure. This strategy can support the reporting obligations under Art.-17 of the EU Habitats Directive in the future.

Chapter 4 demonstrates how combined radar Sentinel-1 and optical Sentinel-2 data can be used to predict forage quantity and quality indicators of semi-natural grassland. A permutation-based variable importance measure indicated a strong contribution of simple-ratio-based optical indices to the model performance. This can support the conservation of semi-natural grassland and a targeted wildlife management in the future.

References

Ali, I., F. Cawkwell, E. Dwyer, B. Barrett, and S. Green. 2016. "Satellite Remote Sensing of Grasslands: From Observation to Management." *Journal of Plant Ecology* 9 (6): 649–671.

Barrett, B., I. Nitze, S. Green, and F. Cawkwell. 2014. "Assessment of Multi-Temporal, Multi-Sensor Radar and Ancillary Spatial Data for Grasslands Monitoring in Ireland Using Machine Learning Approaches." *Remote Sensing of Environment* 152: 109–124.

Belgiu, M., and L. Drăguţ. 2016. "Random Forest in Remote Sensing: A Review of Applications and Future Directions." *ISPRS Journal of Photogrammetry and Remote Sensing* 114: 24–31.

Borer, E.T., E.W. Seabloom, D.S. Gruner, W.S. Harpole, H. Hillebrand, E.M. Lind, P.B. Adler, J. Alberti, T.M. Anderson, and J.D. Bakker. 2014. "Herbivores and Nutrients Control Grassland Plant Diversity via Light Limitation." *Nature* 508 (7497): 517.

Borre, J.V., D. Paelinckx, C.A. Mücher, L. Kooistra, B. Haest, G. De Blust, and A. M. Schmidt. 2011. "Integrating Remote Sensing in Natura 2000 Habitat Monitoring: Prospects on the Way Forward." *Journal for Nature Conservation* 19 (2): 116–125.

Brenning, A. 2005. "Spatial Prediction Models for Landslide Hazards: Review, Comparison and Evaluation." *Natural Hazards and Earth System Science* 5 (6): 853–862.

Buck, O., A. Klink, V.E.G. Millán, K. Pakzad, and A. Müterthies. 2013. "Image Analysis Methods to Monitor Natura 2000 Habitats at Regional Scales–the MS. MONINA State Service Example in Schleswig-Holstein, Germany." *Photogrammetrie-Fernerkundung-Geoinformation* 2013 (5): 415–426.

Bunzel-Drüke, M. 2008. *"Wilde Weiden": Praxisleitfaden Für Ganzjahresbeweidung in Naturschutz Und Landschaftsentwicklung*. Arbeitsgem. Biologischer Umweltschutz im Kreis Soest eV (ABU).

Catchpole, W. R., and C. J. Wheeler. 1992. "Estimating Plant Biomass: A Review of Techniques." *Australian Journal of Ecology* 17 (2): 121–131.

Corbane, C., S. Lang, K. Pipkins, S. Alleaume, M. Deshayes, V.E.G. Millán, T. Strasser, J.V. Borre, S. Toon, and M. Förster. 2015. "Remote Sensing for Mapping Natural Habitats and Their Conservation Status–New Opportunities and Challenges." *International Journal of Applied Earth Observation and Geoinformation* 37: 7–16.

Dahms, T., S. Seissiger, E. Borg, H. Vajen, B. Fichtelmann, and C. Conrad. 2016. "Important Variables of a RapidEye Time Series for Modelling Biophysical Parameters of Winter Wheat." *Photogrammetrie-Fernerkundung-Geoinformation* 2016 (5–6): 285–299.

Dangal, S.R.S., H. Tian, C. Lu, S. Pan, N. Pederson, and A. Hessl. 2016. "Synergistic Effects of Climate Change and Grazing on Net Primary Production of Mongolian Grasslands." *Ecosphere* 7 (5): e01274.

Dengler, J., M. Janišová, P. Török, and C. Wellstein. 2014. "Biodiversity of Palaearctic Grasslands: A Synthesis." *Agriculture, Ecosystems & Environment* 182: 1–14.

Drusch, M., U. Del Bello, S. Carlier, O. Colin, V. Fernandez, F. Gascon, B. Hoersch, C. Isola, P. Laberinti, and P. Martimort. 2012. "Sentinel-2: ESA's Optical High-Resolution Mission for GMES Operational Services." *Remote Sensing of Environment* 120: 25–36.

Dupke, C., C. Bonenfant, B. Reineking, R. Hable, T. Zeppenfeld, M. Ewald, and M. Heurich. 2017. "Habitat Selection by a Large Herbivore at Multiple Spatial and Temporal Scales Is Primarily Governed by Food Resources." *Ecography* 40 (8): 1014–1027.

Einzmann, K., M. Immitzer, S. Böck, O. Bauer, A. Schmitt, and C. Atzberger. 2017. "Windthrow Detection in European Forests with Very High-Resolution Optical Data." *Forests* 8 (1): 21.

European Environment Agency, 2015. Conservation status of species and habitats by ecosystem type from Habitats Directive Article 17 reporting [Internet]. [cited 2018 Aug 16]. Available from: https://www.eea.europa.eu/data-and-maps/daviz/conservation-status-of-species-and

Feilhauer, H., F. Thonfeld, U. Faude, K.S. He, D. Rocchini, and S. Schmidtlein. 2013. "Assessing Floristic Composition with Multispectral Sensors–A Comparison Based on Monotemporal and Multiseasonal Field Spectra." *International Journal of Applied Earth Observation and Geoinformation* 21: 218–229.

Felton, A.M., H.K. Wam, C. Stolter, K.M. Mathisen, and M. Wallgren. 2018. "The Complexity of Interacting Nutritional Drivers behind Food Selection, a Review of Northern Cervids." *Ecosphere* 9 (5): e02230.

Fløjgaard, C., M. De Barba, P. Taberlet, and R. Ejrnæs. 2017. "Body Condition, Diet and Ecosystem Function of Red Deer (Cervus Elaphus) in a Fenced Nature Reserve." *Global Ecology and Conservation* 11: 312–323.

Foody, G.M. 2002. "Status of Land Cover Classification Accuracy Assessment." *Remote Sensing of Environment* 80 (1): 185–201.

Fryxell, J.M. 1991. "Forage Quality and Aggregation by Large Herbivores." *The American Naturalist* 138 (2): 478–98.

Godvik, I.M.R., L.E. Loe, J.O. Vik, V. Veiberg, R. Langvatn, and A. Mysterud. 2009. "Temporal Scales, Trade-Offs, and Functional Responses in Red Deer Habitat Selection." *Ecology* 90 (3): 699–710.

Gómez, C., J.C. White, and M.A. Wulder. 2016. "Optical Remotely Sensed Time Series Data for Land Cover Classification: A Review." *ISPRS Journal of Photogrammetry and Remote Sensing* 116: 55–72.

Harpole, W.S., and D. Tilman. 2007. “Grassland Species Loss Resulting from Reduced Niche Dimension.” *Nature* 446 (7137): 791.

Hautier, Y., P.A. Niklaus, and A. Hector. 2009. “Competition for Light Causes Plant Biodiversity Loss after Eutrophication.” *Science* 324 (5927): 636–638.

Herold, M., Roberts, D.A., Gardner, M.E., Dennison, P.E., 2004. Urban Reflectance Spectra from Santa Barbara. EcoSIS Spectral Library. [Internet]. [cited 2019 March 4]. Available from: http://ecosis.org

Houghton, R.A., J.I. House, J. Pongratz, G. R. Van Der Werf, R.S. DeFries, M.C. Hansen, C. Le Quéré, and N. Ramankutty. 2012. “Carbon Emissions from Land Use and Land-Cover Change.” *Biogeosciences* 9 (12): 5125–5142.

Isselstein J., 2018. Protecting biodiversity in grasslands. In: Marshall, A. and Collins, R. (ed.), *Improving grassland and pasture management in temperate agriculture*. Chapter 16, Burleigh Dodds Science Publishing, Cambridge, UK. ISBN: 978 1 78676 200 9; www.bdspublishing.com.

Isselstein, J., B. Jeangros, and V. Pavlu. 2005. “Agronomic Aspects of Biodiversity Targeted Management of Temperate Grasslands in Europe–a Review.” *Agronomy Research* 3 (2): 139–151.

Jensen, John R. 2009. *Remote Sensing of the Environment: An Earth Resource Perspective 2/e*. Pearson Education India.

Kauth, R. J., and G. S. Thomas. 1976. “The Tasselled Cap–a Graphic Description of the Spectral-Temporal Development of Agricultural Crops as Seen by Landsat.” In *LARS Symposia*, 159.

Lamarque, P., S. Lavorel, M. Mouchet, and F. Quétier. 2014. “Plant Trait-Based Models Identify Direct and Indirect Effects of Climate Change on Bundles of Grassland Ecosystem Services.” *Proceedings of the National Academy of Sciences* 111 (38): 13751–13756.

Li, B.L., Rykiel, E.J., 1996. Introduction to the special issue ‘‘Fuzzy Modelling in Ecology’’. *Ecological Modelling* 90, 109–110.

Lima, S.L., and L.M. Dill. 1990. “Behavioral Decisions Made under the Risk of Predation: A Review and Prospectus.” *Canadian Journal of Zoology* 68 (4): 619–640.

Löw, F., E. Fliemann, I. Abdullaev, C. Conrad, and J.P.A. Lamers. 2015. “Mapping Abandoned Agricultural Land in Kyzyl-Orda, Kazakhstan Using Satellite Remote Sensing.” *Applied Geography* 62: 377–390.

Meißner, M., H. Reinecke, S. Herzog, L. Leinen, and G. Brinkmann. 2012. *Vom Wald ins Offenland: Der Rothirsch auf dem Truppenübungsplatz Grafenwöhr. Raum-Zeit-Verhalten, Lebensraumnutzung, Management*. 1. Aufl. Ahnatal: Frank Fornacon.

Merkle, J.A., K.L. Monteith, E.O. Aikens, M.M. Hayes, K.R. Hersey, D. Middleton, B.A. Oates, H. Sawyer, B.M. Scurlock, and M.J. Kauffman. 2016. “Large Herbivores Surf Waves of Green-up during

Spring." *Proceedings of the Royal Society B: Biological Sciences* 283 (1833): 20160456.

Nagendra, H., R. Lucas, J.P. Honrado, R..H.G. Jongman, C. Tarantino, M. Adamo, and P. Mairota. 2013. "Remote Sensing for Conservation Monitoring: Assessing Protected Areas, Habitat Extent, Habitat Condition, Species Diversity, and Threats." *Ecological Indicators* 33: 45–59.

Pausas, J.G., and W.J. Bond. 2018. "Humboldt and the Reinvention of Nature." *Journal of Ecology*.

Peco, B., A.M. Sánchez, and F.M. Azcárate. 2006. "Abandonment in Grazing Systems: Consequences for Vegetation and Soil." *Agriculture, Ecosystems & Environment* 113 (1–4): 284–294.

Peeters, A., G. Beaufoy, R.M. Canals, A. De Vliegher, C. Huyghe, J. Isselstein, J. Jones, W. Kessler, D. Kirilovsky, and A. Van Den Pol-Van Dasselaar. 2014. "Grassland Term Definitions and Classifications Adapted to the Diversity of European Grassland-Based Systems." In *Grassland Science in Europe*, 19:743–750.

Peña, M.A., and A. Brenning. 2015. "Assessing Fruit-Tree Crop Classification from Landsat-8 Time Series for the Maipo Valley, Chile." *Remote Sensing of Environment* 171: 234–244.

Pettorelli, N., J.O. Vik, A. Mysterud, J.-M. Gaillard, C.J. Tucker, and N.C. Stenseth. 2005. "Using the Satellite-Derived NDVI to Assess Ecological Responses to Environmental Change." *Trends in Ecology & Evolution* 20 (9): 503–10.

Rapinel, S., N. Rossignol, L. Hubert-Moy, J.-B. Bouzillé, and A. Bonis. 2018. "Mapping Grassland Plant Communities Using a Fuzzy Approach to Address Floristic and Spectral Uncertainty." *Applied Vegetation Science*.

Riesch, F., B. Tonn, M. Meißner, N. Balkenhol, and J. Isselstein. 2019. "Grazing by Wild Red Deer: Management Options for the Conservation of Semi-Natural Open Habitats." *Journal of Applied Ecology*.

Riesch, F., H.G. Stroh, B. Tonn, and J. Isselstein. 2018. "Soil PH and Phosphorus Drive Species Composition and Richness in Semi-Natural Heathlands and Grasslands Unaffected by Twentieth-Century Agricultural Intensification." *Plant Ecology & Diversity* 11 (2): 239–253.

Rocchini, D., G.M. Foody, H. Nagendra, C. Ricotta, M. Anand, K.S. He, V. Amici, B. Kleinschmit, M. Förster, and S. Schmidtlein. 2013. "Uncertainty in Ecosystem Mapping by Remote Sensing." *Computers & Geosciences* 50: 128–135.

Rosenthal, G., J. Schrautzer, and C. Eichberg. 2012. "Low-Intensity Grazing with Domestic Herbivores: A Tool for Maintaining and Restoring Plant Diversity in Temperate Europe." *Tuexenia*, no. 32: 167–205.

Ruprecht, E., M.Z. Enyedi, R.L. Eckstein, and T.W. Donath. 2010. "Restorative Removal of Plant Litter and Vegetation 40 Years after Abandonment Enhances Re-Emergence of Steppe Grassland Vegetation." *Biological Conservation* 143 (2): 449–456.

Schmidt, T., C. Schuster, B. Kleinschmit, and M. Förster. 2014. "Evaluating an Intra-Annual Time Series for Grassland Classification–How Many Acquisitions and What Seasonal Origin Are Optimal?" *IEEE Journal of Selected Topics in Applied Earth Observations and Remote Sensing* 7 (8): 3428–3439.

Schmidtlein, S., P. Zimmermann, R. Schüpferling, and C. Weiss. 2007. "Mapping the Floristic Continuum: Ordination Space Position Estimated from Imaging Spectroscopy." *Journal of Vegetation Science* 18 (1): 131–140.

Schönert, M., E. Zillmann, H. Weichelt, J.U.H. Eitel, T.S. Magney, H. Lilienthal, B. Siegmann, and T. Jarmer. 2015. "The Tasseled Cap Transformation for RapidEye Data and the Estimation of Vital and Senescent Crop Parameters." *The International Archives of Photogrammetry, Remote Sensing and Spatial Information Sciences* 40 (7): 101.

Schulze, K.A., G. Rosenthal, and A. Peringer. 2018. "Intermediate Foraging Large Herbivores Maintain Semi-Open Habitats in Wilderness Landscape Simulations." *Ecological Modelling* 379: 10–21.

Schuster, C., M. Förster, and B. Kleinschmit. 2012. "Testing the Red Edge Channel for Improving Land-Use Classifications Based on High-Resolution Multi-Spectral Satellite Data." *International Journal of Remote Sensing* 33 (17): 5583–5599.

Schuster, C., T. Schmidt, C. Conrad, B. Kleinschmit, and M. Förster. 2015. "Grassland Habitat Mapping by Intra-Annual Time Series Analysis–Comparison of RapidEye and TerraSAR-X Satellite Data." *International Journal of Applied Earth Observation and Geoinformation* 34: 25–34.

Sims, D.A., and J.A. Gamon. 2002. "Relationships between Leaf Pigment Content and Spectral Reflectance across a Wide Range of Species, Leaf Structures and Developmental Stages". *Remote Sensing of Environment* 81 (2–3): 337–354.

Song, C., C.E. Woodcock, K.C. Seto, M.P. Lenney, and S.A. Macomber. 2001. "Classification and Change Detection Using Landsat TM Data: When and How to Correct Atmospheric Effects?" *Remote Sensing of Environment* 75 (2): 230–244.

Stenzel, S., H. Feilhauer, B. Mack, A. Metz, and S. Schmidtlein. 2014. "Remote Sensing of Scattered Natura 2000 Habitats Using a One-Class Classifier." *International Journal of Applied Earth Observation and Geoinformation* 33: 211–217.

Stevens, C.J., N.B. Dise, J. O. Mountford, and D.J. Gowing. 2004. “Impact of Nitrogen Deposition on the Species Richness of Grasslands.” *Science* 303 (5665): 1876–1879.

Tang, Z., L. Deng, H. An, W. Yan, and Z. Shangguan. 2017. “The Effect of Nitrogen Addition on Community Structure and Productivity in Grasslands: A Meta-Analysis.” *Ecological Engineering* 99: 31–38.

Terres, J.-M., L.N. Scacchiafichi, A. Wania, M. Ambar, E. Anguiano, A. Buckwell, A. Coppola, A. Gocht, H.N. Källström, and P. Pointereau. 2015. “Farmland Abandonment in Europe: Identification of Drivers and Indicators, and Development of a Composite Indicator of Risk.” *Land Use Policy* 49: 20–34.

Tong, A., and Y. He. 2017. "Estimating and Mapping Chlorophyll Content for a Heterogeneous Grassland: Comparing Prediction Power of a Suite of Vegetation Indices across Scales between Years". *ISPRS Journal of Photogrammetry and Remote Sensing* 126: 146–167.

Valkó, O., S. Venn, M. Żmihorski, I. Biurrun, R. Labadessa, and J. Loos. 2018. “The Challenge of Abandonment for the Sustainable Management of Palaearctic Natural and Semi-Natural Grasslands.” *Hacquetia* 17 (1): 5–16.

Van Wieren, S. E. 1995. “The Potential Role of Large Herbivores in Nature Conservation and Extensive Land Use in Europe.” *Biological Journal of the Linnean Society* 56: 11–23.

Wachendorf, M., T. Fricke, and T. Möckel. 2017. “Remote Sensing as a Tool to Assess Botanical Composition, Structure, Quantity and Quality of Temperate Grasslands.” *Grass and Forage Science*.

Warren, S.D., and R. Büttner. 2008a. “Relationship of Endangered Amphibians to Landscape Disturbance.” *Journal of Wildlife Management* 72 (3): 738–44.

———2008b. “Active Military Training Areas as Refugia for Disturbance-Dependent Endangered Insects.” *Journal of Insect Conservation* 12 (6): 671–76.

Warren, S.D., M. Alt, K.D. Olson, S.D.H. Irl, M.J. Steinbauer, and A. Jentsch. 2014. “The Relationship between the Spectral Diversity of Satellite Imagery, Habitat Heterogeneity, and Plant Species Richness.” *Ecological Informatics* 24: 160–168.

Wilson, R.T., E.J. Milton, and J.M. Nield. 2014. ‘Spatial Variability of the Atmosphere over Southern England, and Its Effect on Scene-Based Atmospheric Corrections’. *International Journal of Remote Sensing* 35 (13): 5198–5218.

Wilson, J.B., R.K. Peet, J. Dengler, and M. Pärtel. 2012. “Plant Species Richness: The World Records.” *Journal of Vegetation Science* 23 (4): 796–802.

Woodhouse, I.H. 2017. *Introduction to Microwave Remote Sensing*. CRC press.

2

CHAPTER 2 – MULTI-TEMPORAL RAPIDEYE TASSELLED CAP DATA FOR LAND COVER CLASSIFICATION USING RANDOM FORESTS

This chapter is submitted as:

Raab, C., B. Tonn, M. Meißner, N. Balkenhol and J. Isselstein. “Multi-temporal RapidEye Tasselled Cap data for land cover classification using Random Forests.” *European Journal of Remote Sensing*.

Abstract

Land cover mapping can be seen as a key element to understand the spatial distribution of habitats and thus to sustainable management of natural resources. Multi-temporal remote sensing data are a valuable data source for land cover mapping. However, the increased amount of data requires effective machine learning approaches. In this study, the Random Forest classification algorithm was applied to (1) a multi-temporal Tasselled-Cap-transformed, (2) top of atmosphere and (3) surface reflectance RapidEye time-series. The overall accuracies were about 91.5% (Kappa = 0.9) for all three datasets. The McNemar test showed, however, significant differences between the Tasselled-Cap-transformed and untransformed mapping results. The profiles for the Tasselled-Cap-transformed RapidEye data indicated a good separability between considered classes. The phenological profiles of vegetated surfaces followed a typical green-up curve for the Greenness Tasselled-Cap-index. A permutation-based variable importance measure indicated that late autumn should be considered as most important phenological phase contributing to the classification model performance. The results suggested that the RapidEye Tasselled Cap Transformation, which was designed for agricultural applications, can be an effective data compression tool, suitable to map heterogeneous landscapes with no measurable negative impact on classification accuracy.

Keywords: land cover; Random Forest; RapidEye; phenological correction, Tasselled Cap Transformation

Introduction

Land cover classification using satellite remote sensing data can be seen as a key element to quantify and monitor changes of the Earth's surface (Gómez et al., 2016). Applications range from global land cover mapping for climate modelling purposes (Houghton et al., 2012) to the delineation of different grassland communities at small scales using RapidEye data (Schuster et al., 2015; Raab et al., 2018). Multi-temporal remote sensing data and indices or transformations can increase the predictive power of a land cover classification model (Schmidt et al., 2014), as more information about the land surface reflectance characteristics can be included. The increased amount of data, however, may require robust machine learning classification algorithms and data compression approaches to cope with high amounts of data, such as Support Vector Machines (Cortes and Vapnik, 1995; Schuster et al., 2012) or Random Forests (RF) (Breiman, 2001; Belgiu and Drăguț, 2016).

The RapidEye earth observation constellation consists of five identical satellites with a theoretical off-nadir revisit time of one day. Spectral data are recorded at a spatial resolution of 6.5 m pixel, which is resampled to 5 m by the data provider (Planet Labs Inc., 2016). The mounted sensors record data not only in the visible blue (440–510 nm), green (520–590 nm) and red (630–685 nm) part of the electromagnetic spectrum, but also in the rededge (690–730 nm) and near-infrared (NIR,

760–850 nm) region (Tyc et al., 2005). In addition to the reflectance recorded by a satellite remote sensing platform, vegetation indices are an established tool for the analysis of plant dynamics and ecosystem monitoring (Pettorelli et al., 2005). The Tasselled Cap Transformation (TCT) represents a group of spectral indices designed for agricultural applications (Kauth and Thomas, 1976). The TCT has been developed for several remote sensing platforms, such as the sensors of the Landsat programme (Baig et al., 2014; Crist and Cicone, 1984; Huang et al., 2002; Kauth and Thomas, 1976), MODIS (Lobser and Cohen, 2007) and RapidEye (Schönert et al., 2014). Similar to the concept of principal component analysis, the original spectral bands are transformed to new bands with defined interpretations. For this, fixed weighting factors are assigned to the original reflectance values of the respective spectral bands. The generated Tasselled-Cap-bands can be associated with biophysical properties of the studied surface. The first Tasselled-Cap-band captures the overall brightness (Brightness), while the second transformation enhances the characteristics of vegetation reflectance (Greenness). Thus, the Greenness can be used as a measure of photosynthetically-active vegetation, with its peak in the NIR domain (Dahms et al., 2016). For RapidEye data, five multi-spectral bands are compressed by the TCT into three new bands with reduced correlation and limited information loss. The Brightness component for the RapidEye sensor summarises the total reflectance as a weighted sum of all spectral bands. Hence, the Brightness is sensitive to changes in the sum of reflectance, but

particularly to an alteration in soil brightness. These two Tasselled-Cap-bands are often complemented by a third transformation, such as Wetness, which is sensitive to surface moisture. For the RapidEye satellites the third Tasselled-Cap-band, Yellowness, is configured to enhance the typical reflectance behaviour of senescent vegetation cover (Schönert et al., 2014).

RapidEye Tasselled-Cap-transformed data has been successfully applied to map abandoned agricultural land (Löw et al., 2015), to estimate windthrow in forests (Einzmann et al., 2017) or for the prediction of biophysical crop parameters (Dahms et al., 2016; Schönert et al., 2015). As the correlation and data intensity is reduced by the TCT, its application can be an attractive approach for multi-temporal land cover mapping, which has not been extensively tested, yet. However, as the TCT-components of the RapidEye sensor are derived from top of atmosphere (TOA) reflectance data (Schönert et al., 2014), potential influences by the atmosphere, due to scattering and absorption (Song et al., 2001), might not be considered sufficiently. This in turn could impact the result of a Tasselled-Cap-transformed multi-temporal land cover classification, because the atmospheric composition can be highly variable over space and time (Wilson et al., 2014). Consequently, this could thwart the advantages of a TCT-based multi-temporal land cover classification. Therefore, an alternative to a land cover classification using Tasselled-Cap-transformed data could be the application of atmospheric corrected surface reflectance data. For this, radiative transfer models can be used to estimate the

atmospheric conditions at the sensing time of an image (Vermote et al., 1997).

Within this context, the purpose of this land cover classification study was to evaluate the performance of a multi-temporal Tasselled-Cap-transformed RapidEye time-series in comparison to TOA and atmospheric corrected surface reflectance (SR) data. We hypothesise that multi-temporal RapidEye Tasselled-Cap-transformed data will capture phenological patterns of vegetated surfaces and that the classification performance will be comparable to using untransformed data, even if they include atmospheric correction.

This hypothesis was tested in an area, the Grafenwoehr Military Training area, which can be considered as a particular challenge to land cover classification. As a result of long-term military use, the Grafenwoehr military training area consists of a relatively fine-scale mosaic composed of open, semi-open, successional and forested areas, compared to the surrounding landscape. Transitions between managed and unmanaged grassland as well as shrub and forest are present, as management has to take into account both military use and nature conservation requirements.

Furthermore, as the acquisition timing can be an important factor influencing the quality of multi-temporal land cover classification (Schmidt et al., 2014; Nitze et al., 2015), a permutation-based variable importance measure was used to estimate the contribution of the three TCT indices the

TOA and SR bands to the respective classification models for different phenological phases.

Materials and methods

Study site

The Grafenwoehr military training area (GTA) is located in the south-east of Germany (Figure 1) and lies at about 450 m (*sd* = 38 m) above sea level in the natural region Upper Palatine-Upper Main Hills. The long-term average temperature and precipitation are 8.3 ± 0.04 °C and 701 ± 4 mm, respectively (1981–2010, mean ± SEM of four weather stations of the German Weather Service (DWD, Deutscher Wetterdienst) in the immediate vicinity). The GTA covers 230 km²; about 85% are part of the Natura 2000 network and contain numerous rare, highly protected habitat types and function as a refuge for many endangered species (Warren and Büttner, 2008a, 2008b; Riesch et al., 2018). About 40% of GTA are covered with open habitats, such as grassland or heath, while about 60% are covered with forest. Parts of the grassland areas are mown once a year around the beginning of July. Wildlife grazing, especially by red deer (*Cervus elaphus*), also plays an important role for vegetation dynamics (Meißner et al., 2012; Riesch et al., 2019).

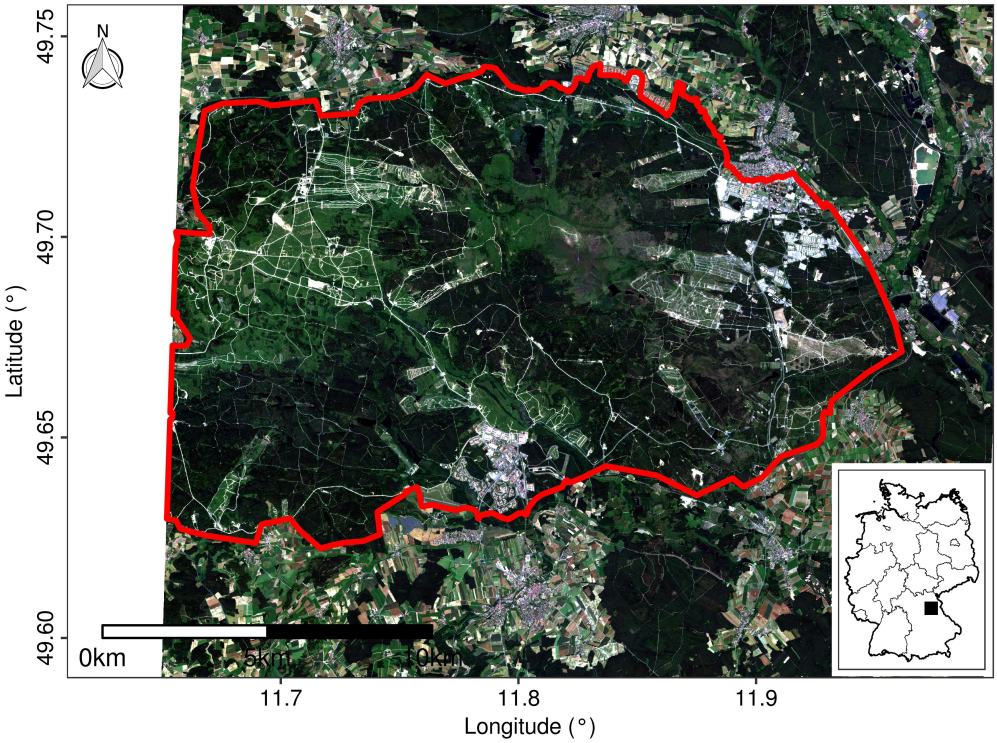

Figure 1: Location the study site Grafenwoehr military training area outlined in red. The location of the study site in Germany is marked with a black square in the lower right map. The background map is based on the 24 June 2016 RapidEye acquisition (Table 1).

Satellite data and pre-processing

A multi-temporal RapidEye time-series consisting of ten images covering the years between 2014 and 2017 (Table 1) was acquired. The ordered processing level 3A was already radiometrically, geometrically, and sensor corrected, and was delivered covering one 25 by 25 km tile (ID-3,262,023).

The pre-processing included a correction of the acquisition dates for shifts in the phenology according to the method proposed by Schmidt et al. (2014). This is an important processing step, because two images from

different years, acquired for the same day of the year and the same area, can differ in their phenology. The actual Julian day of the year was corrected for each acquisition to an adjusted Julian day of the year (Table 1), as outlined in Raab et al. (2018).

Table 1: Multi-annual RapidEye time-series ordered by adjusted Julian day of the year (DOY).

No	Acquisition date	Actual Julian DOY	Adjusted Julian DOY	Sensing time (am)	Sensor view angle (°)	Phenological phase	
1	14 March 2016	74	88	10:45	10.4	prespring (PSP)	DOY 71-102
2	27 March 2017	86	95	10:35	3.5		
3	2 April 2014	92	114	11:17	13.0	first spring (FIS)	DOY 103-131
4	20 April 2016	111	119	11:07	9.6		
5	17 April 2014	107	127	11:14	6.3		
		-				full spring (FUS)	DOY 132-158
6	11 June 2017	162	169	10:31	6.9	early summer (ESU)	DOY 159-179
7	24 June 2016	176	183	10:49	0.3	midsummer (MSU)	DOY 180-220
8	25 August 2017	237	243	10:27	3.5	late summer (LSU)	DOY 221-244
		-				early autumn (EA)	DOY 245-266
		-				full autumn (FA)	DOY 267-284
9	12 October 2015	285	287	11:02	6.3	late autumn (LA)	DOY 285-305
10	16 October 2017	289	290	10:25	6.6		

In order to ensure spatial consistency and to reduce potential classification errors all images were co-registered to the image acquired on 2

April 2014 using the function *coregisterImages*, implemented in the package *RStoolbox* (Leutner and Horning, 2018) in the R statistical programming environment (R Core Team, 2018). TOA was derived according to the product specification by the data provider (Planet Labs Inc., 2016). The Tasselled-Cap-indices Brightness (TCB), Greenness (TCG), and Yellowness (TCY) were derived using the transformation introduced by Schönert et al. (2014). The band specific weighting factors are illustrated in Figure 2. The SR dataset was derived using the Second Simulation of Satellite Signal in the Solar Spectrum (6S) algorithm (Vermote et al., 1997), implemented in the function *i.atcorr* within the open source Geographic Resources Analysis Support System (GRASS GIS), version 7.6 (GRASS Development Team, 2019).

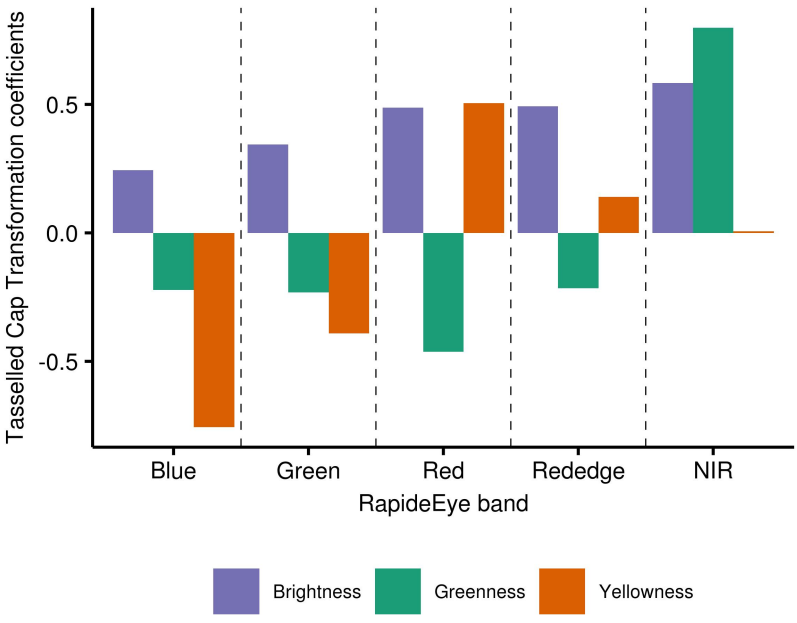

Figure 2: Tasselled Cap Transformation coefficients for Brightness, Greenness and Yellowness for each band according to Schönert et al. (2014).

Training and validation data collection

The classification schema was adopted from the Corine Land Cover level 3 classes. The selected classes included water, moors and heathlands, managed grassland, unmanaged grassland, transitional woodland-shrub, broad-leaved forest, coniferous forest and other (Table 2). The class 'other' summarised areas covered by artificial surfaces and bare soil.

An independent validation set of 410 locations was created by a random sampling approach (Table 2). The distinction between different classes was aided by an aerial image (24 June 2016) as well as the habitat map created as part of the Natura 2000 legal obligations in 2006 (Meißner et al., 2012). Similarly, a total of 4104 training locations were distributed over the GTA (Table 2). As recommended by Millard and Richardson (2015), the proportion of training sample locations per class were adjusted to reflect the actual class proportion in the study area, guided by the Natura 2000 habitat map. Plots of TCB, TCG and TCY against adjusted Julian day of the year were used to visualise vegetation phenology for the selected land cover classes using the extracted information at the training set locations (Pasquarella et al., 2016).

Table 2: Classification schema, respective number of training points and independent validation points.

Number	Class name		Number of training points used for cross-validation	Number of independent validation points used for the McNemar test
1	water	*WA*	120	5
2	moors and heathlands	*MH*	393	14
3	managed grassland	*GM*	433	21
4	unmanaged grassland	*GU*	1059	106
5	broad-leaved forest	*BF*	561	67
6	coniferous forest	*CF*	788	156
7	transitional woodland-shrub	*TW*	316	13
8	other	*OS*	434	28
	Total		4104	410

Classification and validation

The RF machine learning classifier implemented in the package *ranger* (Wright and Ziegler, 2015) was used to relate the TCT, TOA and SR predictor variables to the training sample dataset, respectively. The non-parametric method of RF was selected, because it can handle high-dimensional datasets (Belgiu and Drăguţ, 2016) and its robustness for mapping heterogeneous habitats has been demonstrated by several studies (Barrett et al., 2016; Cutler et al., 2007; Millard and Richardson, 2015; Rodriguez-Galiano et al., 2012). The RF algorithm is an ensemble-based classification tree, from which the predictions are drawn by a majority vote among all trees. The trees are constructed using a subset of training samples drawn through replacement (Belgiu and Drăguţ, 2016). For this, about two

thirds of the training samples are used to train the trees (in-bag samples) and the remaining one third is used to estimate the model performance using internal cross-validation (out of bag samples, OOB). As recommended by Belgiu and Drăguț (2016), the number of trees to be constructed (num.trees) was set to 500. The number of predictor variables randomly sampled as candidates at each split (mtry) was set to the square root of the total number of predictor variables (Gislason et al., 2006). To account for the randomness of the RF algorithm, the classification map was derived from the most frequently predicted class from 100 spatial predictions per pixel. In addition to the classification map, spatial probability values were derived from the RF models, as the mean of 100 predictions.

An important part of land cover classification is the validation, e.g. accuracy assessment by a confusion matrix, of the final map (Foody, 2002). As the internal OOB validation of the RF can be biased (Millard and Richardson, 2015), a *k*-fold cross-validation approach was used instead of the RF OOB classification error estimation. The *k*-fold cross-validation procedure partitions the dataset selected for the model construction randomly into *k* folds, i.e. *k* single parts of the dataset. In this approach, *k*-1 folds are used to train the model and the remaining one fold is used to validate the classification model. This approach has the advantage that, with sufficient repetitions, all the samples can be used to train and validate a model. Hence, a 10-fold cross-validation was used to estimate the models constructed using the training sample set, implemented in the package *mlr*

(Bischl et al., 2016). The validation procedure was repeated 100 times to reduce variance introduced by the cross-validation. Accuracy assessment included overall, user's and producer's accuracy, derived from a standard confusion matrix (Congalton, 1991).

The independent validation set of 410 locations (Table 2) was used to compare the statistical significance of the differences between the land cover predictions derived from TCT, TOA and SR data. For this, the non-parametric McNemar test was used (Foody, 2004), which has been commonly applied to evaluate differences between classification results (Barrett et al., 2016; Rodriguez-Galiano et al., 2012). The significance level was set to 5% with a z-critical value of $z = 1.96$.

Variable importance

Permutation-based variable importance was derived in order to estimate which TCT index, spectral TOA or SR band at which phenological season contributed most to the RF model performance. By excluding one variable and keeping the rest in the model, the contribution to the performance can be estimated in terms of change in classification error rate (Ruß and Brenning, 2010; Peña and Brenning, 2015). Thus, the increase of classification error as a measure of variable importance was estimated with 100 permutations per variable, using the package *mlr*.

Results

Tasselled Cap Transformation time-series

The created training data set was used to extract the TCB, TCG and TCY time-series data and to explore differences in the phenology across the land cover classes. Figure 3 illustrates the seasonal variability with distinct patterns for all eight land cover classes. Values of TCB were generally higher than those of TCG and TCY. The TCY curves showed little variability for all classes with consistently negative values close to zero. The TCG profiles exhibited more pronounced phenological patterns with peaks in the early summer for all classes, except for the non-vegetative ones ‘other’ and ‘water’. The classes ‘unmanaged’ and ‘management grassland’ were well separated according to the TCB and TCG seasonal profiles. The class ‘managed grassland’ showed consistently higher TCB and TCG values compared to ‘unmanaged grassland’. Both TCB and TCG curves captured transitions from leaf-on to leaf-off periods for ‘broad-leaved forest’ and ‘transitional woodland-shrub’ with high seasonal amplitude. The highest TCB values were present for the class ‘other’, which had very low TCG values without a seasonal pattern.

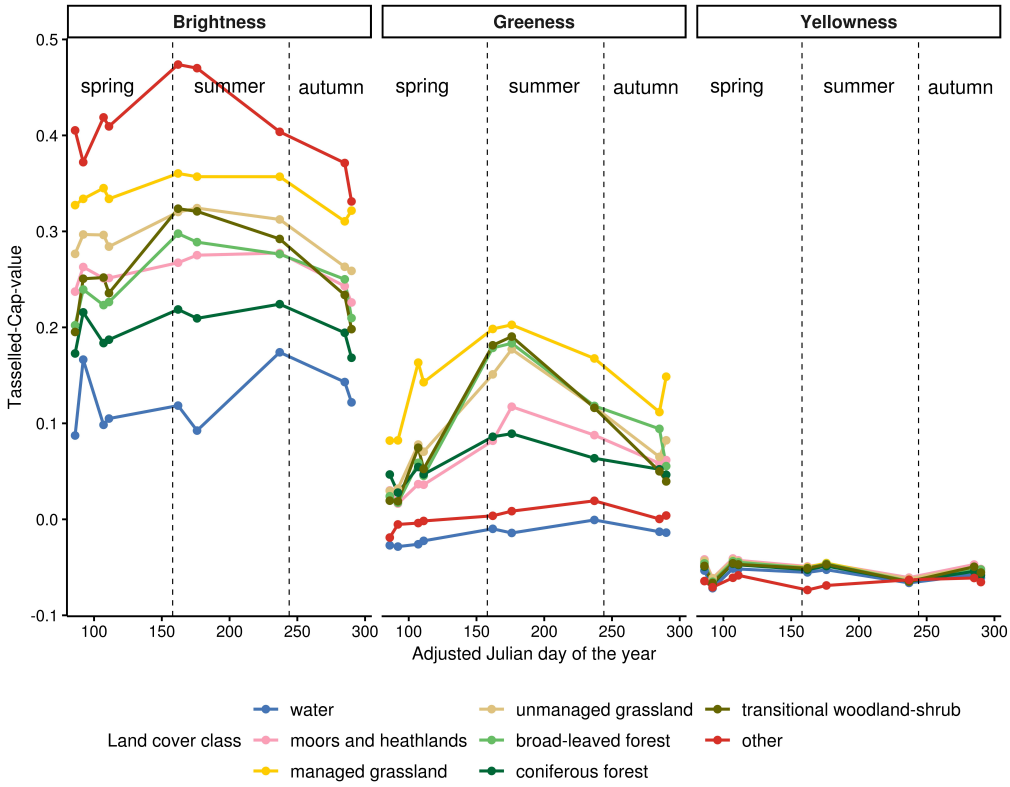

Figure 3: Seasonal Tasselled Cap Brightness, Greenness and Yellowness index plots using the mean value of the extracted training data (Table 2) set per class.

Classification and validation

The accuracy assessment results derived from repeated 10-fold cross-validation for the the TCT, TOA and SR datasets are shown in Table 3. The overall accuracy for all three datasets was about 91.5 % (TCT *sd* = 1.4%, TOA *sd* = 1.4%, SR *sd* = 1.3%). The derived Kappa values were very similar as well. Class-specific omission and commission error rates are illustrated by producer's (PA) and user's accuracy (UA) in Table 3. Lowest PA and UA values were estimated for the classes 'transitional woodland-

shrub' and 'moors and heathlands'. In general, the differences between the three tested datasets were small.

Table 3: Classification results for all three datasets. PA = producer's and UA = user's accuracy.

	Tasselled Cap Transformation	**Top of atmosphere reflectance**	**Surface reflectance**
Overall Accuracy (%)	91.49	91.55	91.49
Kappa	0.90	0.90	0.90
water			
PA	0.97	0.93	0.93
UA	0.97	0.98	0.98
moors and heathlands			
PA	0.87	0.85	0.85
UA	0.82	0.84	0.84
managed grassland			
PA	0.94	0.94	0.94
UA	0.95	0.95	0.95
unmanaged grassland			
PA	0.91	0.91	0.91
UA	0.87	0.86	0.86
broad-leaved forest			
PA	0.92	0.92	0.92
UA	0.93	0.94	0.94
coniferous forest			
PA	0.96	0.95	0.95
UA	0.94	0.94	0.94
transitional woodland-shrub			
PA	0.80	0.82	0.81
UA	0.92	0.95	0.95
other			
PA	0.92	0.95	0.95
UA	0.99	0.98	0.98

The results of the McNemar test between the TCT, TOA and SR classification results using the independent validation set (Table 2) are displayed in Table 4. The null hypothesis, i.e. no significant difference between classification results, was confirmed for TOA and SR. The TCT classification results differed significantly from the TOA and SR results ($p < 0.001$). The overall accuracy estimated by the independent validation set was higher (96.34%) than that of the TOA and SR classification results (89.8–89.3%).

Table 4: Results of the McNemar test for three different datasets, TCT = Tasselled Cap Transformation, TOA = Top of atmosphere reflectance, SR = surface reflectance, OA = overall accuracy.

Map 1	Map 2	|z|	*p* value	OA map 1	OA map 2	Kappa map 1	Kappa map 2
TCT	TOA	4.56	< 0.001	96.34%	89.76%	0.95	0.87
TCT	SR	4.77	< 0.001	96.34%	89.27%	0.95	0.86
TOA	SR	1.41	0.079	89.76%	89.27%	0.87	0.86

The predicted map derived from the TCT RF model is presented in Figure 4. The accompanying predicted probability maps for each class are displayed in the supplemental material Figure S1. The percentages of all land cover classes are shown in Table 5. The differences between TCT, TOA and SR predicted proportion of the land cover were marginal. The dominant vegetation cover classes in all three versions were ‘coniferous forest’ and ‘broad-leaved forest’, making up about 54% of the total area. Most of the ‘transitional woodland-shrub’ cover was in the western part of the study site, predominantly associated with a more fragmented landscape. Larger complexes of ‘managed grassland’ were embedded in this fragmented

mixture of open landscape and ‘transitional woodland-shrub’ and forest. The class ‘unmanaged grassland’ can be found relatively ubiquitously, but with larger complexes in the centre as well as in the western part of the study site. The class ‘other’ covers a larger area in the centre of the study site, which reflects soil scarification due to exploded ordnance. In the eastern part of the study site the class ‘moors and heathlands’ occurred more frequently, compared to the remaining area. This can be related to dryer and less fertile soil conditions for heathlands in the northern and north-eastern part of the study site (Riesch et al., 2018).

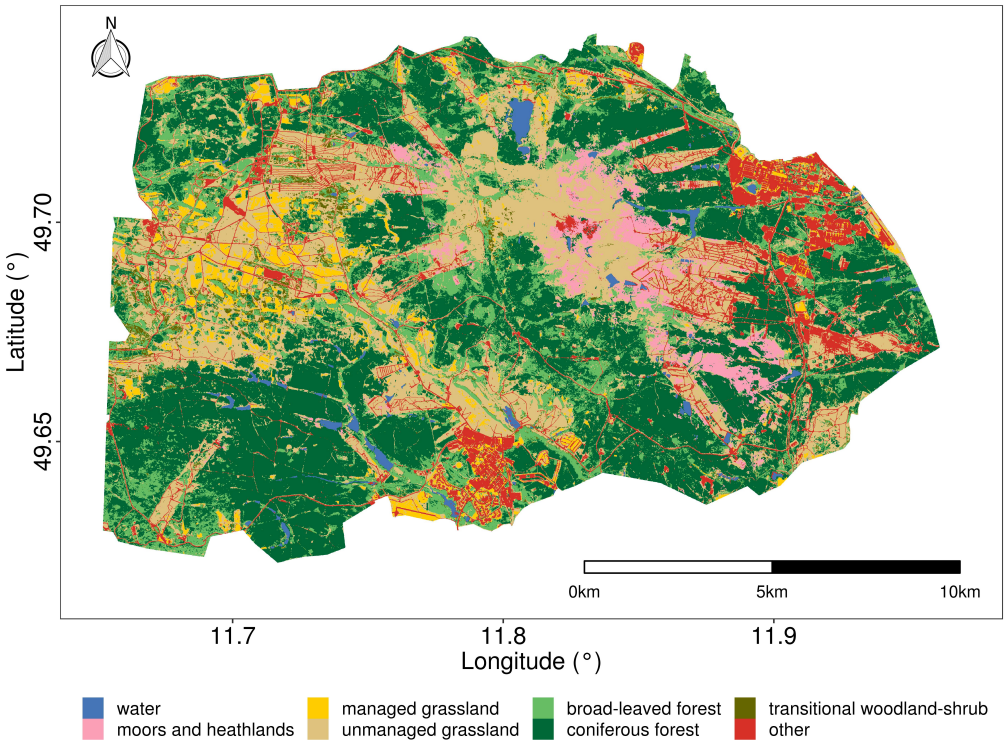

Figure 4: Classification map for the GTA derived from the multi-temporal Tasselled Cap RapidEye times-series, using the Random Forest classification algorithm. To improve the homogeneity of the classification a 3×3 majority filter was applied to the presented map.

Table 5: Share of land cover classes for the Tasselled Cap Transformation (TCT), Top of atmosphere (TOA) and surface reflectance (SR) predicted maps.

Number	Class name	TCT	TOA	SR
		Share of class (%)		
1	water	1.26	1.20	1.20
2	moors and heathlands	3.66	3.57	3.59
3	managed grassland	3.69	3.64	3.65
4	unmanaged grassland	26.31	25.42	25.41
5	broad-leaved forest	15.53	16.18	16.16
6	coniferous forest	38.36	38.09	38.12
7	transitional woodland-shrub	2.75	2.61	2.59
8	other	8.44	9.29	9.28
	Total	100	100	100

Variable importance

The permutation-based variable importance estimated as the mean increase in error rate is shown in Figure 5. For the TOA and SR classification, the most important variable for the RF model was the near-infrared band. This was particularly the case for the phenological seasons early summer and late autumn, which were generally the most important time frames. For the TCT dataset, TCG contributed most to the classification model. The sum of its mean increase in error rate across all considered phenological seasons was about 6.38%. For TCB and TCY, sums of 1.35% and 0.01% were estimated, respectively. The most important phenological season for the TCT model was late autumn. In general, the maximum mean increase in error rate values were higher for the models based on TCT data compared to TOA and SR.

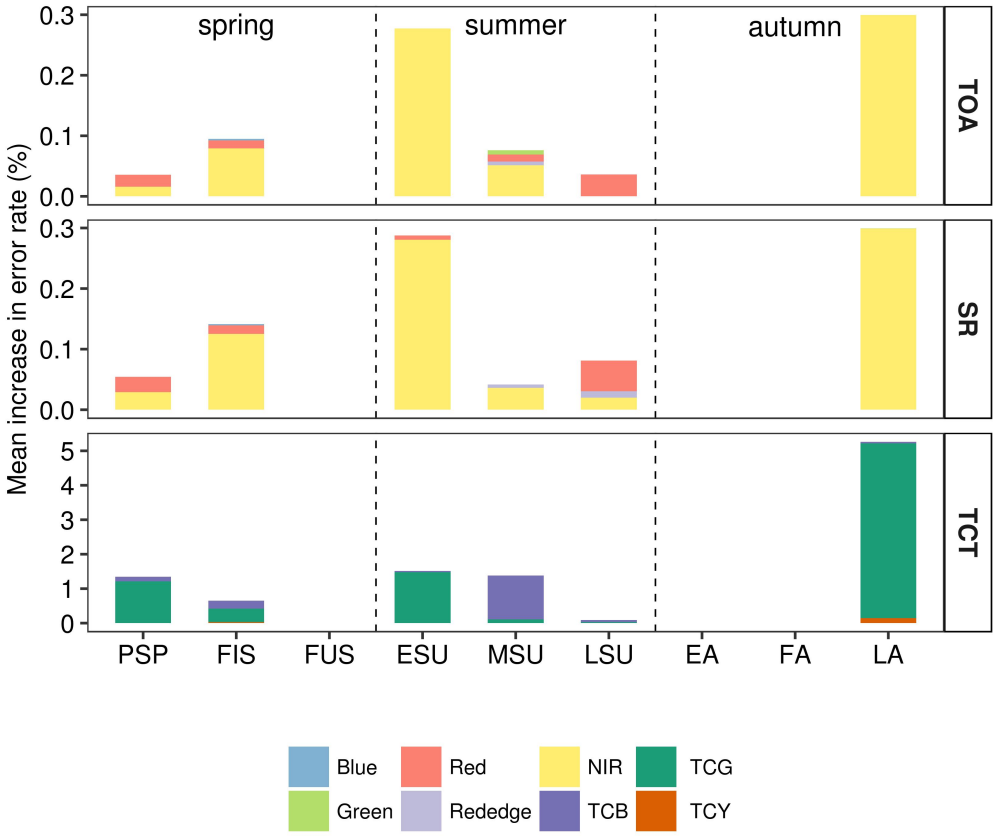

Figure 5: Permutation-based variable importance derived as mean increase in error rate for the top of atmosphere (TOA), surface reflectance (SR) and Tasselled Cap Transformation (TCT) dataset. TCB = Brightness, TCG = Greenness, TCY = Yellowness, PSP = prespring, FIS = first spring, FUS = full spring, ESU = early summer, MSU = midsummer, LSU = late summer, EA =early autumn, FA = full autumn, LA = late autumn.

Discussion

Tasselled Cap Transformation time-series

Similar to the study by Pasquarella et al. (2016), who evaluated Landsat Tasselled Cap time-series to characterise different habitats, distinct phenological profiles of different land cover classes were provided by the RapidEye TCT time-series (Figure 3). As TCG has a high positive weighting factor for the near-infrared band (Figure 2), it covers the spectral variation of live vegetation well. Thus, all TCG-profiles of vegetated surfaces followed a typical green-up curve, similar to the commonly used normalised difference vegetation index (Pettorelli et al., 2005). Most studied land cover classes showed a peak in TCB at the beginning of summer, especially for the class 'other'. As the TCB captures overall brightness and variance in soil brightness (Schönert et al., 2015), this might be attributed to changes in soil conditions, such as moisture.

The Tasselled-Cap-transformed Landsat archive data has been recently recognised as a valuable tool to asses abrupt as well as gradual changes in land cover (Kennedy et al., 2015, 2010; Pasquarella et al., 2016). The available RapidEye archive data should be considered by future studies to evaluate the potential of the high spatial resolution Tasselled-Cap-transformed RapidEye data for change analysis.

Classification and validation

Only marginal differences in classification accuracy between the TCT, TOA and SR datasets were present (Table 3). The McNemar test showed no significant difference between the TOA and SR dataset (Table 4). This was similar to the results provided by Raab et al. (2015), who reported only marginal classification accuracy differences among different atmospheric correction approaches and uncorrected multi-temporal Landsat data. Even though the study area has only small topographic variability, an additional topographic correction could have increased the predictive power of the classification model (Vanonckelen et al., 2013). However, classification results based on TCT differed from both classifications based on untransformed values, and had a c. 6% higher overall accuracy than those. This might be related to a lower model complexity as a smaller number of predictor variables were included, and to a reduced correlation among the predictor variables in the TCT dataset (Millard and Richardson, 2015). The TCT, which was originally developed for agricultural applications, can thus be considered as an effective data compression approach, which can provide similarly high classification accuracies as TOA and SR data.

A variety of alternative land cover classification concepts have been presented using RapidEye data in comparison to the presented pixel-based RF approach. For land cover mapping with single temporal RapidEye data and machine learning techniques, such as Support Vector Machines,

Schuster et al. (2012) and Ustuner et al. (2015) reported OA values ranging from 78.1 to 85.6%. More accurate classification results were reported for multi-temporal data (Zillmann and Weichelt, 2013; Schuster et al., 2015), similar to the results presented in this study. However, the application of Support Vector Machines is computational intensive, since it requires parameter tuning. In a direct comparison of Support Vector Machines and RF for land cover classification in a heterogeneous coastal landscape, Adam et al. (2014) found no significant difference between the performance of both algorithms. The overall accuracy estimated for the RF classification was slightly higher compared to the result using Support Vector Machines. A segmentation-based classification approach aggregates spectrally homogeneous pixels into objects and would most likely increase the overall accuracy compared to the presented pixel-based classification (Förster et al., 2010; Laliberte et al., 2007). This would come with the trade-off of losing information as small features are integrated into bigger objects (Schmidtlein and Sassin, 2004; Liu and Xia, 2010; Schmidt et al., 2017). Therefore, the presented pixel-based TCT classification approach can be seen as a valid approach, from which it would be easy to aggregate classified pixels to objects.

Variable importance

The different magnitudes of the measure mean increase in classification error rate between the TCT and untransformed datasets can be

explained by the compression of information into only three (TCT) instead of five (TOA and SR) uncompressed bands (Figure 5). As most of the surface in the study site was covered with vegetation (Table 5), the high importance of the Greenness TCT-index and the near-infrared band of the TOA and SR dataset was not surprising. The small contribution of the TCY data can be explained by the small variability of this transformation component (Schönert et al., 2014). However, all components of the respective datasets should be considered for mapping land cover, because a potential interdependence between the predictor variables would otherwise be disregarded. The differences between the TOA and SR variable importances were small. For both datasets, the rededge band contributed to the model accuracy, albeit only slightly. Similar results were reported by Schuster et al. (2012).

The phenological correction of acquisition dates allowed to compare how different phenological phases contributed to the classification model. The phenological season late autumn contributed most to the classification model in all three cases. Therefore, the late autumn season must be seen as a critical data acquisition window for mapping land cover by the means of satellite remote sensing in this study. This is supported by Förster et al. (2010), who recommended using image acquisitions originating from the onset of vegetation and the senescence phase to map Natura 2000 habitats. As the remote sensing data available in this study did not cover all

phenological seasons (Table 1), a broad generalisation concerning the importance of all phenological phases was not possible.

Conclusion

The classification of a heterogeneous landscape using Tasselled-Cap-transformed RapidEye data achieved similar high overall accuracies compared to top of atmosphere and surface reflectance data. Thus, the RapidEye Tasselled Cap Transformation can be seen as an effective data compression measure, valuable for the application of multi-temporal land cover mapping. The Tasselled Cap Transformation captured phenological patterns of vegetated surfaces and the late autumn was identified as the most influential image acquisition window. A phenological correction of image acquisition dates must be seen as a pivotal pre-processing step for the analysis of satellite remote sensing data originating from different years. Future research should evaluate the potentials of the Tasselled-cap-transformed RapidEye data to study environmental changes at very high resolutions.

Acknowledgements

We thank Friederike Riesch and Laura Richter for comments on earlier versions of this manuscript. The project was supported by funds of German government's Special Purpose Fund held at Landwirtschaftliche Rentenbank (28 RZ 7007). We thank the Federal Forests Division

(Bundesforst) of the German Institute for Federal Real Estate (Bundesanstalt für Immobilienaufgaben) and the Institut für Wildbiologie Göttingen und Dresden e.V. for close cooperation and support. We acknowledge the DLR for the delivery of RapidEye images as part of the RapidEye Science Archive (RESA) – proposal 00226.

References

Adam, E., O. Mutanga, J. Odindi, and E.M. Abdel-Rahman. 2014. "Land-Use/Cover Classification in a Heterogeneous Coastal Landscape Using RapidEye Imagery: Evaluating the Performance of Random Forest and Support Vector Machines Classifiers". *International Journal of Remote Sensing* 35 (10): 3440–3458.

Baig, M.H. Ali, L. Zhang, T. Shuai, and Q. Tong. 2014. "Derivation of a Tasselled Cap Transformation Based on Landsat 8 At-Satellite Reflectance". *Remote Sensing Letters* 5 (5): 423–431.

Barrett, B., C. Raab, F. Cawkwell, and S. Green. 2016. "Upland Vegetation Mapping Using Random Forests with Optical and Radar Satellite Data". *Remote Sensing in Ecology and Conservation* 2 (4): 212–231.

Belgiu, M., and L. Drăguț. 2016. "Random Forest in Remote Sensing: A Review of Applications and Future Directions". *ISPRS Journal of Photogrammetry and Remote Sensing* 114: 24–31.

Bischl, B., M. Lang, L. Kotthoff, J. Schiffner, J. Richter, E. Studerus, G. Casalicchio, and Z.M. Jones. 2016. "Mlr: Machine Learning in R". *The Journal of Machine Learning Research* 17 (1): 5938–5942.

Breiman, L. 2001. "Random Forests". *Machine Learning* 45 (1): 5–32.

Congalton, R.G. 1991. "A Review of Assessing the Accuracy of Classifications of Remotely Sensed Data". *Remote Sensing of Environment* 37 (1): 35–46.

Cortes, C., and V. Vapnik. 1995. "Support-Vector Networks". *Machine Learning* 20 (3): 273–297.

Crist, .P., and R.C. Cicone. 1984. "Application of the Tasseled Cap Concept to Simulated Thematic Mapper Data". *Ann Arbor* 1001: 48107.

Cutler, D.R., T.C. Edwards, K.H. Beard, A. Cutler, K.T. Hess, J. Gibson, and J.J. Lawler. 2007. "Random Forests for Classification in Ecology". *Ecology* 88 (11): 2783–2792.

Dahms, T., S. Seissiger, E. Borg, H. Vajen, B. Fichtelmann, and C. Conrad. 2016. "Important Variables of a RapidEye Time Series for Modelling Biophysical Parameters of Winter Wheat". *Photogrammetrie-Fernerkundung-Geoinformation* 2016 (5–6): 285–299.

Einzmann, K., M. Immitzer, S. Böck, O. Bauer, A. Schmitt, and C. Atzberger. 2017. "Windthrow Detection in European Forests with Very High-Resolution Optical Data". *Forests* 8 (1): 21.

Foody, G.M. 2002. "Status of Land Cover Classification Accuracy Assessment". *Remote Sensing of Environment* 80 (1): 185–201.

———2004. "Thematic Map Comparison". *Photogrammetric Engineering & Remote Sensing* 70 (5): 627–633.

Förster, M., A. Frick, C. Schuster, and B. Kleinschmit. 2010. "Object-Based Change Detection Analysis for the Monitoring of Habitats in the Framework of the NATURA 2000 Directive with Multi-Temporal

Satellite Data". *The International Archives of the Photogrammetry, Remote Sensing and Spatial Information Sciences* 38: 4.

Gislason, P.O., J.A. Benediktsson, and J.R. Sveinsson. 2006. "Random Forests for Land Cover Classification". *Pattern Recognition Letters* 27 (4): 294–300.

Gómez, C., J.C. White, and M.A. Wulder. 2016. "Optical Remotely Sensed Time Series Data for Land Cover Classification: A Review". *ISPRS Journal of Photogrammetry and Remote Sensing* 116: 55–72.

GRASS Development Team. 2019. *Geographic Resources Analysis Support System (GRASS GIS) Software, Version 7.6*. Open Source Geospatial Foundation. http://grass.osgeo.org.

Houghton, R.A., J.I. House, J. Pongratz, G.R. Van Der Werf, R.S. DeFries, M.C. Hansen, C. Le Quéré, and N. Ramankutty. 2012. "Carbon Emissions from Land Use and Land-Cover Change". *Biogeosciences* 9 (12): 5125–5142.

Huang, C., B. Wylie, L. Yang, C. Homer, and G. Zylstra. 2002. "Derivation of a Tasselled Cap Transformation Based on Landsat 7 At-Satellite Reflectance". *International Journal of Remote Sensing* 23 (8): 1741–1748.

Kauth, R. J., and G. S. Thomas. 1976. "The Tasselled Cap–a Graphic Description of the Spectral-Temporal Development of Agricultural Crops as Seen by Landsat". In *LARS Symposia*, 159.

Kennedy, R.E., Z. Yang, J. Braaten, C. Copass, N. Antonova, C. Jordan, and P. Nelson. 2015. "Attribution of Disturbance Change Agent from Landsat Time-Series in Support of Habitat Monitoring in the Puget Sound Region, USA". *Remote Sensing of Environment* 166: 271–285.

Kennedy, R.E., Z. Yang, and W.B. Cohen. 2010. "Detecting Trends in Forest Disturbance and Recovery Using Yearly Landsat Time Series: 1. LandTrendr—Temporal Segmentation Algorithms". *Remote Sensing of Environment* 114 (12): 2897–2910.

Laliberte, A.S., E.L. Fredrickson, and A. Rango. 2007. "Combining Decision Trees with Hierarchical Object-Oriented Image Analysis for Mapping Arid Rangelands". *Photogrammetric Engineering & Remote Sensing* 73 (2): 197–207.

Leutner, B., and N. Horning. 2018. "RStoolbox: Tools for Remote Sensing Data Analysis". *R Package Version 0.2.4*.

Liu, D., and F. Xia. 2010. "Assessing Object-Based Classification: Advantages and Limitations". *Remote Sensing Letters* 1 (4): 187–194.

Lobser, S.E., and W.B. Cohen. 2007. "MODIS Tasselled Cap: Land Cover Characteristics Expressed through Transformed MODIS Data". *International Journal of Remote Sensing* 28 (22): 5079–5101.

Löw, F., E. Fliemann, I. Abdullaev, C. Conrad, and J.P.A. Lamers. 2015. "Mapping Abandoned Agricultural Land in Kyzyl-Orda, Kazakhstan Using Satellite Remote Sensing". *Applied Geography* 62: 377–390.

Meißner, M., H. Reinecke, S. Herzog, L. Leinen, and G. Brinkmann. 2012. *Vom Wald ins Offenland: Der Rothirsch auf dem Truppenübungsplatz Grafenwöhr. Raum-Zeit-Verhalten, Lebensraumnutzung, Management*. 1. Aufl. Ahnatal: Frank Fornacon.

Millard, K., and M. Richardson. 2015. "On the Importance of Training Data Sample Selection in Random Forest Image Classification: A Case Study in Peatland Ecosystem Mapping". *Remote Sensing* 7 (7): 8489–8515.

Nitze, I., B. Barrett, and F. Cawkwell. 2015. "Temporal Optimisation of Image Acquisition for Land Cover Classification with Random Forest and MODIS Time-Series". *International Journal of Applied Earth Observation and Geoinformation* 34: 136–46.

Pasquarella, V.J., C.E. Holden, L. Kaufman, and C.E. Woodcock. 2016. "From Imagery to Ecology: Leveraging Time Series of All Available Landsat Observations to Map and Monitor Ecosystem State and Dynamics". *Remote Sensing in Ecology and Conservation* 2 (3): 152–170.

Peña, M. A., and A. Brenning. 2015. "Assessing Fruit-Tree Crop Classification from Landsat-8 Time Series for the Maipo Valley, Chile". *Remote Sensing of Environment* 171: 234–244.

Pettorelli, N., J.O. Vik, A. Mysterud, J.-M. Gaillard, C. J. Tucker, and N. C. Stenseth. 2005. "Using the Satellite-Derived NDVI to Assess Ecological Responses to Environmental Change". *Trends in Ecology & Evolution* 20 (9): 503–10.

Planet Labs Inc. 2016. "Satellite Imagery Product Specifications". *Satellite Imagery Product Specifications: Version 6.1*.

R Core Team. 2018. *R: A Language and Environment for Statistical Computing*. R Foundation for Statistical Computing. https://www.R-project.org/.

Raab, C., B. Barrett, F. Cawkwell, and S. Green. 2015. "Evaluation of Multi-Temporal and Multi-Sensor Atmospheric Correction Strategies for Land-Cover Accounting and Monitoring in Ireland". *Remote Sensing Letters* 6 (10): 784–793.

Raab, C., H.G. Stroh, B. Tonn, M. Meißner, N. Rohwer, N. Balkenhol, and J. Isselstein. 2018. "Mapping Semi-Natural Grassland Communities Using Multi-Temporal RapidEye Remote Sensing Data". *International Journal of Remote Sensing* 39 (17): 5638–5659.

Riesch, F., B. Tonn, M. Meißner, N. Balkenhol, and J. Isselstein. 2019. "Grazing by Wild Red Deer: Management Options for the Conservation of Semi-Natural Open Habitats". *Journal of Applied Ecology*.

Riesch, F., H.G. Stroh, B. Tonn, and J. Isselstein. 2018. "Soil PH and Phosphorus Drive Species Composition and Richness in Semi-Natural Heathlands and Grasslands Unaffected by Twentieth-Century Agricultural Intensification". *Plant Ecology & Diversity* 11 (2): 239–253.

Rodriguez-Galiano, V.F., B. Ghimire, J. Rogan, M. Chica-Olmo, and J. P. Rigol-Sanchez. 2012. "An Assessment of the Effectiveness of a Random Forest Classifier for Land-Cover Classification". *ISPRS Journal of Photogrammetry and Remote Sensing* 67: 93–104.

Ruß, G., and A. Brenning. 2010. "Spatial Variable Importance Assessment for Yield Prediction in Precision Agriculture". *Advances in Intelligent Data Analysis IX*, 184–195.

Schmidt, J., F.E. Fassnacht, M. Förster, and S. Schmidtlein. 2017. "Synergetic Use of Sentinel-1 and Sentinel-2 for Assessments of Heathland Conservation Status". *Remote Sensing in Ecology and Conservation*.

Schmidt, T., C. Schuster, B. Kleinschmit, and M. Förster. 2014. "Evaluating an Intra-Annual Time Series for Grassland Classification–How Many Acquisitions and What Seasonal Origin Are Optimal?" *IEEE Journal of Selected Topics in Applied Earth Observations and Remote Sensing* 7 (8): 3428–3439.

Schmidtlein, S., and J. Sassin. 2004. "Mapping of Continuous Floristic Gradients in Grasslands Using Hyperspectral Imagery". *Remote Sensing of Environment* 92 (1): 126–138.

Schönert, M., H. Weichelt, E. Zillmann, and C. Jürgens. 2014. "Derivation of Tasseled Cap Coefficients for RapidEye Data". In *SPIE Remote Sensing*, 92450Q–92450Q. International Society for Optics and Photonics.

Schönert, M., E. Zillmann, H. Weichelt, J.U.H. Eitel, T.S. Magney, H. Lilienthal, B. Siegmann, and T. Jarmer. 2015. "The Tasseled Cap Transformation for RapidEye Data and the Estimation of Vital and Senescent Crop Parameters". *The International Archives of Photogrammetry, Remote Sensing and Spatial Information Sciences* 40 (7): 101.

Schuster, C., M. Förster, and B. Kleinschmit. 2012. "Testing the Red Edge Channel for Improving Land-Use Classifications Based on High-Resolution Multi-Spectral Satellite Data". *International Journal of Remote Sensing* 33 (17): 5583–5599.

Schuster, C., T. Schmidt, C- Conrad, B. Kleinschmit, and M. Förster. 2015. "Grassland Habitat Mapping by Intra-Annual Time Series Analysis–Comparison of RapidEye and TerraSAR-X Satellite Data". *International Journal of Applied Earth Observation and Geoinformation* 34: 25–34.

Song, C., C.E. Woodcock, K.C. Seto, M.P. Lenney, and S.A. Macomber. 2001. "Classification and Change Detection Using Landsat TM Data: When and How to Correct Atmospheric Effects?" *Remote Sensing of Environment* 75 (2): 230–244.

Tyc, G., J. Tulip, D. Schulten, M. Krischke, and M. Oxfort. 2005. "The RapidEye Mission Design". *Acta Astronautica* 56 (1): 213–219.

Ustuner, M., F.B. Sanli, and B. Dixon. 2015. "Application of Support Vector Machines for Landuse Classification Using High-Resolution RapidEye

Images: A Sensitivity Analysis". *European Journal of Remote Sensing* 48 (1): 403–422.

Vanonckelen, S., S. Lhermitte, and A. Van Rompaey. 2013. "The Effect of Atmospheric and Topographic Correction Methods on Land Cover Classification Accuracy". *International Journal of Applied Earth Observation and Geoinformation* 24: 9–21.

Vermote, E.F., D. Tanré, J.L. Deuze, M. Herman, and J.-J. Morcette. 1997. "Second Simulation of the Satellite Signal in the Solar Spectrum, 6S: An Overview". *IEEE Transactions on Geoscience and Remote Sensing* 35 (3): 675–686.

Warren, S.D., and R. Büttner. 2008a. "Relationship of Endangered Amphibians to Landscape Disturbance". *Journal of Wildlife Management* 72 (3): 738–44.

———2008b. "Active Military Training Areas as Refugia for Disturbance-Dependent Endangered Insects". *Journal of Insect Conservation* 12 (6): 671–76.

Wilson, R.T., E.J. Milton, and Joanna M. Nield. 2014. "Spatial Variability of the Atmosphere over Southern England, and Its Effect on Scene-Based Atmospheric Corrections". *International Journal of Remote Sensing* 35 (13): 5198–5218.

Wright, M.N., and A. Ziegler. 2015. "Ranger: A Fast Implementation of Random Forests for High Dimensional Data in C++ and R". *ArXiv Preprint ArXiv:1508.04409*.

Zillmann, E., and H. Weichelt. 2013. "Grassland Identification Using Multi-Temporal RapidEye Image Series". In *MultiTemp 2013: 7th International Workshop on the Analysis of Multi-temporal Remote Sensing Images*, 1-4. IEEE, 2013.

Supporting information to the paper

Raab, C., B. Tonn, M. Meißner, N. Balkenhol and J. Isselstein. "Multi-temporal RapidEye Tasselled Cap data for land cover classification using Random Forests." *European Journal of Remote Sensing.*

Supplementary figures

Figure S1: Probability maps for the GTA derived from the multi-temporal Tasselled Cap RapidEye time series, using the Random Forest classification algorithm.

R code example

Appendix 1: A practical example.

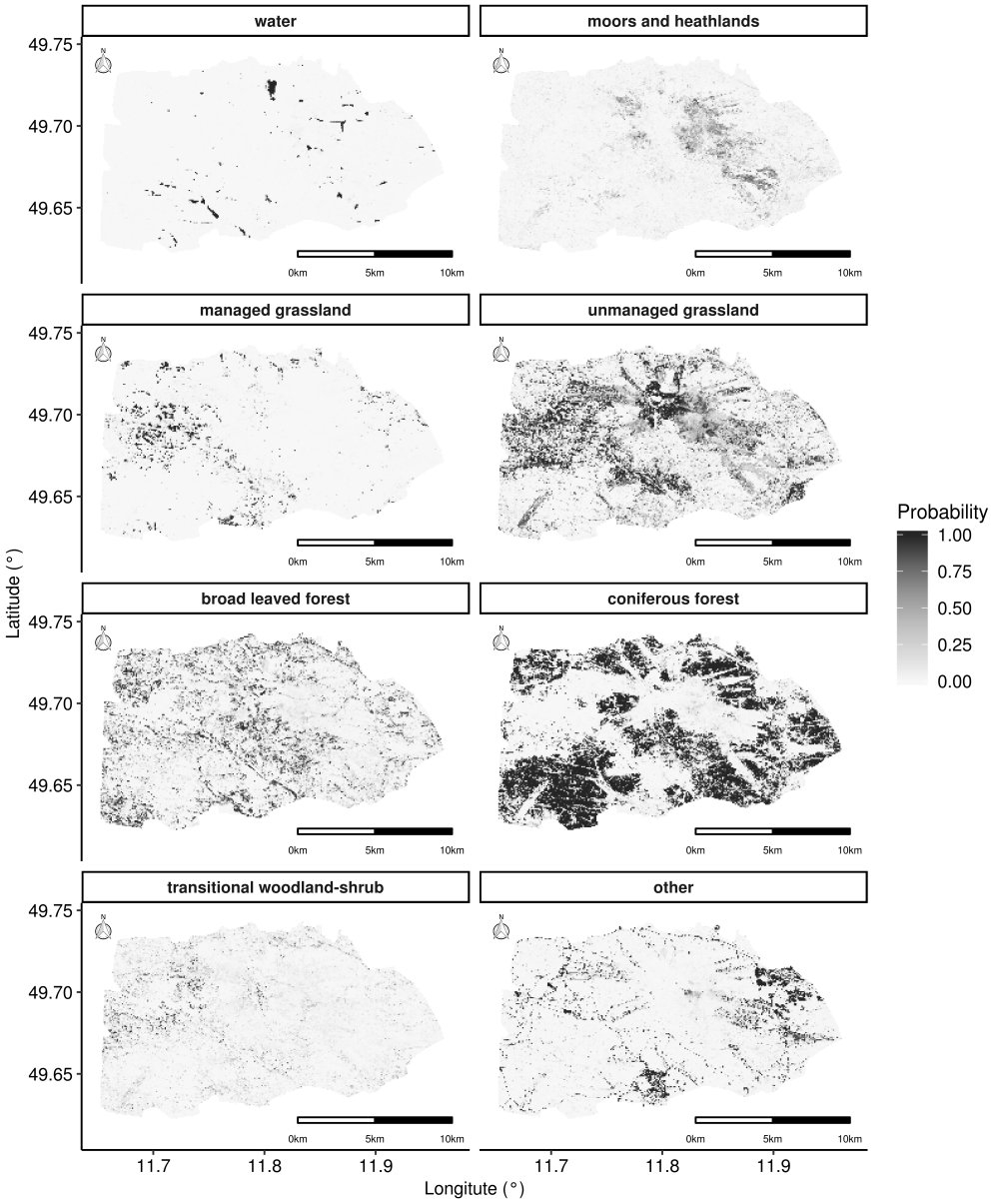

Figure S1: Probability maps for the GTA derived from the multi-temporal Tasselled Cap RapidEye time series, using the Random Forest classification algorithm.

Appendix 1: A practical example

To illustrate how the random forest algorithm can be used for remote sensing classification purposes, we make use of a data set compilation provided by the book "Remote Sensing and GIS for Ecologists: Using Open Source Software" (Wegmann et al., 2016). The data can be accessed under the following URL:

http://book.ecosens.org/data/

The aim of this exercise is to demonstrate how land cover classification can be performed using R.

Data preparation

First we will load the required packages and subsequently the data:

```
library(raster)
library(rgdal)
library(mlr)
library(ranger)
library(RStoolbox)
library(ggplot2)

lsat <- brick("data_book/raster_data/LT52240632011210.tif")

train <- readOGR("data_book/vector_data", "training_2011")
test <- readOGR("data_book/vector_data", "validation_2011")
```

Training data samples

We merge the provided training and testing data set, because we will use the spatial boundaries of both to generate random samples for the model training and validation:

```
train_polygon <- rbind(train,test)
# 500 random points to be generated
```

```
set.seed(123)
train_points <- spsample(train_polygon, type = "random", n = 500)
# spatial overlay between the polygons and generated points
vals <- over(train_points, train_polygon)
# add class name as response column
train_points$response <- vals$class_name


table(train_points$response)
##
##   forest noforest    water
##      360       98       42
```

Visualisation

```
train_points_df <- as.data.frame(train_points)
train_poly_df <- fortify(train_polygon)
ggplot() + Rstoolbox::ggRGB(lsat,
                            r=3,
                            g=2,
                            b=1,
                            stretch = "lin",
                            ggLayer = TRUE)+
  geom_point(data=train_points_df,
             aes(x=x, y=y, color=response))+
  scale_colour_manual(values = c("noforest"="red", "forest"="green",
"water"="blue"))+
  geom_polygon(data= train_poly_df,
               aes(x=long,y=lat, group=group),
               colour="yellow",
               fill=NA)+
  coord_equal()
```

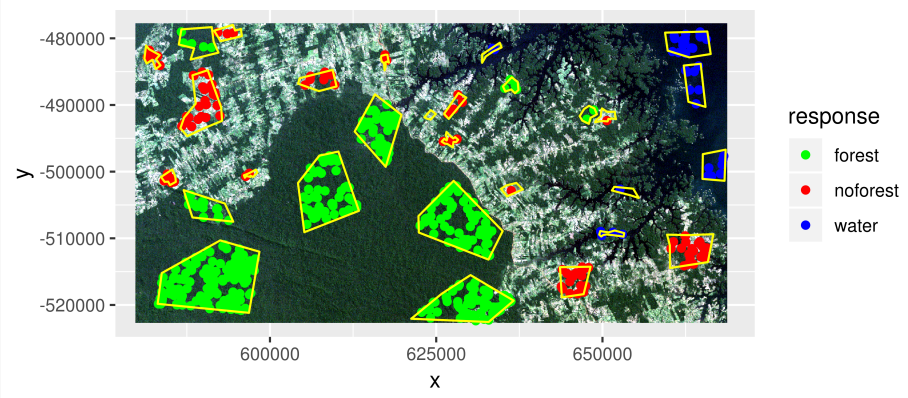

Now we can use the generated samples in order to extract the respective reflectance values recorded by the satellite:

```
train_extracted <- data.frame(extract(lsat,
                              y=train_points,
                              cellnumbers = TRUE,
                              sp=TRUE))

# remove potential dublicates
train_extracted  <- train_extracted [!duplicated(train_extracted$cells), -2]
train_df <- train_extracted[c(1:8)]
train_coordinates <- train_extracted[c(9:10)]
```

Model parameter settings

Here we adjust the parameter setting for the random forest classification model:

```
#number of predictor variables randomly sampled as candidates at each split
mtry <- round(sqrt(length(names(train_df))))
# number of trees to be constructed
num.trees <- 500
# number of folds
k <- 5
# number of repetitions
reps <- 10
```

Model validation

```
# define task and learner
nsp_task <- makeClassifTask(id = "lsat_nsp",
                    data = train_df,
                    target = "response")
# define learner
rf_learner <- setHyperPars(makeLearner("classif.ranger"),
                      par.vals = list(mtry = mtry,
                                      num.trees = num.trees))
#define non-spatial, repeated cross-validation
rdesc = makeResampleDesc("RepCV",
                    reps=reps,
                    folds=k,
                    predict = "test")
```

```
# validation
res_nsp <- mlr::resample(learner = rf_learner,
                         task = nsp_task,
                         resampling = rdesc,
                         measures = list(
                           setAggregation(acc, test.mean),
                           setAggregation(acc, test.sd),
                           setAggregation(kappa,test.mean),
                           setAggregation(kappa,test.sd)),
                         models = FALSE,
                         show.info = FALSE)

res_nsp$aggr
##   acc.test.mean     acc.test.sd kappa.test.mean   kappa.test.sd
##      0.91660000      0.02200278      0.80656936      0.05586579
```

Prediction

After the model performance was evaluated using cross-validation we apply the model to each pixel, in order to generate a classified land cover map.

```
# get predictor variable names
ff <- names(train_df)[c(2:8)]

# create formula for the random forest model
fo <- as.formula(paste("response ~", paste(ff, collapse="+")))

# model paramters
ntree <- 500
mtry <- round(sqrt(length(ff)))

# construct predictive model
rf_model <- ranger(formula = fo,
                   data=train_df,
                   mtry=mtry,
                   num.trees = ntree,
                   num.threads = 1,
                   classification=TRUE,
                   write.forest = TRUE,
                   probability=FALSE)
```

```
#https://stackoverflow.com/questions/46354103/image-classification-raster-stack-with-random-forest-package-ranger

lsat_prediction <- predict(lsat,
                           rf_model,
                           type='response',
                           num.threads=1,
                           progress = 'text',
                           fun = function(model, ...) predict(model, ...)$predictions)
# save prediction result
res <- writeRaster(lsat_prediction, "lsat_prediction")
hdr(res, format = "ENVI")
rm(res)
```

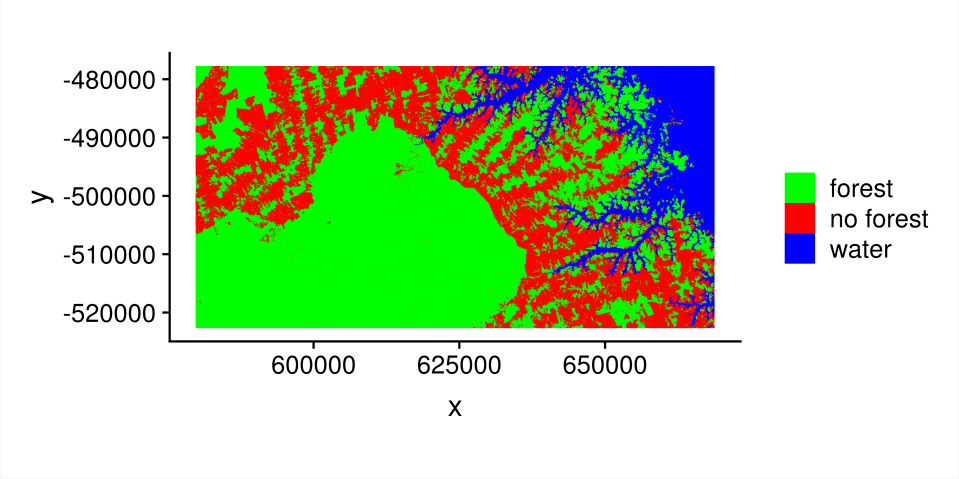


```
library(rasterVis)

cols <- c("A" = 'green', "B" = 'red', "C" = 'blue')

gplot(lsat_prediction,length(values(lsat_prediction))) +
  geom_raster(aes(fill=factor(value, labels=c("A", "B", "C"))))+
  scale_fill_manual(values = cols,
                    breaks = c("A", "B", "C"),
                    labels = c("forest", "no forest", "water"),
                    name= " ")+
  coord_equal()
```

References

Wegmann, M., Leutner, B., Dech, S., 2016. “Remote Sensing and GIS for Ecologists: Using Open Source Software.” *Pelagic Publishing Ltd.*

3

CHAPTER 3 – MAPPING SEMI-NATURAL GRASSLAND COMMUNITIES USING MULTI-TEMPORAL RAPIDEYE REMOTE SENSING DATA

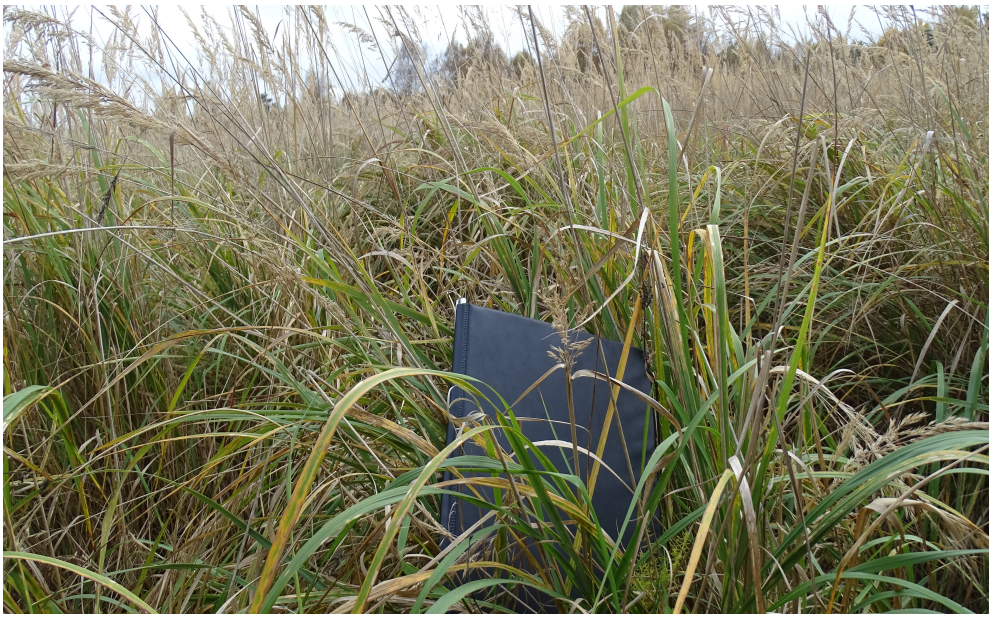

This chapter is published as:

Raab, C., H-G. Stroh, B. Tonn, M. Meißner, N. Rohwer, N. Balkenhol, J. Isselstein. 2018. "Mapping semi-natural grassland communities using multi-temporal RapidEye remote sensing data". *International Journal of Remote Sensing*. 39, 5638–5659.

Abstract

Mapping semi-natural grassland has become increasingly important with regard to climate variability, invasive species, and the intensification of land use. At the same time, adequate field data collection is of pivotal importance for national and international reporting obligations, such as the European Habitats Directive. We present a remote-sensing-based monitoring framework for a Natura 2000 site with a heterogeneous composition of different grassland communities, using the Random Forest algorithm. Automated training data selection was successfully implemented based on the Random Forest proximity measure (Overall Accuracy ranging from 77.5-86.5%). RapidEye acquisitions originating from onset of vegetation (prespring and first spring) and senescence (late summer and first autumn) were identified as important phenological phases for mapping semi-natural grassland communities. The derived probability maps of occurrences for each grassland class captured transitions between grassland communities and are therefore a better approximation of real world conditions compared to classical, discrete maps.

Keywords: European Habitats Directive, monitoring, Random Forest, proximity, training data, variable importance, probability maps

Introduction

Semi-natural grasslands are habitats with high biodiversity (Dengler et al., 2014). They are characterised by indigenous, naturally occurring plant communities which have not been substantially modified, e.g. by sowing or fertilization. Unlike natural grassland, semi-natural grasslands have their origin in human activities, such as mowing or grazing, and depend on active management for their conservation (Peeters et al., 2014). Mapping and monitoring these habitats with their structural and botanical heterogeneity at very fine scales is a challenging task, but becomes increasingly relevant with regard to intensification of land use, land abandonment, climate variability and invasive species (Stenzel et al., 2014; Wachendorf et al., 2017). National and international nature conservation and management activities, such as the European Habitats Directive (Council Directive 92/43/EEC 1992) may even impose legal obligations to set up a monitoring framework for grasslands (Borre, et al., 2011). Typically, grassland habitats are mapped and monitored through field surveys, which are time- and labour-intensive. In addition, they are difficult to reproduce, prone to subjective interpretation in the field, and in some cases limited by access restrictions. Remote-sensing-based mapping and monitoring offer unique possibilities to derive spatially-explicit vegetation maps on large geographical areas using automated process chains (Borre et al., 2011; Buck et al., 2013; Nagendra et al., 2013; Stenzel et al.,

2014; Corbane et al., 2015). Thus, remote-sensing-derived products can easily be updated on regular intervals.

The availability of remote sensing platforms applicable for land monitoring has experienced a tremendous boost since the 1970s (Belward and Skøien, 2015). The increased amount of remote sensing images, however, requires effective supervised machine learning algorithms, such as Support Vector Machines (Cortes and Vapnik, 1995; Mountrakis et al., 2011) or Random Forests (Breiman, 2001; Belgiu and Drăguț, 2016) to extract relevant information from high-dimensional spectral data. The Random Forest classifier can be described as an ensemble of decision trees, from which the prediction is drawn by a majority vote. In contrast to Maximum Likelihood classifiers, no assumptions about the distribution of the data are required for the non-parametric Random Forest. Moreover, the Random Forest algorithm is insensitive to overfitting and its good performance for mapping vegetation has been demonstrated in several studies (Gislason et al., 2006; Cutler et al., 2007; Rodriguez-Galiano et al., 2012; Feilhauer et al., 2014; Barrett et al., 2016; Maxwell et al., 2018).

All supervised machine learning algorithms require a set of training data, which adequately represent the spectral characteristics of targeted vegetation classes. The training sampling strategy impacts classification accuracy and often leads to either over- or underrepresentation of classes in the final map (Millard and Richardson, 2015; Ustuner et al., 2016). Manual training sample selection is a time-consuming and subjective task (Rocchini

et al., 2013), and so is the collection of test samples in the field, especially at transitions between different vegetation cover types.

Automated training data generation, derived e.g. from existing reference maps, can be a potential solution to maintain objectivity in a cost- and labour-efficient way. For this, robust computer algorithms are needed to screen the initial training data set for incorrectly labeled samples, also called outliers. The Random Forest proximity of two training samples is a function of the ratio between the number of trees in which both samples share the same terminal node and the total number of trees in the forest (Belgiu and Drăguț, 2016). As pointed out by Gislason et al. (2006), Verikas et al. (2011) and Touw et al. (2012), this measure can be used to detect and consequently exclude outliers in a training data set. Thus, by using the Random Forest proximity measure, uncertainties (e.g. at the transition between two vegetation communities) introduced by the training data sampling strategy or reference field mapping can be reduced.

In addition to the training data sampling design, the acquisition time of remote sensing data can be seen as an important factor influencing the quality of the mapping result (Nitze et al., 2015). Multi-seasonal remote sensing time series can support the discrimination of spectrally very similar land cover types, such as semi-natural grassland types, by incorporating temporal characteristics (Schmidt et al., 2014). The identification of important temporal windows for classifying land cover types is not only of

value to decrease model complexity and computation intensity, but also allows for a very targeted study design.

In this article, we explore the use of multi-annual, multi-seasonal remote sensing data combined with the Random Forest machine learning algorithm to discriminate semi-natural grassland communities identified by field mapping. The aims of this study were to:

- develop a framework to automatically derive training data by reducing uncertainties introduced by field mapping and sampling strategy,
- map the probability of spatial occurrence of different grassland communities,
- identify phenological seasons supporting the discrimination of different grassland communities.

The work was divided into a field mapping and data pre-processing part followed by the training data selection process. For each grassland class, the probability of occurrence was derived. Finally, permutation-based variable importance (Ruß and Brenning, 2010) were calculated. The presented processing framework will help to improve current and future mapping and monitoring obligations, such as required by the European Habitats Directive.

Materials and Methods

In this section, we provide an introduction to the study area and field mapping process, followed by our main study aim: automated selection of

training data. In addition, we present how the derived training data can be applied for mapping the probability of occurrence of grassland at community level. Important temporal windows for mapping semi-natural grassland are estimated using a permutation based approach. A conceptual overview of methods applied in this manuscript is given in Figure 1.

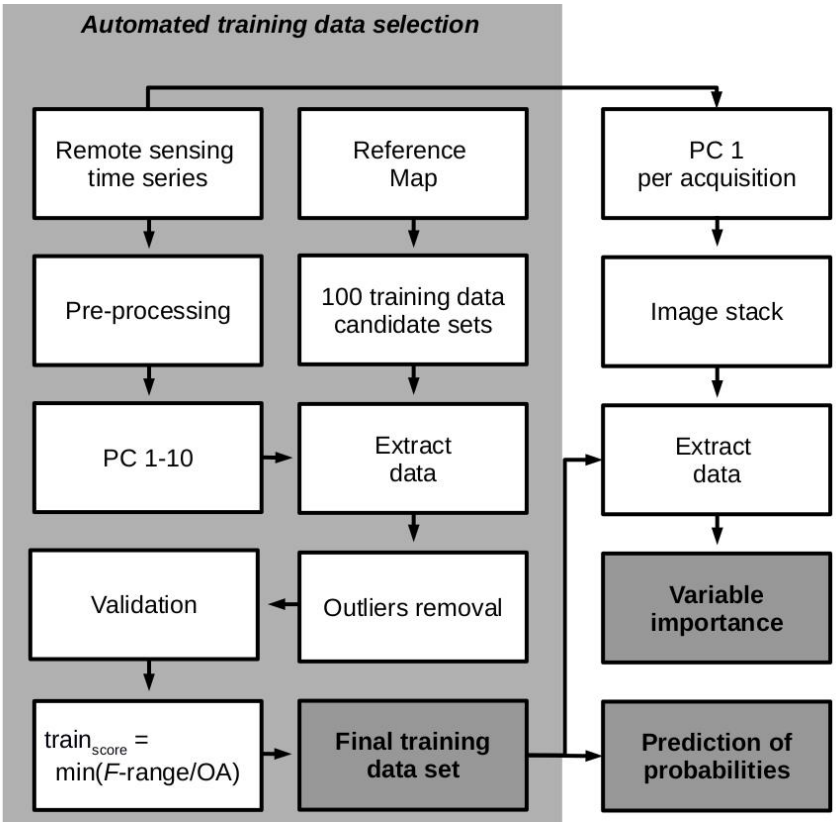

Figure 1: Schematic illustration of the automated training data selection process highlighted by a gray box. The right part of this figure emphasises the application of the derived training data set to calculate spatially explicit probability maps and to identify important phenological seasons for the discrimination of different grassland communities.

Study area

The Grafenwoehr military training area (GTA) is located in the south-east of Germany (Bavaria) and lies at about 445 m above sea level in the natural region Upper Palatine-Upper Main Hills (Figure 2). Long-term

annual averages of temperature and precipitation are 8.3 ± 0.04 °C and 701 ± 4 mm, respectively (1981-2010, mean ± SEM, of four weather stations of the German Weather Service (DWD, Deutscher Wetterdienst) in the immediate vicinity). The GTA extends about 223 km². Roughly 85% are part of the Natura 2000 network and contain numerous rare and highly protected habitat types, forming a refuge for many endangered species (Warren and Büttner, 2008a, 2008b; Riesch et al., 2018). About 130 km² of the GTA are covered with forest and around 63 km² with semi-natural grasslands. The majority of the open areas are mown or mulched once per year between July and August. Fire and wildlife grazing, especially by red deer (*Cervus elaphus*), also play a role in some of these areas (Meißner et al., 2012).

In order to demonstrate the feasibility of monitoring semi-natural grassland communities via remote sensing in areas with limited access, we focused on two study sites, Sommerhau and Hoehenberg. Situated in the north of the GTA (Figure 2), about 71 ha of the total Hoehenberg site can be described as heterogeneous grassland, surrounded by forest. The northern two thirds of the Hoehenberg site consist of a plain, underlain by Keuper sandstone, with only slight differences in the relief. Parts of the area are mulched once a year around the middle of July, mainly for fire safety reasons.

In contrast, the Sommerhau site is situated in the western part of the GTA (Figure 2). This area of about 140 ha is characterised by a mixture of grassland, fallow land and hedgerows, mainly underlain by more or less

calcareous rock. In addition to some smaller forest stands, a larger continuous forested area can be found in the south. Compared to the Hoehenberg site, more anthropogenic infrastructure is present and the management regime includes mowing once a year around the middle of July.

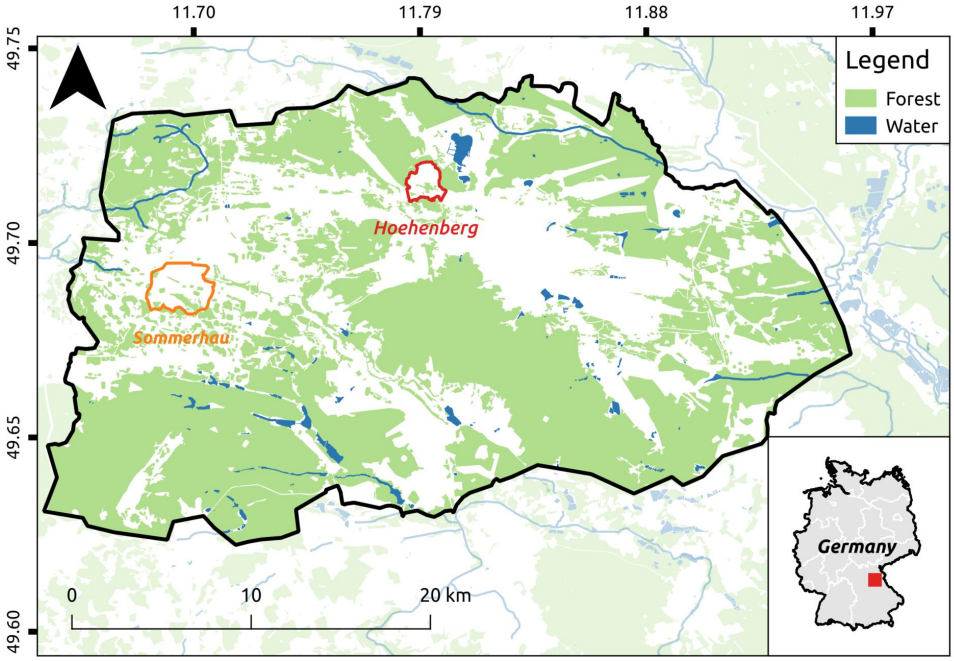

Figure 2: Location of the two study sites Sommerhau (orange) and Hoehenberg (red) in the Grafenwoehr military training area. The location of the study site in Germany is marked with a red square. The map is based on data provided by ©OpenStreetMap contributors.

Field mapping

Field data were collected at the two study sites between 2015 and 2017, mainly during summer. The collection of field data was limited by access restrictions due to military training activities. Even though geographical (Figure 2) and management differences exist, a large quantity of the same common species can be found in both study sites. The field data collection aimed to derive vegetation units based on floristic composition as

well as on dominance of individual species and structural properties. To this end, reference relevés were surveyed according to the EU Habitats Directive habitat types of Bavaria (BayLFU, 2012). A selection of plant sociological literature aided the mapping process to adequately depict special local habitat types (Dierschke, 1997; Dierschke and Briemle, 2002; Burkart et al., 2004), as a restriction to the units in the Habitat Directive would have led to an inadequate depiction of unlisted local habitat types. Vegetation units (communities) were formed based on the surveyed reference plots and are outlined in Table 1 and Table 2, respectively. To derive a spatial grassland community map for each site, spatial boundaries were drawn according to the collected relevés data and visual interpretation in the field. This was supported by an aerial image taken during the midsummer season.

Table 1: Mapped grassland communities and share of total area for Sommerhau in percentage (%).

ID	Description	Share (%)
SG1	**Mown grassland dominated by short grasses (< 40%) - pasture-like lowland hay meadow**	**39.4**
SG11	Species-rich pasture-like lowland hay meadow**,** cover of *Trifolium repens* < 10%	16.0
SG12	Species-rich pasture-like lowland hay meadow, cover of *Trifolium repens* > 10%	22.0
SG13	Species-rich o pasture-like lowland hay meadow with species of dry calcerous grassland	0.5
SG14	*Lolium-perenne-Trifolium repens* pasture**,** cover of *Trifolium repens* >10%	1.0
SG2	**Mown grassland dominated by tall grasses (> 40%) - typical lowland hay meadow**	**35.4**
SG21	Species-rich lowland hay meadow**,** cover of *Trifolium repens* <10%	19.1
SG22	Species-rich lowland hay meadow with nutrient indicator species**,** cover of *Trifolium repens* >10%	7.3
SG24	Species-rich or species-poor, disturbed lowland hay meadow	3.9
SG25	Species-rich lowland hay meadow with high cover of ruderal species	5.0
SB	**Fallow grassland**	**25.2**
SB10	Species-rich grassland fallow land, mesophilic sites	12.1
SB30	Species-poor grassland fallow land, mesophilic sites	11.3
SB40	Grassland fallow land, wet to dry locations	1.7
	Total area	138.4 ha

Table 2: Mapped grassland communities and share of total area for Sommerhau in percentage (%).

ID	Description	Share (%)
HM1	**Vegetation dominated by short grasses, cover of tall grasses < 15%**	**47.1**
HM11	Species-rich *Festuca-rubra-Agrostis capillaris* meadow	13.9
HM12	Species-rich *Festuca-rubra-Agrostis capillaris* meadow, with grazing indicators	9.6
HM14	Species-rich *Festuca-rubra-Agrostis capillaris*, transition to *Nardus* grassland	20.9
HM15	Species-rich *Festuca-rubra-Agrostis capillaris* meadow, transition to oligotrophic siliceous grassland	2.8
HM2	**Vegetation dominated by tall grasses >20%**	**27.5**
HM21	Species-rich meadow-like grassland	27.5
HM3	***Nardus* grassland**	**1.9**
HM30	*Nardus* grassland, cover of *Calluna vulgaris* < 30%	1.9
HM4	**Oligotrophic siliceous grassland**	**0.9**
HM40	Oligotrophic siliceous grassland	0.9
HB	**Fallow grassland**	**22.5**
HB50	*Calamagrostis-epigejos*-dominated	7.5
HB60	*Molinia* meadows, *Molinia caerulea* > 40%	8.1
HB70	Eutrophic wet grasslands, *Cyperaceae* > 50%	6.9
	Total area	71.0 ha

Satellite data and pre-processing

We acquired a multi-annual RapidEye time series (2014 - 2017) of 17 images (Table 3) with different temporal coverage for the Sommerhau and Hoehenberg sites. The processing level 3A that was used is already radiometrically, geometrically, and sensor corrected, and is delivered as 25 by 25 km tiles (ID-3262023).

Launched in 2008, the RapidEye satellite constellation consists of five identical satellites with a theoretically daily off-nadir recording interval

(5.5 days at nadir) (Tyc et al., 2005). The high spatial resolution of 6.5 m pixel size is resampled to 5 m during the ortho-rectification by the data-provider. In addition to the visible part of the electromagnetic spectrum, blue (440-510 nm), green (520-590 nm) and red (630-685 nm), the RapidEye satellites acquire top-of-atmosphere radiation in the rededge (690-730 nm) and near-infrared (NIR, 760-850 nm) part.

Temporal differences of phenological phases across years are a challenge when working with multi-annual time series remote sensing data (Schmidt et al., 2014). Climate and local weather conditions affect the entry times of vegetation stages (phenological phases/seasons), therefore two satellite images from the same date but different years covering the study area may capture different phenological seasons. To account for this, Foerster et al. (2012) introduced a correction approach, which was successfully applied on multi-annual RapidEye data by Schmidt et al. (2014). To consider shifts in the phenology, we used observations of plant phenological seasons from the DWD, within a buffer distance of up to 30 km from the GTA centroid, to calculate the average entry time of each phenological season (Table 3) for the years 1951-2013. To estimate the deviation of each study year 2014-2017 from the long-term recordings, the averaged values were fitted to actual phenological observations of the respective year, using a third order polynomial (Schmidt et al., 2014). Based on these models, we calculated an adjusted Julian day of the year from the actual image acquisition dates (Table 3).

Table 3: Multi-annual RapidEye time series ordered by adjusted DOY (Julian day of the year). Study sites: Hoehenberg (H) and Sommerhau (S).

No	Acquisition date	Study site	Actual DOY	Adjusted DOY	Phenological phase
1	14 March 2016	H,S	74	88	
2	18 March 2015	S	77	89	Prespring (PSP), DOY 71-102
3	18 March 2016	H,S	78	91	
4	27 March 2017	H	86	95	
5	2 April 2014	H,S	92	114	
6	20 April 2016	H,S	111	119	First spring (FIS), DOY 103-131
7	17 April 2014	H,S	107	127	
8	22 Mai 2016	H,S	143	149	Full spring (FUS) DOY 132-158
9	26 Mai 2017	H	146	154	
10	11 June 2017	H,S	162	169	Early summer (ESU), DOY 159-179
11	8 June 2014	H,S	159	174	
12	24 June 2016	H,S	176	183	Midsummer (MSU), DOY 180-120
13	1 August 2016	H,S	214	221	Late summer (LSU), DOY 121-244
14	5 August 2015	H,S	217	227	
		-			Early autumn (EA), DOY 245-266
15	28 September 2014	S	271	277	Full autumn (FA), DOY 267-284
16	12 October 2015	H,S	285	287	Late autumn (LA), DOY 285- 305

All images were reprojected to the German DHDN/3-degree Gauss-Kruger zone 4 (EPSG:31468) reference system and co-registered (RMSE ≤ 0.5). Image correction included the transformation of raw Digital Numbers (DN) to radiance and top-of-atmosphere-reflectance (Planet Labs Inc, 2016). Atmospheric correction was performed using the Second Simulation of Satellite Signal in the Solar Spectrum (6S) (Vermote et al., 1997) algorithm, as implemented in the *i.atcorr* function in the open source Geographic Resources Analysis Support System (GRASS GIS) version 7.2 (GRASS

Development Team, 2017). To account for distortions introduced by the topography, a C-factor correction (Teillet et al., 1982) was applied using a sun illumination model derived from the European Digital Elevation Model (EU-DEM), version 1.1 (25 m spatial resolution).

Training data sampling

The training data selection was performed in a fully automated process chain, illustrated as a generalised flow chart in Figure 1. The key elements of the proposed procedure include a stratified random sampling based on a reference map (derived as described in section 2.2), the removal of potential outliers followed by validation and the selection of a final training data set.

As recommended by Colditz (2015), training points were randomly allocated proportional to the area covered by each class in the respective reference map (Figure 3). Since we converted each pixel location into one point, no double sampling was possible. In addition, all non-grassland pixels were manually excluded from the study in advance by visual interpretation. To prevent a low representation of rare grassland communities, the minimum amount of training samples per class was set to 1% of the total number of training points (Colditz, 2015). The total number of samples for each initial training data candidate set per study site was set to 15% of available pixels (8,453 pixels for Sommerhau and 4,261 for Hoehenberg).

We repeated the random sampling 100 times, resulting in 100 initial training data candidate sets.

To reduce the complexity and to save calculation time, a Principal Component Analysis (PCA) was carried out for both study sites using all data available in the respective multi-seasonal RapidEye time series. Subsequently, the initial training data candidate sets were used to extract the first ten Principal Component (PC) bands (PC1-10), explaining about 96% of the time series data for both Sommerhau and Hoehenberg.

Potential outliers were excluded based on the sample proximity measurement provided by the Random Forest (Breiman, 2001; Gislason et al., 2006). The reduction of the 100 initial training data candidate sets was carried out using the function *rfOutliers* (threshold = 10) implemented in the *CORElearn package* (Robnik-Šikonja et al., 2017) in R (R Core Team, 2017).

To estimate the performance of each reduced training data candidate set we applied a 5-fold cross-validation approach with 100 repetitions using the *mlr* package (Bischl et al., 2016) and the Random Forest algorithm implemented in the *ranger* package (Wright and Ziegler, 2015). In this study, all Random Forest models were constructed with 500 trees (num.trees) with the number of variables randomly sampled as candidates at each split (mtry) set to the square root of the number of input variables (Belgiu and Drăguț, 2016).

The decision for the final training data set was based on the ratio of overall accuracy and the range of a class-specific performance measure (*F*-score). The *F*-score is calculated as the harmonic mean of user's and producer's accuracy, derived from the confusion matrix. The used range refers to the respective *F*-score values for all considered classes. This $train_{score}$ ratio measure was chosen in order to ensure a balance between class-related accuracy and overall performance.

Spatial probability of occurrence

Instead of classifying each pixel into discrete grassland classes, we used the final training data set for each study site to predict the spatial probability of occurrence for each class (Malley et al., 2012). Due to its randomness, a constructed Random Forest model is always unique and would slightly differ from a second model that is constructed from the same data with the same settings. To account for these uncertainties, we averaged the predicted probabilities of 100 Random Forest models. The probabilities were predictions using the first ten PC bands of the respective RapidEye time series.

Variable importance

To determine which image acquisition dates (Table 3) are most relevant for estimating the spatial distribution of semi-natural grassland communities, we calculated permutation-based variable importance, recorded as an increase in classification error caused by excluding one

variable and keeping the rest in the model. Thus, important dates contributing to model performance can be estimated. For this purpose, we compressed the main variance of all five bands of each image from the multi-seasonal RapidEye time series by extracting only the first Principal Component (PC1) per acquisition. On average, about 73% (sd = 6.5) of variance was explained by the first PC for Sommerhau and 84% (sd = 10.2) for Hoehenberg. Permutation was embedded in an additional cross-validation procedure with 100 repetitions, repeated 100 times on fold level, using the *mlr* and *ranger* packages.

Results

Field mapping

The field mapping revealed a high diversity of grassland communities for both study sites. Results of the field mapping are displayed in Figure 3. The mapped communities are outlined in Table 1 for Sommerhau and in Table 2 for Hoehenberg. The highest proportion of the Sommerhau site was covered with mown grassland dominated by short grasses (39.4%, SG11-SG14). The grassland class boundaries mostly followed the management (e.g. mowing). Fallow grassland classes could be found in the northern and western part, covering about one quarter of the area (SB10-SB40). In contrast, a much more heterogeneous mosaic of less intensively managed grassland communities could be found in the Hoehenberg site. Short-grass dominated areas covered about one half of the

site (HM11-HM15). With about 27%, stands dominated by tall grasses (HM21) were the most widespread class, occurring mainly in the northern two thirds of the area.

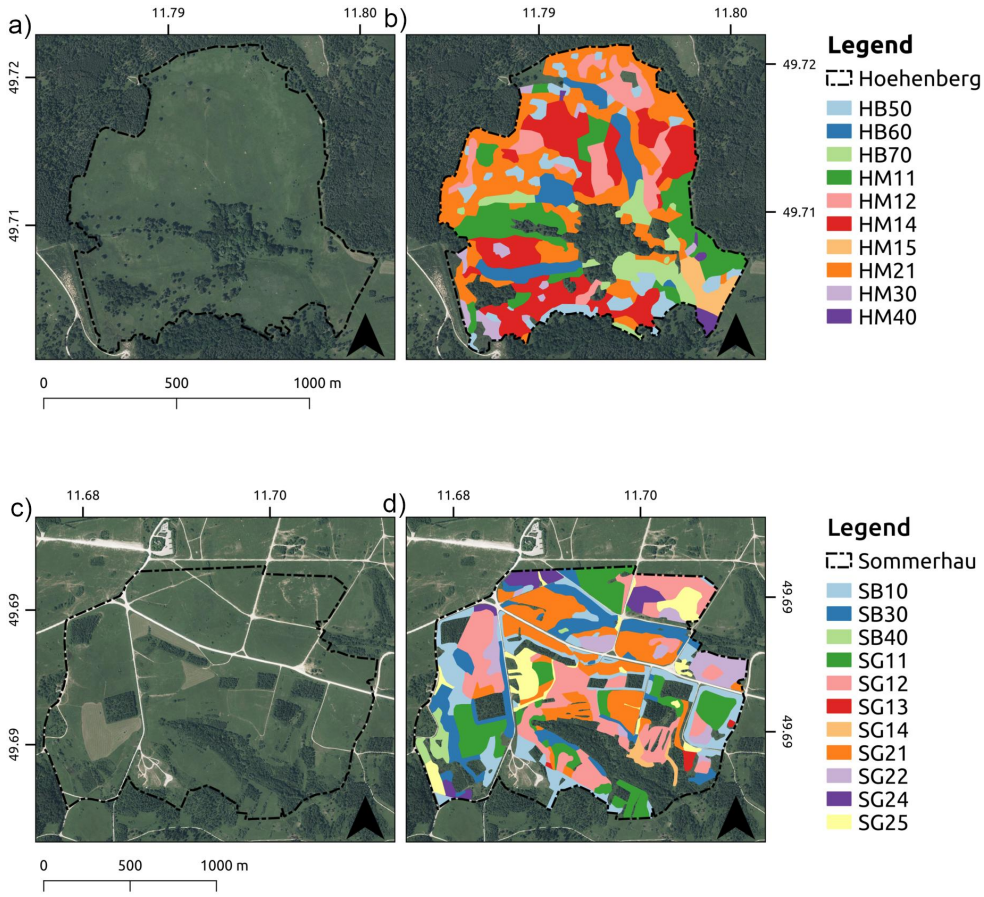

Figure 3: Aerial image (24 June 2016) of the Hoehenberg a) and Sommerhau c) (geodata based on: Bayerische Vermessungsverwaltung, 2018). The result of field vegetation mapping for Hoehenberg b) and Sommerhau d). Explanations of the legend items can be found in Table 1 and Table 2.

Training data sampling

Using a proportional training data selection strategy along with a Random Forest proximity-based outliers detection, the mean number of points remaining in each of the 100 reduced training data candidate sets

were 6,350 (sd = 134) points for Sommerhau and 3,331 (sd = 82) for Hoehenberg. On average 2,147 (sd = 133) outliers were excluded from the initial training data candidate sets for Sommerhau and 932 (sd = 83) for Hoehenberg. A detailed overview of class-specific values for both sites are outlined in Table 4 and Table 5, respectively. No outliers were detected for the classes SG12 and SG14, as well as for HM30 and HM40.

Table 4: Results of the training data sampling procedure for all classes (Table 1) of the Sommerhau site, reported as the amount of points per class. The performance is given by the harmonic mean of user's and producer's accuracy (*F*-score). sd = standard deviation.

	SB10	**SB30**	**SB40**	**SG11**	**SG12**	**SG13**	**SG14**	**SG21**	**SG22**	**SG24**	**SG25**
Mean number of points	647	690	133	1049	1449	84	84	1164	445	231	374
sd	21	16	3	18	20	-	-	21	12	9	14
Mean number of outliers	357	260	8	279	373	-	-	418	164	96	192
sd	21	16	3	18	20	-	-	21	11	9	14
Mean *F*-score	82.2	80.6	68.3	92.4	87.4	77.6	66.0	88.3	81.3	86.8	86.1
sd *F*-score	1.3	1.0	3.7	0.6	0.6	2.9	4.6	0.7	1.6	1.6	1.2
Number of points of the selected training set	663	688	134	979	1400	84	84	1171	443	203	356
Number of detected outliers points of the selected training set	341	256	6	306	422	-	-	411	166	108	209
***F*-score of the selected training set**	84.9	82.2	73.1	92.5	87.3	77.7	73.6	89.5	77.6	86.4	86.2
sd *F*-score of the selected training set	0.6	0.5	2.1	0.3	0.3	2.0	2.7	0.3	1.0	1.0	0.8

Table 5: Results of the training data sampling procedure for all classes (Table 2) of the Hoehenberg site, reported as the amount of points per class. The performance is given by the harmonic mean of user's and producer's accuracy (*F*-score). sd = standard deviation.

	HB50	**HB60**	**HB70**	**HM11**	**HM12**	**HM14**	**HM15**	**HM21**	**HM30**	**HM40**
Mean number of points	215	280	256	412	353	676	113	901	82	43
sd	10	7	5	15	8	16	2	19	-	-
Mean number of outliers	104	65	39	179	55	214	4	272	-	-
sd	10	7	5	15	8	16	3	19	-	-
Mean *F*-score	78.3	86.8	85.2	78.9	68.6	76.5	83.4	77	68.7	79.4
sd *F*-score	2.8	1.7	1.8	2.0	2.2	1.5	2.6	1.0	4.4	4.0
Number of points of the selected training set	206	286	251	431	349	671	115	916	82	43
Number of detected outliers points of the selected training set	113	59	44	157	59	219	2	255	-	-
***F*-score of the selected training set**	77.7	84.9	83.3	79.2	73.6	72.7	83.5	76.8	74.5	81.7
sd *F*-score of the selected training set	1.0	0.7	0.9	0.9	1.0	0.8	1.2	0.4	2.4	2.7

The average estimated performance of the 100 reduced training data candidate sets in terms of overall accuracy was about 9% higher for the Sommerhau (OA = 86%, Kappa = 0.84) compared to the Hoehenberg (OA = 78%, Kappa = 0.73) site (Table 6). The average *F*-score range was 8% higher for the Sommerhau compared to the Hoehenberg site.

Table 6: Results of 5-fold cross-validation with 100 repetitions of the 100 reduced training data candidate sets and the selected training data set. OA = overall accuracy, sd = standard deviation, *F*-range = range of class-specific *F*-scores.

	OA	**OA sd**	**Kappa**	**Kappa sd**	***F*-range**	***F*-range sd**	***F*-range/OA**
Sommerhau selected training set	86.5	0.2	0.84	0.0027	20.1	2.1	0.23
Sommerhau mean of all models	86	0.4	0.84	0.005	27.9	6.7	0.32
Hoehenberg selected training set	77.5	0.4	0.73	0.0045	12.2	1.4	0.16
Hoehenberg mean of all models	78	0.7	0.73	0.0088	20.1	3.2	0.26

The final training data set for all subsequent calculations was determined by the lowest *F*-score range:OA ratio. For Sommerhau the best training set in terms of this ratio resulted in an OA of 86.5% (sd = 0.2). A lower value was obtained for the Hoehenberg data set (OA: 77.5%, sd = 0.4). In comparison to the respective mean values of all training sets, the selected sample sets showed more balanced *F*-score values.

The cross-validated confusion matrix of the Random Forest classification applied on PC1-10 data of the RapidEye time series yielded good class-specific results for Sommerhau (Table 7) and Hoehenberg (Table 8). The lowest user's and producer's accuracies were estimated for relatively rare classes, such as HM40 and SG14.

Table 7: Confusion matrix of grassland communities classified by Random Forest applied on the first ten Principal Component bands of the Sommerhau RapidEye time series. Data is averaged over 100 cross-validation repetitions.

		Reference												
		SB10	SB30	SB40	SG11	SG12	SG13	SG14	SG21	SG22	SG24	SG25	**Total**	User's accuracy
Prediction	SB10	564	62	14	1	0	6	0	11	0	2	4	**664**	0.85
	SB30	74	596	38	0	0	1	0	41	1	1	3	**755**	0.79
	SB40	1	2	82	0	0	0	1	0	0	0	0	**86**	0.94
	SG11	12	7	0	943	33	1	6	5	3	5	2	**1017**	0.93
	SG12	0	1	0	68	1273	8	22	26	63	21	35	**1517**	0.84
	SG13	0	0	0	0	1	56	1	0	0	0	2	**60**	0.93
	SG14	0	0	0	0	3	0	51	0	0	0	0	**54**	0.94
	SG21	11	23	0	3	31	4	0	1068	61	10	5	**1216**	0.88
	SG22	0	0	0	0	29	0	0	19	312	0	3	**363**	0.86
	SG24	0	0	1	1	10	0	0	1	0	177	1	**191**	0.93
	SG25	0	2	0	5	19	7	2	1	2	3	302	**343**	0.88
	Total	**662**	**693**	**135**	**1021**	**1399**	**83**	**83**	**1172**	**442**	**219**	**357**		
	Producer's accuracy	0.85	0.86	0.61	0.92	0.91	0.67	0.60	0.91	0.71	0.81	0.85		

Table 8: Confusion matrix of grassland communities classified by Random Forest applied on the first ten Principal Component bands of the Hoehenberg RapidEye time series. Data is averaged over 100 cross-validation repetitions.

		Reference											
		HB50	HB60	HB70	HM11	HM12	HM14	HM15	HM21	HM30	HM40	**Total**	User's accuracy
Prediction	HB50	145	0	4	1	0	14	0	2	1	0	**167**	0.86
	HB60	4	234	9	1	1	3	0	12	0	0	**264**	0.88
	HB70	4	12	201	2	0	0	0	10	0	0	**229**	0.87
	HM11	2	1	1	320	1	24	6	12	6	2	**375**	0.85
	HM12	5	10	0	2	250	28	1	33	1	0	**330**	0.76
	HM14	10	4	1	45	29	473	6	55	9	0	**632**	0.75
	HM15	3	0	0	2	0	2	92	0	1	4	**104**	0.88
	HM21	31	25	34	56	66	126	6	794	9	0	**1147**	0.69
	HM30	1	0	0	2	2	1	0	0	53	1	**60**	0.88
	HM40	0	0	0	2	0	0	3	0	2	35	**42**	0.83
	Total	**205**	**286**	**250**	**433**	**349**	**671**	**114**	**918**	**82**	**42**		
	Producer's accuracy	0.70	0.82	0.80	0.74	0.72	0.71	0.80	0.86	0.65	0.81		

In addition, we analysed the spatial characteristics of the excluded outliers summed up for all initial training data candidate sets, illustrated as a density raster in Figure 4. For both sites, core areas with no outliers can be observed. The density of outliers for the Sommerhau site followed the spatial patterns of infrastructure, e.g. roads. Both cases provide evidence for a general edge effect, characterised by high density of outliers present at transitions between different grassland communities.

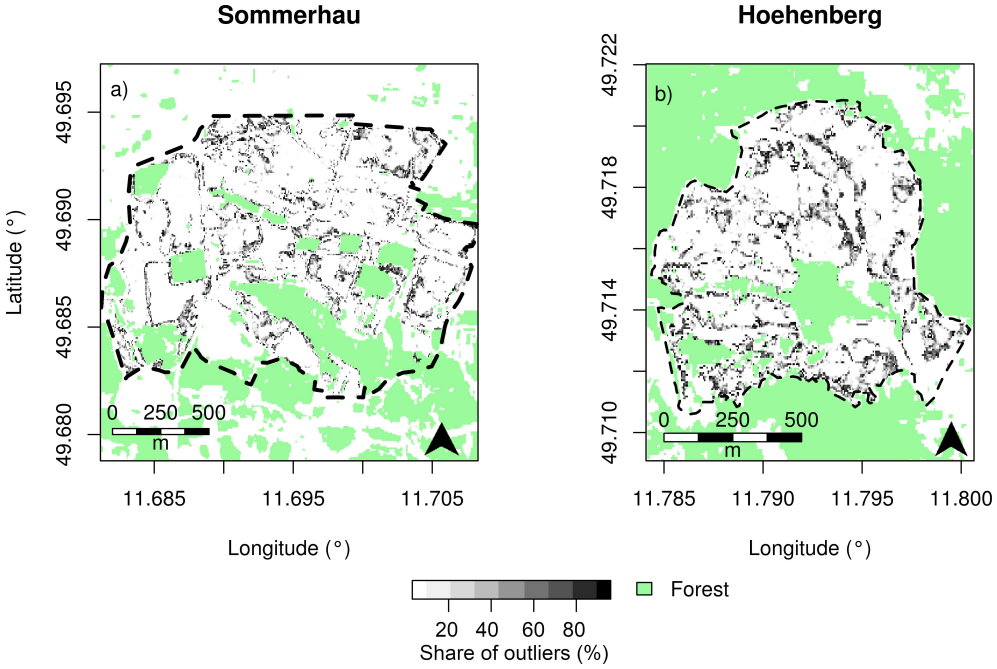

Figure 4: Share of outliers divided by the total amount of members of training data candidate sets per pixel expressed as percentage. Sommerhau a) and Hoehenberg b).

Spatial probability of occurrence

For each class, we derived the modelled probability of occurrence for each pixel, averaged over 100 repetitions. The exemplary results for the classes SG21 and SG14 for the Sommerhau site and HM21 and HB70 for the Hoehenberg site are illustrated in Figure 5.

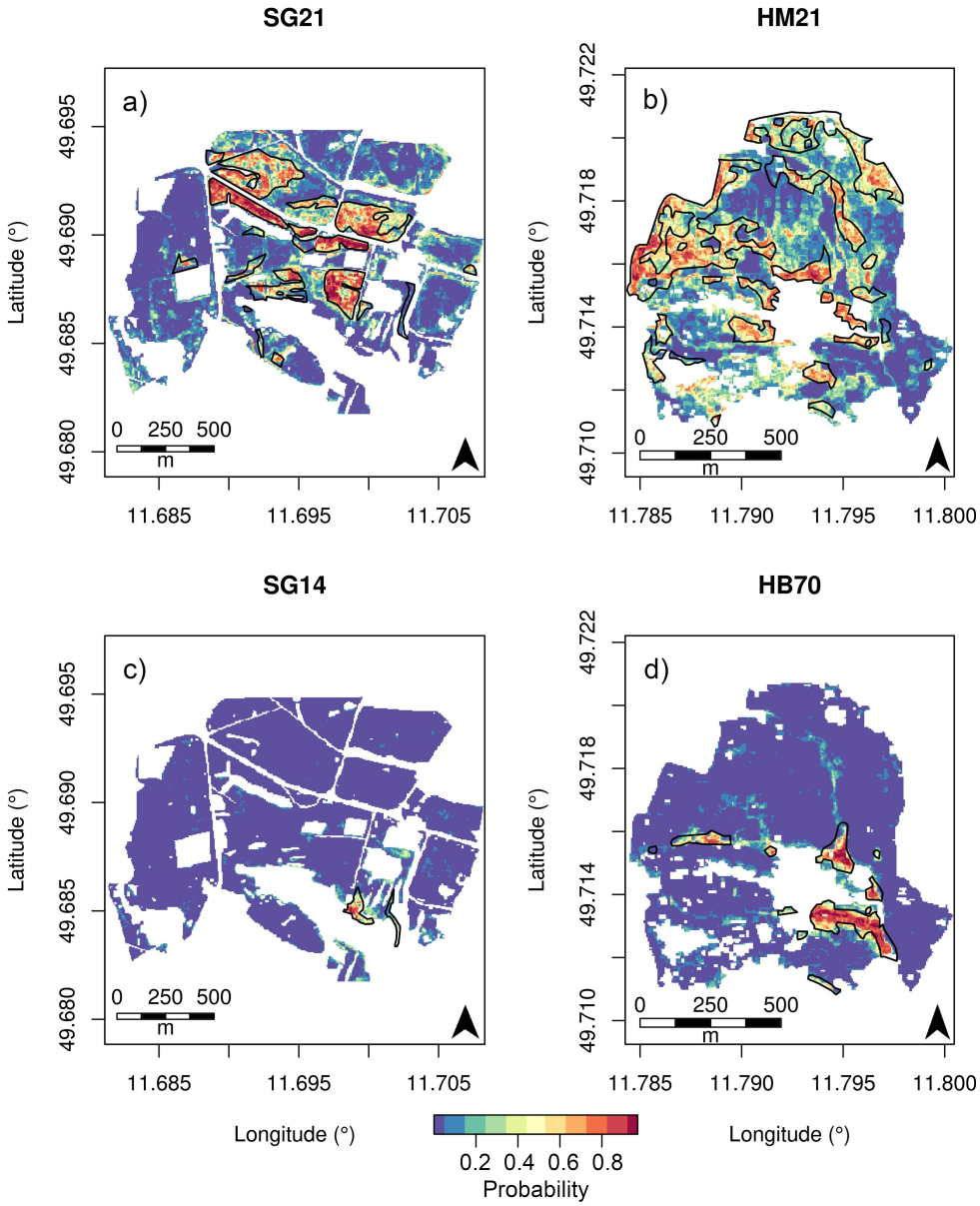

Figure 5: Exemplary results for the spatial probability of occurrence for the Sommerhau classes SG21 a) and SG14 c), as well as the Hoehenberg classes HM21 b) and HB70 d). The field mapping results are drawn as black polygons. Detailed descriptions of the classes can be found in Table 1 and Table 2.

For all other grassland communities the results are displayed in Figure S1-S17 in the supplementary material. Very high class probabilities

can be observed within the field-mapped boundaries for all grassland communities and both sites. In general, areas with lower probabilities can be found mostly in the direct vicinity of the mapped boundaries, with a gradual decrease with distance.

Variable importance

Permutation-based variable importance, derived from increase in classification error, were used to identify important acquisition dates. As illustrated in Figure 6, the importance across and within phenological seasons varied, with a maximum increase in classification error of about 20% for the first autumn (FA) image number 15 in Sommerhau. The cumulative importance for all prespring (PSP) acquisitions was much higher for Sommerhau than in Hoehenberg, but relatively similar between the two sites for the first spring (FIS) season. In general, for both sites the late summer (LSU) season appeared to be relevant for mapping grassland at community level, and for Sommerhau especially also the first autumn (FA). Unfortunately, no image for this period was available for a comparison with Hoehenberg.

In summary, the least important phenological seasons for mapping semi-grassland at community level, in terms of an increase in classification error, were the full spring (FUS) and early summer (ESU) for both study sites.

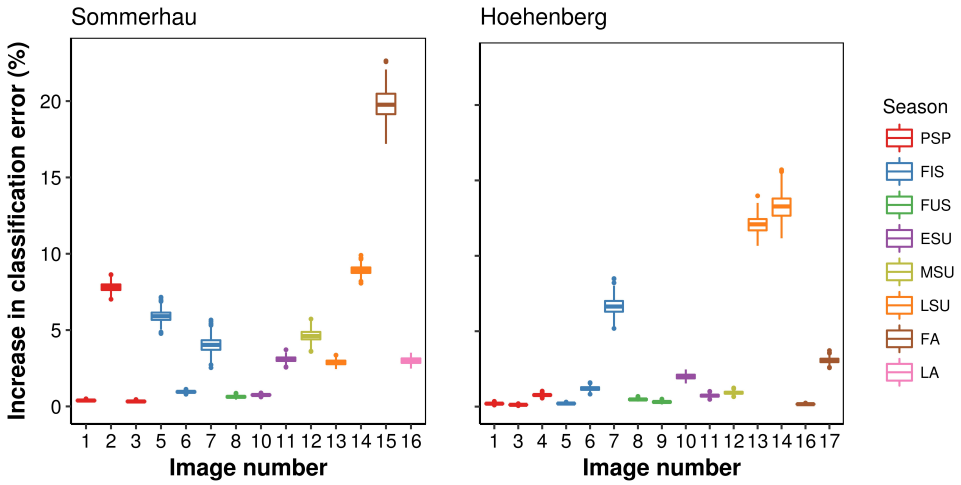

Figure 6: Permutation-based variable importance in terms of increase in classification error caused by excluding the PC1 band for one date and keeping the rest in the model. Explanations to the image number of the x-axis and the phenological seasons of the legend can be found in Table 3.

Discussion

The field mapping of both study sites was challenged by access limitations and, given the heterogeneous grassland community composition, a labour-intensive and time-consuming task. Similar circumstances for field data collection are reported by Ghimire et al. (2012), and are probably quite common on many military training areas, which often support high levels of biodiversity and are of major management and conservation concern (e.g. Benton et al., 2008). Uncertainty in training data due to the subjectivity of field surveys, as well as the mixed pixel problem, are major challenges in remote sensing (Rocchini et al., 2013). In our study, the applied screening of training data for potential outliers excluded about 25% of the initial field reference set for both study sites. As the training data set were screened for outliers, potential uncertainties were reduced. High accuracies were

estimated for the respective final training data set, based on the PC1-10 response variables (Sommerhau: OA = 86.5%, Kappa = 0.84 and Hoehenberg: OA = 77.5%, Kappa = 0.73). The performance with a Random Forest proximity threshold of 10 was good. The proximity measure can be related to the spectral distance of two samples and a more conservative, i.e. smaller, threshold value would lead to more homogeneous training points for the respective classes. For very low threshold values, the model would be trained with pure pixels only, and would therefore not be able to reliable classify mixed pixels. In general, there is a need to explore the sensitivity of results to the threshold setting for the Random-Forest-based outliers detection method (Belgiu and Drăguț, 2016). In addition, its potential to identify subclasses by grouping samples with similar proximities to all other training points of the same class should be explored in future research activities (Touw et al., 2012).

The spatial distribution of detected outliers for several iterations (Figure 4) highlights areas with potential mapping errors, as well as uncertainties about the discrete spatial boundaries between grassland communities drawn during the mapping process. These areas can be specifically addressed by a following mapping iteration to revise the spatial class boundaries. This can be especially useful for long-term monitoring strategies in combination with probability maps to detect potential early warning signals for the decline of a high-value grassland community in terms of conservation.

The estimated performance during the training data selection procedure was consistently better for the Sommerhau site compared to Hoehenberg. This can be attributed to a more heterogeneous land cover for the Hoehenberg site and different land management practices. The amount of initial training points per study site (15% of the area) can be regarded as relatively high compared to common recommendations (Colditz, 2015; Belgiu and Drăguț, 2016), even though about one quarter was subsequently excluded by the outliers screening. However, in contrast to a fixed number of training points related to the study site size, Millard and Richardson (2015) recommended that the training set should be as large as possible and randomly distributed, while accounting for the proportion of land covered by each class. In addition, studies showed that the Random Forest benefits to a great extent from large sample sizes (Fassnacht, et al., 2014; Ma, et al., 2017).

The selection of the most important variables contributing to a classification model has gained a lot of attention over the last decade (Diaz-Uriarte, 2007; Pal and Foody, 2010; Verikas et al., 2011; Rodriguez-Galiano et al., 2012; Chutia et al., 2017), and methods to select most influential variables include backward elimination (Dash and Liu, 1997) and forward selection strategies (Langley, 1994). The Random Forest algorithm provides a relative measure of variable importance in the form of the change of an internal classification error measure and the Gini index caused by excluding one variable and keeping the rest in the model (Breiman, 2001; Rodriguez-

Galiano et al., 2012). These variable importance measures can, however, display a bias when variables are correlated (Strobl et al., 2008). In this case high importance can be observed in favour of insignificant variables correlated with significant variables at the cost of reduced importance measures for significant, uncorrelated variables (Nicodemus and Malley, 2009; Conn et al., 2015). In addition, the Random Forest variable importance is not reliable when the predictor variables vary in scale or number of categories (Strobl et al., 2007). Introduced by Strobl et al. (2008), the conditional variable importance for Random Forest is one approach to address the discussed importance measure problems, but is known to be very calculation intensive (Nicodemus et al., 2010). Therefore, a permutation-based variable importance estimation can be seen as a valid alternative.

The results of the permutation-based variable importance of this study indicate a general importance of the first spring (FIS) and late summer (LSU) season for both sites. Particularly for Sommerhau, the first autumn (FA) can bee seen as the most influential temporal window, with an estimated mean increase of about 20% in classification error when excluded from the model. Full spring (FUS) and early summer (ESU) were the least important phenological seasons for both sites in this study. This finding is not supported by Schmidt et al. (2014), who identified early summer (ESU) – followed by full spring (FUS), late summer (LSU) and midsummer (MSU) – as the most important phenological seasons to discriminate semi-natural grasslands in Northern Germany. However, the inconsistent important dates

for accurately mapping northern versus southern German grassland communities can likely be attributed to differences in the location, management and grassland composition between studied areas. However, Förster et al. (2010) suggested to use RapidEye acquisitions during the onset of vegetation and senescence phases to monitor Natura 2000 habitats, which was indicated by our findings as well.

When the probability values of occurrence (Figure 5 and Figure S1-S17 in the supplementary material) are plotted together with the mapping results, a good spatial agreement can be observed, even for rare grassland communities (e.g. SG14, Figure 5). Some probability values higher than the expected value of zero can be found outside the mapped boundaries. For the example of class HB70 this can be linked to the topography, e.g. related to a ditch going from the north to the south. Areas with lower probabilities can be attributed to continuous transitions due to self-organisation in vegetation and changes in environmental conditions (Rocchini et al., 2013). While a common pixel-based classification of such gradual transitions into a fixed number of discrete classes would not have reflected the true reality of the Earth's surface, the proposed mapping approach captures gradual transitions by probabilities of occurrence. A segmentation-based mapping approach would most likely increase the overall accuracies for high spatial resolution data by aggregating spectrally homogeneous pixels into objects (Laliberte et al., 2007; Förster et al., 2010), but with the trade-off of losing fine-scale information as small features are swallowed into bigger objects (Schmidtlein

and Sassin, 2004; Schmidt et al., 2017). In addition, it is easy to aggregate pixels to objects for reporting purposes, while the reverse is impossible.

Conclusion

In this study we showed that training data for mapping and monitoring vegetation cover can automatically be derived in an objective way and that multi-annual, multi-seasonal remote sensing data can be successfully applied to monitor semi-natural grassland vegetation types at a fine scale. The introduced training data sampling framework can help to identify potential uncertainties in the reference data. Pivotal for this is the collection of baseline data by field mapping. With regard to the reporting obligations under Art.-17 of the EU Habitats Directive, the proposed mapping strategy can locate hot-spot areas of change by incorporating future remote sensing data. Thus, an effective field work strategy can be designed to target areas of special interest. Full spring (FUS) and early summer (ESU) were identified as the least important phenological seasons for mapping semi-natural grassland. Future research should consider the synergistic possibilities of combining multi-spectral and radar data for monitoring semi-natural grassland (Schuster et al., 2011; Metz et al., 2012; Bargiel, 2013).

Acknowledgements

The project was supported by funds of German government's Special Purpose Fund held at Landwirtschaftliche Rentenbank (28 RZ 7007). We thank the

Federal Forests Division (Bundesforst) of the German Institute for Federal Real Estate (Bundesanstalt für Immobilienaufgaben) and the Institut für Wildbiologie Göttingen und Dresden e.V. for close cooperation and support. We acknowledge the DLR for the delivery of RapidEye images as part of the RapidEye Science Archive (RESA) – proposal 00226.

References

Bargiel, D. 2013. “Capabilities of High Resolution Satellite Radar for the Detection of Semi-Natural Habitat Structures and Grasslands in Agricultural Landscapes.” *Ecological Informatics* 13: 9–16.

Barrett, B., C. Raab, F. Cawkwell, and S. Green. 2016. “Upland Vegetation Mapping Using Random Forests with Optical and Radar Satellite Data.” *Remote Sensing in Ecology and Conservation* 2 (4):212–231.

BayLFU, (Bayerisches Landesamt für Umwelt). 2012. “Biotopkartierung - Kartieranleitungen - LfU Bayern.” Kartieranleitungen. 2012. https://www.lfu.bayern.de/natur/biotopkartierung_flachland/kartieranleitungen/index.html.

Belgiu, M., and L. Drăguț. 2016. “Random Forest in Remote Sensing: A Review of Applications and Future Directions.” *ISPRS Journal of Photogrammetry and Remote Sensing* 114:24–31.

Belward, A.S., and J.O. Skøien. 2015. “Who Launched What, When and Why; Trends in Global Land-Cover Observation Capacity from Civilian Earth Observation Satellites.” *ISPRS Journal of Photogrammetry and Remote Sensing* 103:115–128.

Benton, N., J.D. Ripley, and F. Powledge. 2008. “Conserving Biodiversity on Military Lands: A Guide for Natural Resources Managers.” *Arlington (VA): NatureServe*.

Bischl, B., M. Lang, L. Kotthoff, J. Schiffner, J. Richter, E. Studerus, G. Casalicchio, and M.Z. Jones. 2016. “Mlr: Machine Learning in R.” *Journal of Machine Learning Research* 17 (170): 1–5.

Borre, J.V., D. Paelinckx, C.A. Mücher, L. Kooistra, B. Haest, G. De Blust, and A.M. Schmidt. 2011. “Integrating Remote Sensing in Natura 2000 Habitat Monitoring: Prospects on the Way Forward.” *Journal for Nature Conservation* 19 (2):116–125.

Breiman, L. 2001. “Random Forests.” *Machine Learning* 45 (1):5–32.

Buck, O., A. Klink, V.E.G. Millán, K. Pakzad, and A. Müterthies. 2013. “Image Analysis Methods to Monitor Natura 2000 Habitats at Regional Scales–the MS. MONINA State Service Example in Schleswig-Holstein, Germany.” *Photogrammetrie-Fernerkundung-Geoinformation* 2013 (5):415–426.

Burkart, M., H. Dierschke, N. Holzel, B. Nowak, and T. Fartmann. 2004. “Molinio-Arrhenatheretea (E1)-Teil 2: Molinietalia.” *Synopsis*, no. 9:1–103.

Chutia, D., D.K. Bhattacharyya, J. Sarma, and P.N.L. Raju. 2017. “An Effective Ensemble Classification Framework Using Random Forests and a Correlation Based Feature Selection Technique.” *Transactions in GIS*.

Colditz, R.R. 2015. “An Evaluation of Different Training Sample Allocation Schemes for Discrete and Continuous Land Cover Classification Using Decision Tree-Based Algorithms.” *Remote Sensing* 7 (8):9655–9681.

Conn, D., T. Ngun, G. Li, and C. Ramirez. 2015. “Fuzzy Forests: Extending Random Forests for Correlated, High-Dimensional Data.”

Corbane, C., S. Lang, K. Pipkins, S. Alleaume, M. Deshayes, V.E.G.Millán, T. Strasser, J.V. Borre, S. Toon, and M. Förster. 2015. “Remote Sensing for Mapping Natural Habitats and Their Conservation Status–New Opportunities and Challenges.” *International Journal of Applied Earth Observation and Geoinformation* 37: 7–16.

Cortes, C., and V. Vapnik. 1995. “Support-Vector Networks.” *Machine Learning* 20 (3):273–297.

Cutler, D.R., T.C. Edwards, K.H. Beard, A. Cutler, K.T. Hess, J. Gibson, and J. J. Lawler. 2007. “Random Forests for Classification in Ecology.” *Ecology* 88 (11): 2783–2792.

Dash, M., and H. Liu. 1997. “Feature Selection for Classification.” *Intelligent Data Analysis* 1 (1–4):131–156.

Dengler, J., M. Janišová, P. Török, and C. Wellstein. 2014. “Biodiversity of Palaearctic Grasslands: A Synthesis.” *Agriculture, Ecosystems & Environment* 182: 1–14.

Diaz-Uriarte, R. 2007. “GeneSrF and VarSelRF: A Web-Based Tool and R Package for Gene Selection and Classification Using Random Forest.” *BMC Bioinformatics* 8 (1):328.

Dierschke, H. 1997. “Molinio-Arrhenatheretea (E1)-Kulturgrasland Und Verwandte Vegetationstypen, Teil 1: Arrhenatheretalia-Wiesen Und Weiden Frischer Standorte.” *Synopsis Der Pflanzengesellschaften Deutschlands*, no. 3.

Dierschke, H., and G. Briemle. 2002. *Kulturgrasland: Wiesen, Weiden Und Verwandte Staudenfluren; 20 Tabellen*. Ulmer.

Feilhauer, H., C. Dahlke, D. Doktor, A. Lausch, S. Schmidtlein, G. Schulz, and S. Stenzel. 2014. “Mapping the Local Variability of Natura 2000 Habitats with Remote Sensing.” *Applied Vegetation Science* 17 (4): 765–779.

Fassnacht, F.E., F. Hartig, H. Latifi, C. Berger, J. Hernández, P. Corvalán, and B. Koch. 2014. “Importance of Sample Size, Data Type and Prediction Method for Remote Sensing-Based Estimations of Aboveground Forest Biomass.” *Remote Sensing of Environment* 154:102–114.

Foerster, S., K. Kaden, M. Foerster, and S. Itzerott. 2012. “Crop Type Mapping Using Spectral–temporal Profiles and Phenological Information.” *Computers and Electronics in Agriculture* 89:30–40.

Förster, M., A. Frick, C. Schuster, and B. Kleinschmit. 2010. “Object-Based Change Detection Analysis for the Monitoring of Habitats in the Framework of the NATURA 2000 Directive with Multi-Temporal Satellite Data.” *The International Archives of the Photogrammetry, Remote Sensing and Spatial Information Sciences* 38: 4.

Ghimire, B., J. Rogan, V.R. Galiano, P. Panday, and N. Neeti. 2012. "An Evaluation of Bagging, Boosting, and Random Forests for Land-Cover Classification in Cape Cod, Massachusetts, USA." *GIScience & Remote Sensing* 49 (5):623–643.

Gislason, P.O., J.A. Benediktsson, and J.R. Sveinsson. 2006. "Random Forests for Land Cover Classification." *Pattern Recognition Letters* 27 (4):294–300.

GRASS Development Team. 2017. *Geographic Resources Analysis Support System (GRASS GIS) Software, Version 7.2*. Open Source Geospatial Foundation. http://grass.osgeo.org.

Laliberte, A.S., E.L. Fredrickson, and A. Rango. 2007. "Combining Decision Trees with Hierarchical Object-Oriented Image Analysis for Mapping Arid Rangelands." *Photogrammetric Engineering & Remote Sensing* 73 (2): 197–207.

Langley, P. 1994. "Selection of Relevant Features in Machine Learning." In *Proceedings of the AAAI Fall Symposium on Relevance*, 184:245–271.

Ma, L., T. Fu, T. Blaschke, M. Li, D. Tiede, Z. Zhou, X. Ma, and D. Chen. 2017. "Evaluation of Feature Selection Methods for Object-Based Land Cover Mapping of Unmanned Aerial Vehicle Imagery Using Random Forest and Support Vector Machine Classifiers" 6 (2):51.

Malley, J.D., J. Kruppa, A. Dasgupta, K. G. Malley, and A. Ziegler. 2012. "Probability Machines: Consistent Probability Estimation Using Nonparametric Learning Machines." *Methods of Information in Medicine* 51 (1): 74.

Maxwell, A.E., T.A. Warner, and F. Fang. 2018. "Implementation of Machine-Learning Classification in Remote Sensing: An Applied Review." *International Journal of Remote Sensing* 39 (9): 2784–2817.

Meißner, M., H. Reinecke, S. Herzog, L. Leinen, and G. Brinkmann. 2012. *Vom Wald ins Offenland: Der Rothirsch auf dem Truppenübungsplatz Grafenwöhr. Raum-Zeit-Verhalten, Lebensraumnutzung, Management*. 1. Aufl. Ahnatal: Frank Fornacon.

Metz, A., A. Schmitt, T. Esch, P. Reinartz, S. Klonus, and M. Ehlers. 2012. "Synergetic Use of TerraSAR-X and Radarsat-2 Time Series Data for Identification and Characterization of Grassland Types-a Case Study in Southern Bavaria, Germany." In *Geoscience and Remote Sensing Symposium (IGARSS), 2012 IEEE International*, 3560–3563. IEEE.

Millard, K., and M. Richardson. 2015. "On the Importance of Training Data Sample Selection in Random Forest Image Classification: A Case Study in Peatland Ecosystem Mapping." *Remote Sensing* 7 (7):8489–8515.

Mountrakis, G., J. Im, and C. Ogole. 2011. "Support Vector Machines in Remote Sensing: A Review." *ISPRS Journal of Photogrammetry and Remote Sensing* 66 (3):247–259.

Nagendra, H., R. Lucas, J.P. Honrado, R. HG Jongman, C. Tarantino, M. Adamo, and P. Mairota. 2013. "Remote Sensing for Conservation

Monitoring: Assessing Protected Areas, Habitat Extent, Habitat Condition, Species Diversity, and Threats." *Ecological Indicators* 33:45–59.

Nicodemus, K.K., and J.D. Malley. 2009. "Predictor Correlation Impacts Machine Learning Algorithms: Implications for Genomic Studies." *Bioinformatics* 25 (15):1884–1890.

Nicodemus, K.K, J.D. Malley, C. Strobl, and A. Ziegler. 2010. "The Behaviour of Random Forest Permutation-Based Variable Importance Measures under Predictor Correlation." *BMC Bioinformatics* 11 (1): 110.

Nitze, I., B. Barrett, and F. Cawkwell. 2015. "Temporal Optimisation of Image Acquisition for Land Cover Classification with Random Forest and MODIS Time-Series." *International Journal of Applied Earth Observation and Geoinformation* 34:136–46.

Pal, M., and G. M. Foody. 2010. "Feature Selection for Classification of Hyperspectral Data by SVM." *IEEE Transactions on Geoscience and Remote Sensing* 48 (5):2297–2307.

Peeters, A., G. Beaufoy, R.M. Canals, A.D. Vliegher, C. Huyghe, J. Isselstein, J. Jones, W. Kessler, D. Kirilovsky, and A. V. D. P.-V. Dasselaar. 2014. "Grassland Term Definitions and Classifications Adapted to the Diversity of European Grassland-Based Systems." In *Grassland Science in Europe*, 19:743–750.

Planet Labs Inc, . 2016. "Satellite Imagery Product Specifications." *Satellite Imagery Product Specifications: Version 6.1*.

R Core Team. 2017. *R: A Language and Environment for Statistical Computing*. R Foundation for Statistical Computing. https://www.R-project.org/.

Riesch, F., H.G. Stroh, B. Tonn, and J. Isselstein. 2018. "Soil PH and Phosphorus Drive Species Composition and Richness in Semi-Natural Heathlands and Grasslands Unaffected by Twentieth-Century Agricultural Intensification." *Plant Ecology & Diversity*, no. just-accepted.

Robnik-Šikonja, M., P. Savicky, and J. Adeyanju Alao. 2017. "CORElearn: Classification, Regression and Feature Evaluation, R Package Version 1.51.2 (2017)."

Rocchini, D., G.M. Foody, H. Nagendra, C. Ricotta, M. Anand, K.S. He, V. Amici, B. Kleinschmit, M. Förster, and S. Schmidtlein. 2013. "Uncertainty in Ecosystem Mapping by Remote Sensing." *Computers & Geosciences* 50:128–135.

Rodriguez-Galiano, V.F., M. Chica-Olmo, F. Abarca-Hernandez, P.M. Atkinson, and C. Jeganathan. 2012. "Random Forest Classification of Mediterranean Land Cover Using Multi-Seasonal Imagery and Multi-Seasonal Texture." *Remote Sensing of Environment* 121:93–107.

Ruß, G., and A. Brenning. 2010. "Spatial Variable Importance Assessment for Yield Prediction in Precision Agriculture." *Advances in Intelligent Data Analysis IX*, 184–195.

Schmidt, T., C. Schuster, B. Kleinschmit, and M. Förster. 2014. "Evaluating an Intra-Annual Time Series for Grassland Classification—How Many Acquisitions and What Seasonal Origin Are Optimal?" *IEEE Journal of Selected Topics in Applied Earth Observations and Remote Sensing* 7 (8):3428–3439.

Schmidt, J., F.E. Fassnacht, M. Förster, and S. Schmidtlein. 2017. "Synergetic Use of Sentinel-1 and Sentinel-2 for Assessments of Heathland Conservation Status." *Remote Sensing in Ecology and Conservation*.

Schmidtlein, S., and J. Sassin. 2004. "Mapping of Continuous Floristic Gradients in Grasslands Using Hyperspectral Imagery." *Remote Sensing of Environment* 92 (1): 126–138.

Schuster, C., I. Ali, P. Lohmann, A. Frick, M. Förster, and B. Kleinschmit. 2011. "Towards Detecting Swath Events in TerraSAR-X Time Series to Establish NATURA 2000 Grassland Habitat Swath Management as Monitoring Parameter." *Remote Sensing* 3 (7): 1308–1322.

Schuster, C., M. Förster, and B. Kleinschmit. 2012. "Testing the Red Edge Channel for Improving Land-Use Classifications Based on High-Resolution Multi-Spectral Satellite Data." *International Journal of Remote Sensing* 33 (17):5583–5599.

Stenzel, S., H. Feilhauer, B. Mack, A. Metz, and S. Schmidtlein. 2014. "Remote Sensing of Scattered Natura 2000 Habitats Using a One-Class Classifier." *International Journal of Applied Earth Observation and Geoinformation* 33:211–217.

Strobl, C., A.-L. Boulesteix, T. Kneib, T. Augustin, and A. Zeileis. 2008. "Conditional Variable Importance for Random Forests." *BMC Bioinformatics* 9 (1):307.

Strobl, C., A.-L. Boulesteix, A. Zeileis, and T. Hothorn. 2007. "Bias in Random Forest Variable Importance Measures: Illustrations, Sources and a Solution." *BMC Bioinformatics* 8 (1):25.

Teillet, P.M., B. Guindon, and D.G. Goodenough. 1982. "On the Slope-Aspect Correction of Multispectral Scanner Data." *Canadian Journal of Remote Sensing* 8 (2):84–106.

Touw, W.G., J.R. Bayjanov, L. Overmars, L. Backus, J. Boekhorst, M. Wels, and S.AFT van Hijum. 2012. "Data Mining in the Life Sciences with Random Forest: A Walk in the Park or Lost in the Jungle?" *Briefings in Bioinformatics* 14 (3):315–326.

Tyc, G., J. Tulip, D. Schulten, M. Krischke, and M. Oxfort. 2005. "The RapidEye Mission Design." *Acta Astronautica* 56 (1):213–219.

Ustuner, M., F.B. Sanli, and S. Abdikan. 2016. "Balanced VS Imbalanced Training Data: Classifying Rapideye Data with Support Vector Machines." *ISPRS-International Archives of the Photogrammetry, Remote Sensing and Spatial Information Sciences*, 379–384.

Verikas, A., A. Gelzinis, and M. Bacauskiene. 2011. "Mining Data with Random Forests: A Survey and Results of New Tests." *Pattern Recognition* 44 (2):330–349.

Vermote, E.F., D. Tanré, J.L. Deuze, M. Herman, and J.-J. Morcette. 1997. "Second Simulation of the Satellite Signal in the Solar Spectrum, 6S: An Overview." *IEEE Transactions on Geoscience and Remote Sensing* 35 (3):675–686.

Wachendorf, M., T. Fricke, and T. Möckel. 2017. "Remote Sensing as a Tool to Assess Botanical Composition, Structure, Quantity and Quality of Temperate Grasslands." *Grass and Forage Science*.

Warren, S.D., and R. Büttner. 2008a. "Relationship of Endangered Amphibians to Landscape Disturbance." *Journal of Wildlife Management* 72 (3):738–44.

2008b. "Active Military Training Areas as Refugia for Disturbance-Dependent Endangered Insects." *Journal of Insect Conservation* 12 (6):671–76.

Wright, M.N., and A. Ziegler. 2015. "Ranger: A Fast Implementation of Random Forests for High Dimensional Data in C++ and R." *ArXiv Preprint ArXiv:1508.04409*.

Supporting information to the paper

Raab, C., H.G. Stroh, B. Tonn, M. Meißner, N. Rohwer, N. Balkenhol, J. Isselstein. 2018. "Mapping semi-natural grassland communities using multi-temporal RapidEye remote sensing data". *International Journal of Remote Sensing*. 39, 5638–5659.

Supplementary figures

Figure S1: Predicted spatial probability for the class SG11.

Figure S2: Predicted spatial probability for the class SG12.

Figure S3: Predicted spatial probability for the class SG13.

Figure S4: Predicted spatial probability for the class SG22.

Figure S5: Predicted spatial probability for the class SG24.

Figure S6: Predicted spatial probability for the class SG25.

Figure S7: Predicted spatial probability for the class SB10.

Figure S8: Predicted spatial probability for the class SB30.

Figure S9: Predicted spatial probability for the class SB40.

Figure S10: Predicted spatial probability for the class HM11.

Figure S11: Predicted spatial probability for the class HM12.

Figure S12: Predicted spatial probability for the class HM14.

Figure S13: Predicted spatial probability for the class HM15.

Figure S14: Predicted spatial probability for the class HM30.

Figure S15: Predicted spatial probability for the class HM40.

Figure S16: Predicted spatial probability for the class HB50.

Figure S17: Predicted spatial probability for the class HB60.

R code example

Appendix 1: A practical example.

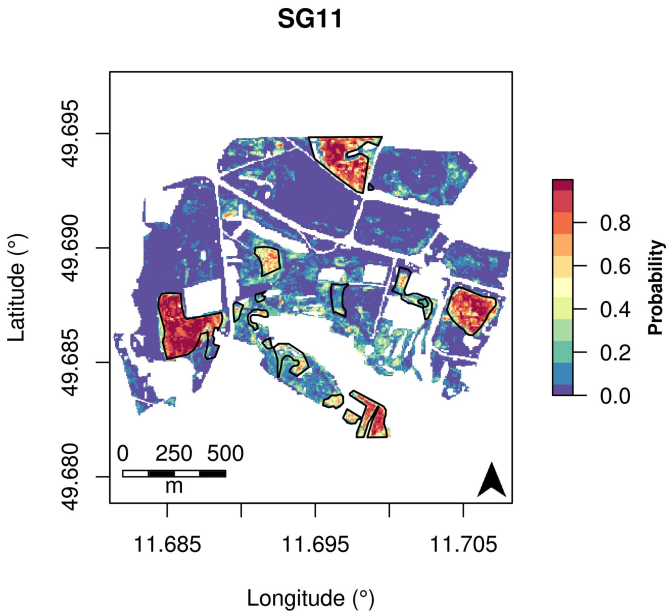

Figure S1: Predicted spatial probability for the class SG11. The field mapping results are drawn as black polygons.

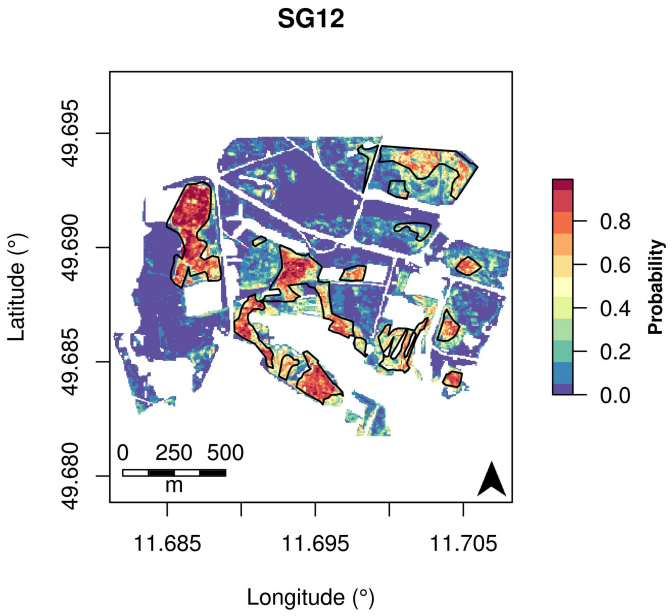

Figure S1: Predicted spatial probability for the class SG12. The field mapping results are drawn as black polygons.

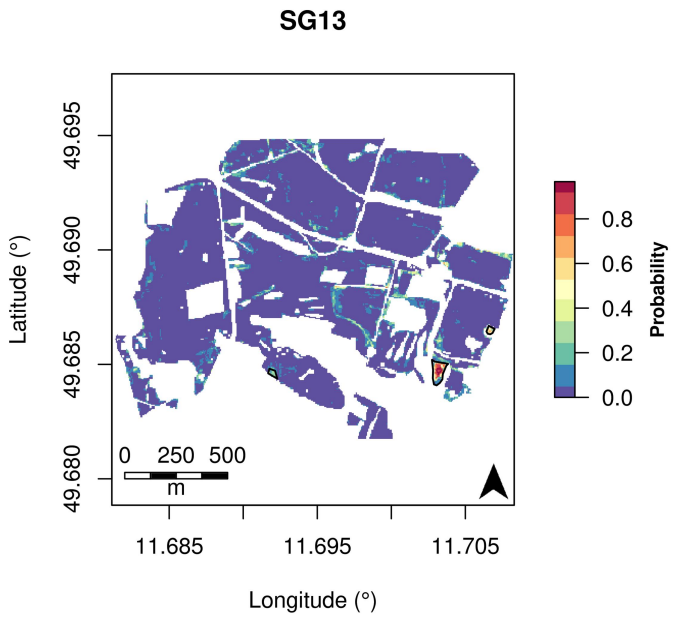

Figure S3: Predicted spatial probability for the class SG13. The field mapping results are drawn as black polygons.

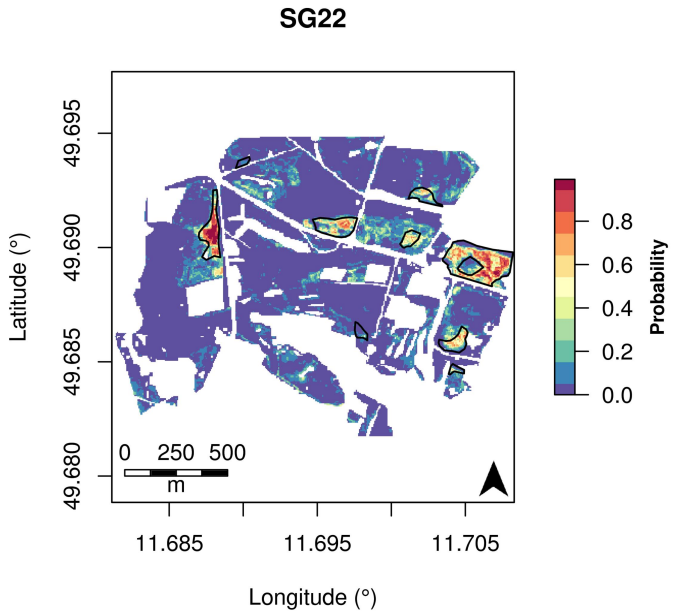

Figure S4: Predicted spatial probability for the class SG22. The field mapping results are drawn as black polygons.

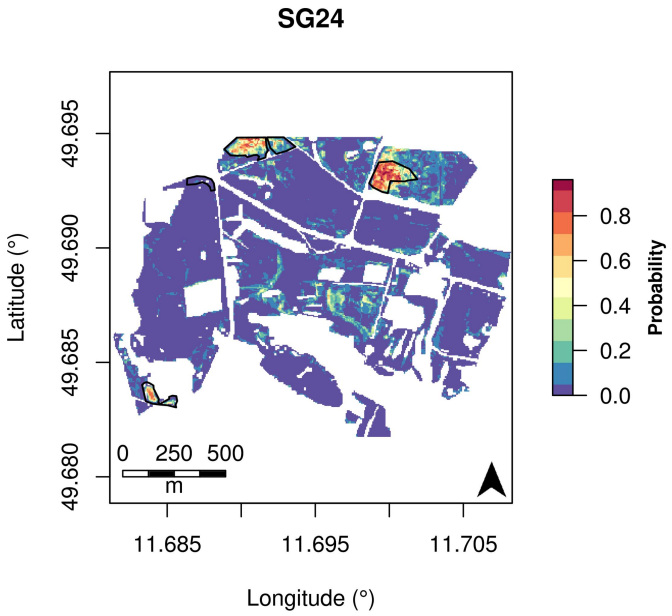

Figure S5: Predicted spatial probability for the class SG24. The field mapping results are drawn as black polygons.

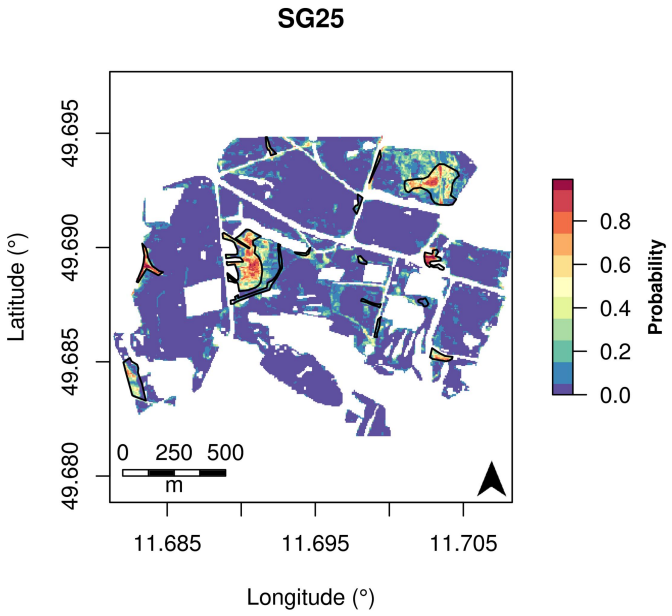

Figure S6: Predicted spatial probability for the class SG25. The field mapping results are drawn as black polygons.

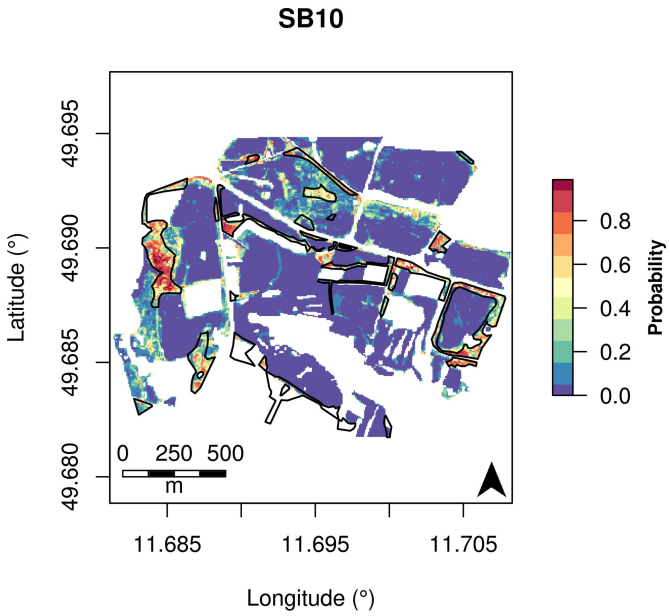

Figure S7: Predicted spatial probability for the class SB10. The field mapping results are drawn as black polygons.

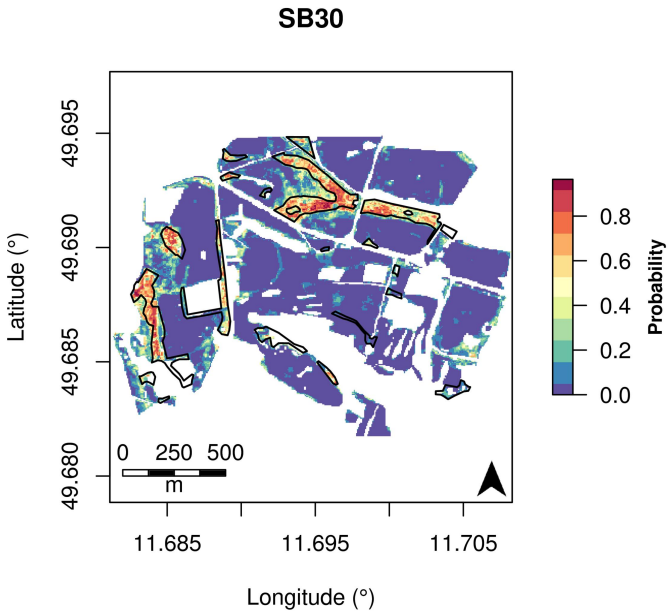

Figure S8: Predicted spatial probability for the class SB30. The field mapping results are drawn as black polygons.

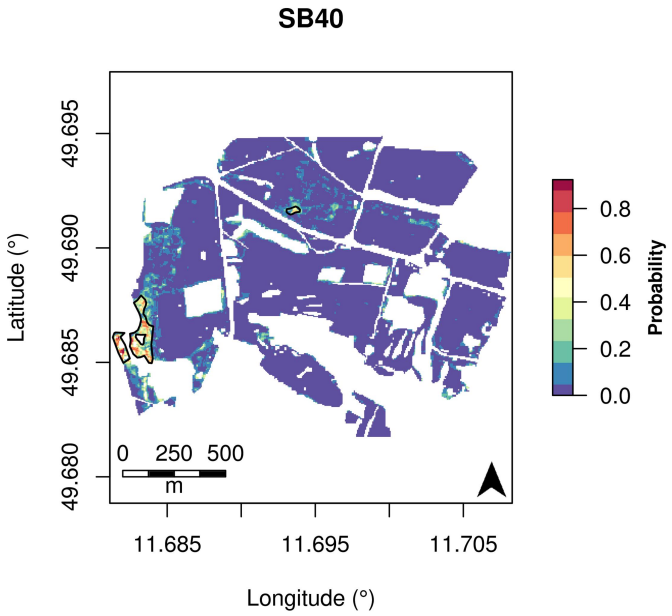

Figure S9: Predicted spatial probability for the class SB40. The field mapping results are drawn as black polygons.

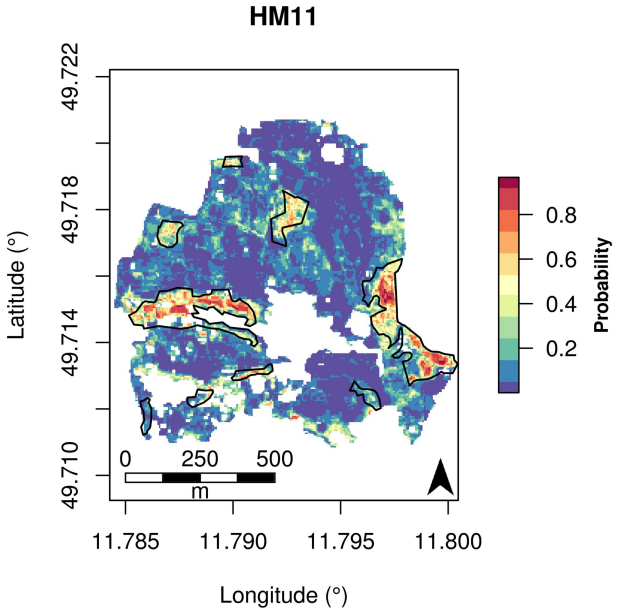

Figure S10: Predicted spatial probability for the class HM11. The field mapping results are drawn as black polygons.

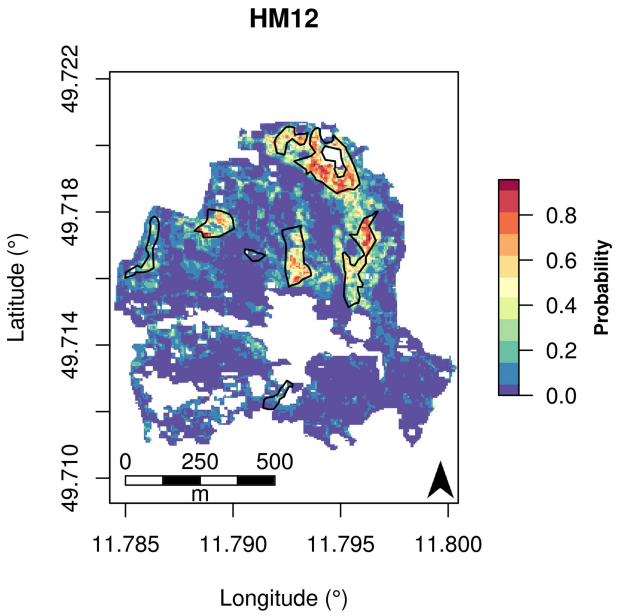

Figure S11: Predicted spatial probability for the class HM12. The field mapping results are drawn as black polygons.

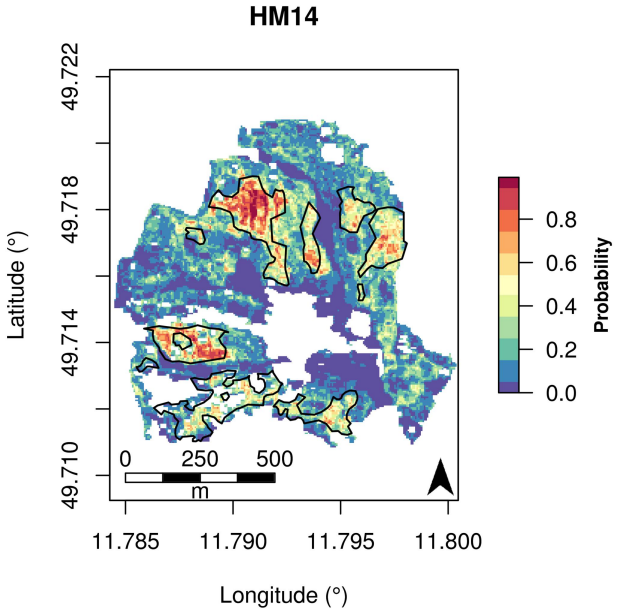

Figure S12: Predicted spatial probability for the class HM14. The field mapping results are drawn as black polygons.

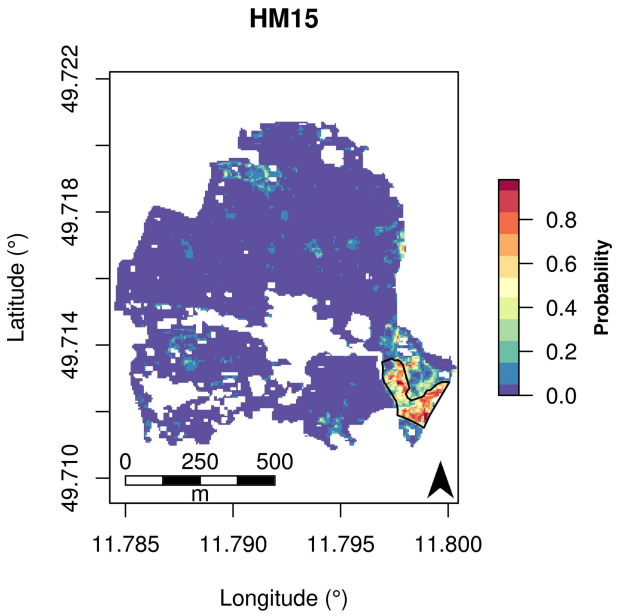

Figure S13: Predicted spatial probability for the class HM15. The field mapping results are drawn as black polygons.

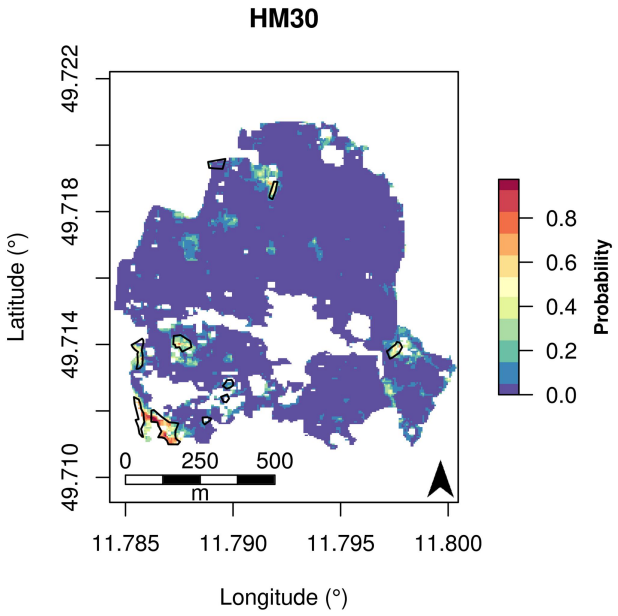

Figure S14: Predicted spatial probability for the class HM30. The field mapping results are drawn as black polygons.

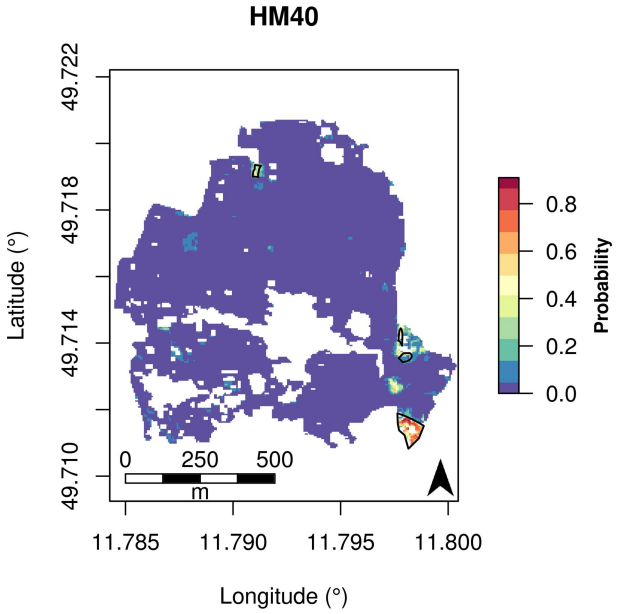

Figure S15: Predicted spatial probability for the class HM40. The field mapping results are drawn as black polygons.

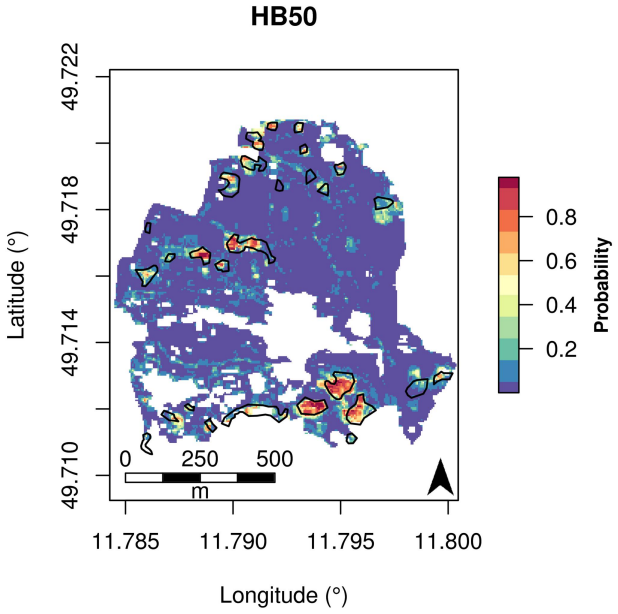

Figure S16: Predicted spatial probability for the class HB50. The field mapping results are drawn as black polygons.

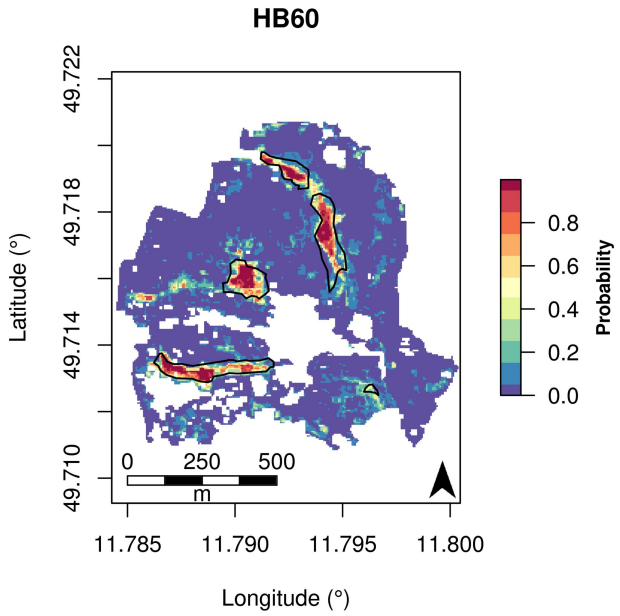

Figure S17: Predicted spatial probability for the class HB60. The field mapping results are drawn as black polygons.

Appendix 1: A practical example

In this practical example we will illustrate how the Random Forest algorithm can be used for automated training data sampling and remote sensing classification purposes. For this, we make use of a data set compilation provided by the book "Remote Sensing and GIS for Ecologists: Using Open Source Software" (Wegmann et al., 2016). The data can be accessed under the following URL:

http://book.ecosens.org/data/

Data preparation

First we load the required packages and subsequently the data:

```
library(raster)
library(RStoolbox)

lsat <- brick("data_book/raster_data/LT52240632011210.tif")
names(lsat) <- paste0("b",rep(1:7))

lsat <- crop(lsat, extent(650000,665046,-519107,-498509))
```

Dummy mapping results

Now we use an unsupervised classification to create a dummy map with three classes, which represent our field mapping result for this short example. For this, we convert the unsupervised classification raster will be to polygons, because field-mapping results are often available in such a format.

```
# unsupervised classification
lsat_map <- unsuperClass(lsat, nClasses = 3)$map
# majority filter (3*3) to smooth the result and add some error
```

```
lsat_map <-focal(lsat_map, w=matrix(1,11,11), fun=modal)

lsat_map_poly <- rasterToPolygons(lsat_map,
                                  dissolve=TRUE)

plot(lsat_map)
plot(lsat_map_poly, add=TRUE)
```

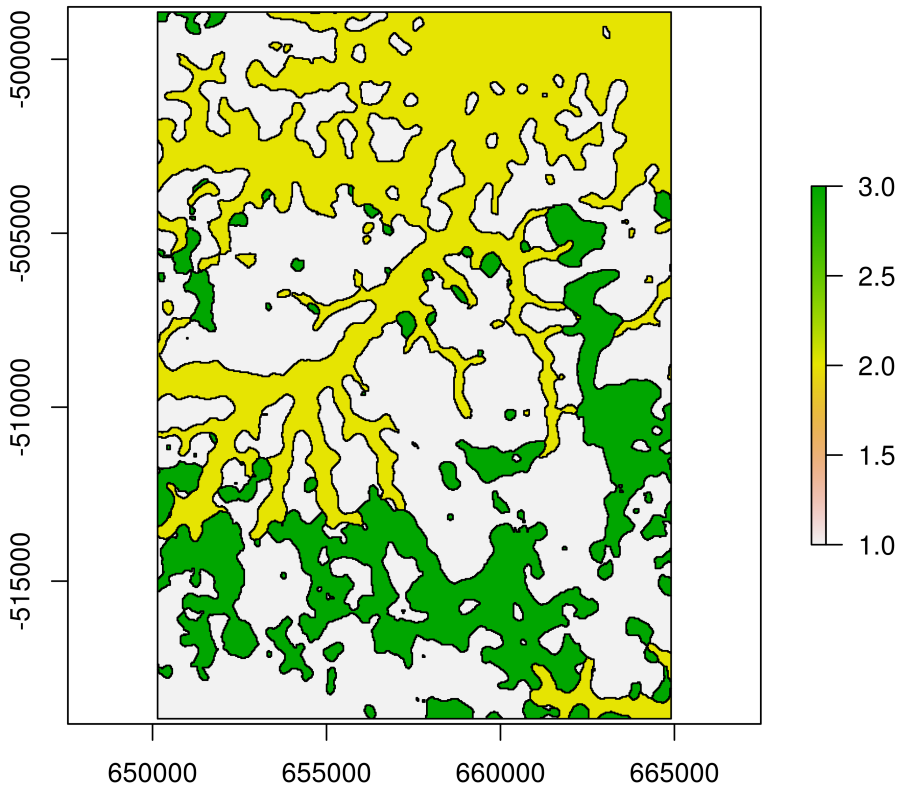

Sampling

```
#calculate area per class
lsat_map_poly$area <- area(lsat_map_poly)

# check resolution of the satellite image
res(lsat)
## [1] 30 30
# calcualte how many pixels are available per class
lsat_map_poly$pixels <- lsat_map_poly$area /(30*30)
```

```
# calcualte how many pixels should be included for the sampling
lsat_map_poly$no_samples <- round(lsat_map_poly$pixels/100 *1)

# now we will iterate over all unique classes
data_sampling <- lapply(unique(lsat_map_poly$layer), function(x){
  # first subset data according to the respective class
  sub <- subset(lsat_map_poly, layer == x)
  # create random sample points
  sub_sampled <- spsample(sub, n = sub$no_samples, type = "random")
  # add class name as response column
  sub_sampled$response <- rep(x,length(sub_sampled))
  return(sub_sampled)

  })

# combine the sampling results for all classes
data_sampling <- do.call(rbind,data_sampling)

# extract reflectance values from the satellite image
train_extracted <- data.frame(extract(lsat,
                              y=data_sampling,
                              cellnumbers = TRUE,
                              sp=TRUE))

# remove potential dublicates
train_extracted  <- train_extracted [!duplicated(train_extracted$cells), -2]
table(train_extracted$response)
##
##    1    2    3
## 1741  984  589
```

Outlier detection

Because no convenient function was available in the randomForest or range package, we make use of the CORElearn package to exclude potential outliers based in the Random Forest proximity measure.

```
library(CORElearn)

# subset data
train_df <- train_extracted[c(1:8)]
# we use factor in case of classification
train_df$response <- factor(train_df$response)
# model construction
```

```
md <- CoreModel(response ~ .,
                train_df,
                model="rf",
                rfNoTrees=500,
                maxThreads=1)

# calculate outier measure
outliers <- rfOutliers(md, train_df)

plot(md, train_df, rfGraphType="outliers")
abline(h = 10)
```

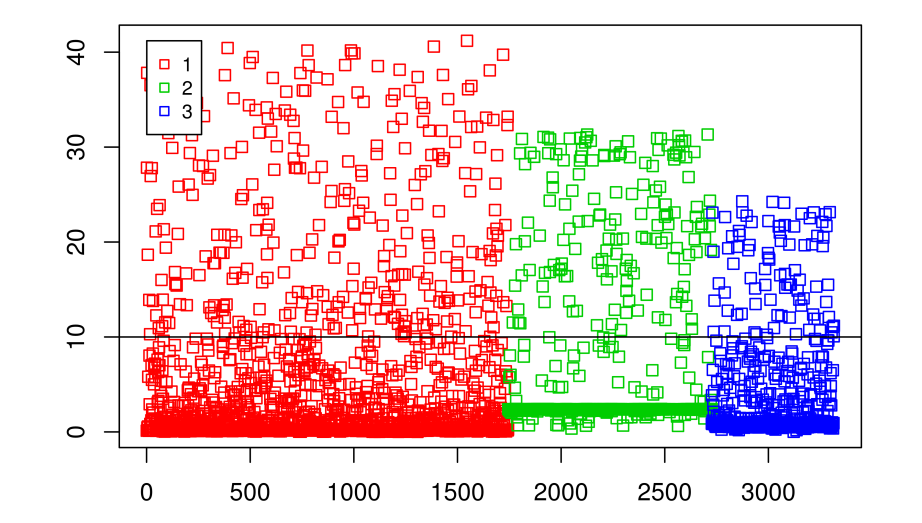


```
# clean up
destroyModels(md)
train_df$out <- abs(outliers)
```

Model validation

We use a cut-off value of 10 to exclude all samples considered as outlier.

```
library(ranger)
library(mlr)

train_df_cleaned <- train_df[train_df$out < 10,]

# Number of excluded outliers per class
table(train_df$response) - table(train_df_cleaned$response)
```

```
##
##   1   2   3
## 318 168 100
train_df_uncleaned <- train_df[c(1:8)]
train_df_cleaned <- train_df_cleaned[c(1:8)]

#number of predictor variables randomly sampled as candidates at each split
mtry <- round(sqrt(length(names(train_df_cleaned))))
# number of trees to be constructed
num.trees <- 500
# number of folds
k <- 5
# number of repetitions
reps <- 10

# define task and learner for cleaned sample dataset
cleaned_task <- makeClassifTask(id = "lsat_cleaned",
                                data = train_df_cleaned,
                                target = "response")

# define learner
rf_learner <- setHyperPars(makeLearner("classif.ranger"),
                           par.vals = list(mtry = mtry,
                                           num.trees = num.trees))

#define non-spatial, repeated cross-validation
rdesc = makeResampleDesc("RepCV",
                         reps=reps,
                         folds=k,
                         predict = "test")

# validation
res_cleaned <- mlr::resample(learner = rf_learner,
                             task = cleaned_task,
                             resampling = rdesc,
                             measures = list(
                               setAggregation(acc, test.mean),
                               setAggregation(acc, test.sd),
                               setAggregation(kappa,test.mean),
                               setAggregation(kappa,test.sd)),
                             models = FALSE,
                             show.info = FALSE)

# define task and learner for the uncleaned sample dataset
uncleaned_task <- makeClassifTask(id = "lsat_uncleaned",
                          data = train_df_uncleaned,
                          target = "response")
```

```
# validation
res_uncleaned <- mlr::resample(learner = rf_learner,
                               task = uncleaned_task,
                               resampling = rdesc,
                               measures = list(
                                 setAggregation(acc, test.mean),
                                 setAggregation(acc, test.sd),
                                 setAggregation(kappa,test.mean),
                                 setAggregation(kappa,test.sd)),
                               models = FALSE,
                               show.info = FALSE)
```

Comparison

```
#"uncleaned" training data
res_uncleaned$aggr
##   acc.test.mean     acc.test.sd kappa.test.mean   kappa.test.sd
##     0.905190906     0.008311368     0.842784621     0.014300796
#"cleaned" training data
res_cleaned$aggr
##   acc.test.mean     acc.test.sd kappa.test.mean   kappa.test.sd
##               1               0               1               0
```

Prediction of probabilities

```
# construct model with probability = TRUE
ranger_model <-ranger(response ~ .,
                      data=train_df_cleaned,
                      probability=TRUE,
                      num.threads = 1)
# convert raster to data.frame with coordinates
img_df <- as.data.frame(lsat, xy=TRUE)
# Run predictions
rf_proba <- predict(object=ranger_model,
                               data=img_df[3:length(names(img_df))],
                               type="response",
                               num.threads=1,
                               num.trees = ranger_model$num.trees,
                               probability = TRUE)
proba_rast <- rasterFromXYZ(cbind(img_df[1:2], data.frame(rf_proba$predictions)))
names(proba_rast) <- c(paste0("p", colnames(rf_proba$predictions)))

plot(proba_rast)
```

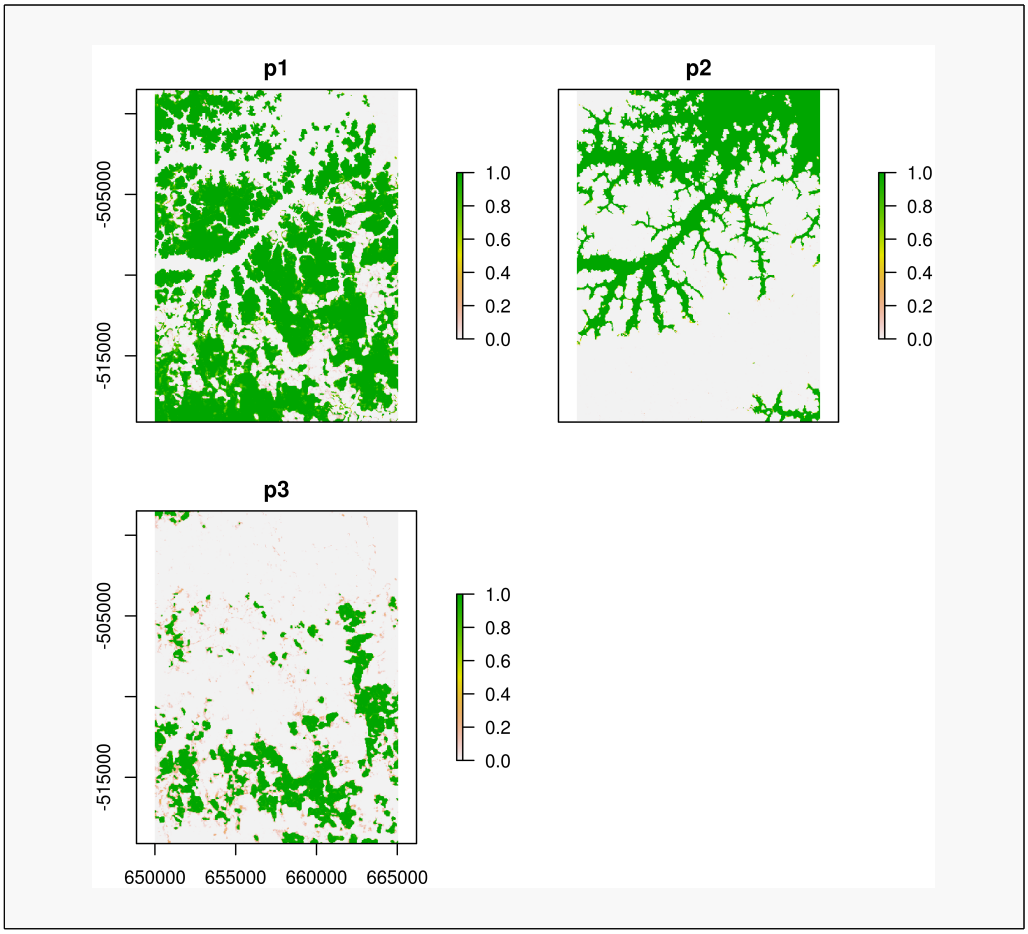

References

Wegmann, M., Leutner, B., Dech, S., 2016. “Remote Sensing and GIS for Ecologists: Using Open Source Software.” *Pelagic Publishing Ltd.*

4

CHAPTER 4 – COMBINING SENTINEL-1 AND SENTINEL-2 DATA FOR ESTIMATING FORAGE QUANTITY AND QUALITY OF SEMI-NATURAL GRASSLAND IN GERMANY TO SUPPORT A TARGET-ORIENTED HABITAT AND WILDLIFE MANAGEMENT

Raab, C., F. Riesch, B. Tonn, B. Barrett, M. Meißner, N. Balkenhol and J. Isselstein. "Combining Sentinel-1 and Sentinel-2 data for estimating forage quantity and quality of semi-natural grassland in Germany to support a target-oriented habitat and wildlife management."

Highlights

- Radar (Sentinel-1) and multispectral (Sentinel-2) data were evaluated for mapping semi-natural grassland forage quantity and quality indicators.

- The predictor dataset was optimised using permutation-based variable importance, maximising the predictive power of the random forest regression models.

- Simple ratios between the narrow near-infrared and red-edge region were among the most important variables.

Abstract

Semi-natural grasslands represent ecosystems with high biodiversity. Their conservation depends on the removal of biomass, e.g. through grazing by livestock or wildlife. For this, spatially-explicit information about grassland forage quantity and quality is a prerequisite for an efficient management. The recent advancements of the Sentinel satellite mission, providing valuable information with a high spatiotemporal resolution, offer new possibilities to support the conservation of semi-natural grasslands. In this study, the combined use of radar (Sentinel-1) and multispectral (Sentinel-2) data to predict forage quantity and quality indicators of semi-natural grassland in Germany was investigated. Field data for organic acid detergent fibre concentration (oADF), crude protein concentration (CP), compressed sward height (CSH), and standing biomass dry weight (DM) collected between 2015 and 2017 were related to remote sensing data using the random forest regression algorithm. In total, 102 optical- and radar-based predictor variables were used to derive an optimised dataset, maximising the predictive power of the respective model. High R^2 values were obtained for the grassland quality indicators oADF (R^2 = 0.79, RMSE = 2.29%) and CP (R^2 = 0.72, RMSE = 1.70%) using 15 and eight predictor variables, respectively. Lower R^2 values were achieved for the quantity indicators CSH (R^2 = 0.60, RMSE = 2.77 cm) and DM (R^2 = 0.45, RMSE = 90.84 g/m²). A permutation-based variable importance measure indicated a strong contribution of simple-ratio-based optical indices to the model performance. In particular, the ratios between the narrow near-infrared and red-edge region were among the most important variables. The model performance for oADF, CP and CSH was only marginally increased by adding Sentinel-1 data. For DM, no positive effect on the model performance was observed by combining Sentinel-1 and Sentinel-2 data. Thus, optical Sentinel-2 data resampled to a resolution of 10 m might be sufficient to

accurately predict forage quality, and to some extent also quantity indicators of semi-natural grassland.

Keywords: semi-natural grassland, Sentinel, forage quality and quantity, random forest, variable selection, satellite, radar

Introduction

Grassland ecosystems cover approximately 30% of the Earth's terrestrial surface and are habitats with high biodiversity (Dengler et al., 2014; Gibson, 2009; Riesch et al., 2018; Scurlock and Hall, 1998; Wilson et al., 2012). The conservation of semi-natural grasslands depends on management, as they originate from human activities, such as livestock grazing or mowing (Peeters et al., 2014). In the last decades, it has become pivotal to actively conserve semi-natural grasslands due to various threats including intensification of land use (Isselstein et al., 2005, Isselstein 2018), land abandonment (Valkó et al., 2018) and climate change (Dangal et al., 2016; Lamarque et al., 2014). From a conservation perspective, extensive grazing with livestock species and wildlife has become an established and suitable tool to maintain semi-natural grasslands (Borer et al., 2014; Bunzel-Drüke, 2008; Rosenthal et al., 2012; Van Wieren, 1995). The spatial distribution and activities of large herbivores are affected by the availability and quality of potential forage areas, and so is their impact on the ecosystem through grazing, trampling and dispersion of wastes (Catorci et al., 2016; Fløjgaard et al., 2017; Merkle et al., 2016; Palmer et al., 2003; Raynor et al., 2016). Therefore, spatially-explicit information about forage quantity and quality is of critical importance for active grazing management to conserve semi-natural grasslands. However, collecting field data is a labour-intensive and time-consuming task (Catchpole and Wheeler, 1992). Satellite remote

sensing offers unique possibilities to evaluate and predict grassland forage quantity and quality for large areas using empirical models (John et al., 2018; Mutanga et al., 2004). For this, regression techniques are used to relate field information to the data recorded by a satellite.

Earth observation sensors with high temporal and spatial coverage can be the preferred choice to establish a robust relationship between field and remote sensing reflectance data. The application of such data, for example recorded by the Moderate Resolution Imaging Spectroradiometer (MODIS) at 250−500 m spatial resolution or by the Medium Resolution Imaging Spectrometer (MERIS) at 300−1200 m spatial resolution, has been successfully applied in several geographical regions, such as the Xilingol steppe situated in the central part of Inner Mongolia (Kawamura et al., 2005), intensively managed grassland in Ireland (Ali et al., 2017) and agricultural and semi-natural grassland in the north of the Netherlands (Si et al., 2012). But the structural and botanical heterogeneity of semi-natural grasslands may require higher spatial and spectral resolutions. Hyperspectral remote sensing systems draw on the possibilities of the entire electromagnetic spectrum to relate remotely sensed reflectance data to chemical components or biomass of the vegetation cover (Cho and Skidmore, 2009; Darvishzadeh et al., 2014; Knox et al., 2011; Mutanga et al., 2004; Pellissier et al., 2015; Skidmore et al., 2010). However, hyperspectral remote sensing data are usually not commonly available and very high resolution multispectral satellites, such as RapidEye (Ramoelo et

al., 2012) (provides multispectral data at 5 m spatial resolution) or WorldView-2 (Ramoelo et al., 2015) (records multispectral data at 1.8 m spatial resolution) are operated by commercial companies. This can introduce financial constraints for the application of these data in long-term monitoring for conservation purposes. One freely available alternative could therefore be the medium resolution Operational Land Imager (OLI) sensor (records multispectral data at 30 m spatial resolution), mounted on the Landsat-8 satellite (Marsett et al., 2006). The higher spatial resolution of the recently started satellite mission Sentinel-2 (records multispectral data at 10, 20 and 60 m) of the European Space Agency offers further advantages, such as a higher spectral and temporal resolution (Delegido et al., 2011; Frampton et al., 2013; Ramoelo et al., 2015; Punalekar et al., 2018). In particular, Ramoelo et al. (2015) demonstrated for simulated multispectral Sentinel-2 data that the red-edge and short-wave-infrared regions of the electromagnetic spectrum were robust predictors for modelling the spatial distribution of nitrogen and therefore crude protein, in the Lowveld savanna of South-Africa. Similarly, promising results were recently shown by Punalekar et al. (2018) who used Sentinel-2 data to successfully estimate grassland biomass at farm level. The results showed a good agreement between compressed sward height measurements and the derived biomass maps.

All these spectral-based approaches depend on image acquisitions with a low cloud contamination rate and thus are restricted by weather

conditions. Synthetic aperture radar (SAR) sensors, such as the Sentinel-1 constellation operated by the European Space Agency, can penetrate through clouds and are less dependent on illumination conditions. In addition, SAR-systems can provide valuable information about vegetation structure and moisture content (Barrett et al., 2014; Ali et al., 2016; Wachendorf et al., 2017). The application of SAR-data has been successfully tested for agricultural applications, such as the detection of grassland mowing events (Tamm et al., 2016; Voormansik et al., 2016, 2013) or the estimation of grassland vegetation height and biomass (Zalite et al., 2016). When combined with multispectral remote sensing data, SAR-data might help to model biophysical properties of rapidly changing vegetation composition and structure at small scales (Dusseux et al., 2014).

In this article, the potential advantages of using combined Sentinel-1 and Sentinel-2 data to predict semi-natural grassland forage quantity and quality were explored. For this purpose, the random forest regression (Breiman, 2001) algorithm was applied on 102 potential predictor variables, including multispectral and SAR-indices. The study site was located in the south-east of Germany and is extensively grazed by wild red deer (*Cervus elaphus*) (Riesch et al., 2019). The following research questions were evaluated:

- Does combining multispectral (Sentinel-2) and radar (Sentinel-1) remote sensing data improve the mapping of semi-natural grassland forage quantity and quality?

- Can an optimised subset of the predictor dataset increase the random forest regression model performance?

Materials and methods

Study area

The study was carried out in the Grafenwoehr military training area (GTA) located in the south-east of Germany (Bavaria), extending over approximately 230 km² (Figure 1). GTA is part of the natural region of Upper Palatine-Upper Main Hills, bordering the Franconian Jura in the west, with elevations between 450 and 500 m above sea level. The long-term average temperature and precipitation are 8.3 ± 0.04 °C and 701 ± 4 mm, respectively (1981−2010, mean ± SEM, of four weather stations of the German Weather Service (DWD, Deutscher Wetterdienst) in the immediate vicinity). About 40% of GTA is covered with open habitats, such as semi-natural grassland, while forest covers the majority of the area (ca. 60%). Approximately 85% of GTA is part of the Natura 2000 network and contains many rare and highly protected habitat types, forming a refuge for numerous endangered species (Warren et al., 2014; Warren and Büttner, 2008a). The grasslands in the western third of GTA are underlain by more or less calcareous soils (Warren and Büttner 2008b, 2008a). Since 1947, GTA is used as a United States Army Garrison. This means that preserving the open landscape is of high importance for military use as well as for maintaining their conservation status. Soil fertility in the study area is low, comparable

with a pre-industrialised soil nutrient status of the first half of the 20th century (Riesch et al., 2018).

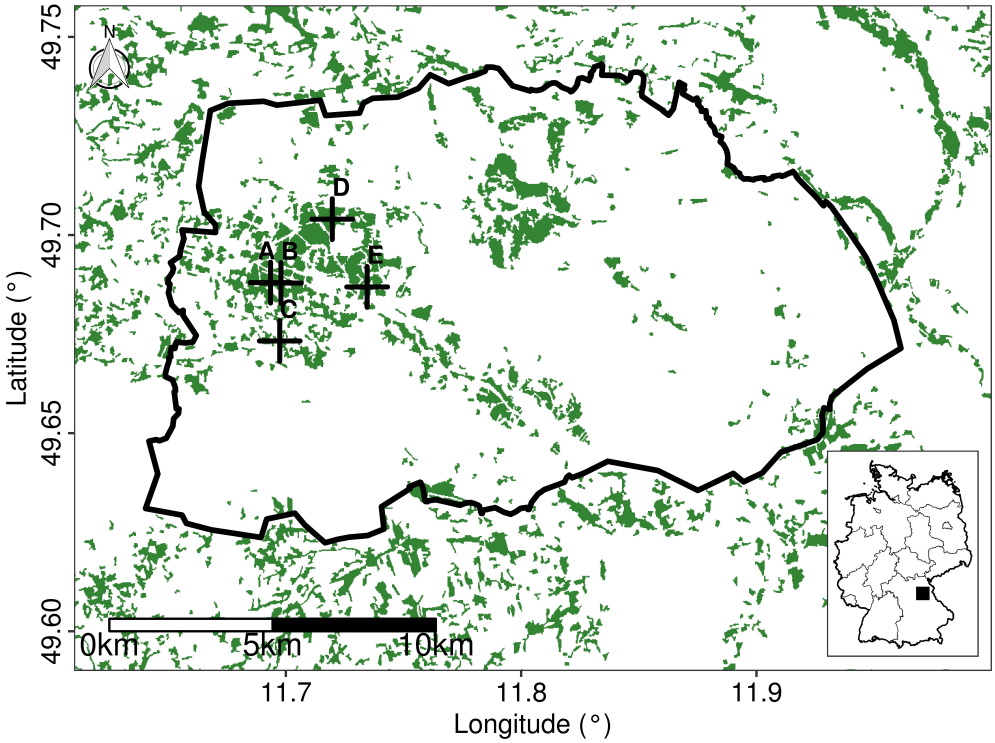

Figure 1: Location of the study site Grafenwoehr Military Training Area. The location of the study site in Germany is highlighted with a black square (lower right corner). The five sampling locations are marked with black crosses and labelled from A-E. The grassland layer is based on data provided by the Copernicus High Resolution Layer: Grassland (GRA) 2015 (© European Union, Copernicus Land Monitoring Service 2018, European Environment Agency (EEA)), illustrated in green.

Field data

Various methods exist to assess the quantity of available forage (t'Mannetje, 2000). A method that is particularly suitable for heterogeneous vegetation is measuring the compressed sward height (CSH) with a rising plate meter (Sanderson et al., 2001, Correll et al., 2003). This measurement can be converted to standing biomass dry weight (DM) based on calibration cuts (t'Mannetje and Jones, 2000). Forage quality depends on a large

number of chemical and physical biomass characteristics. Among these, the concentrations of crude protein (CP) and organic acid detergent fibre (oADF) are particularly useful parameters (Adesogan et al., 2000).

For this study, the forage quantity and quality dataset provided by the study of Riesch et al. (2019) was used, who investigated the grazing effect of red deer on plot level in GTA between 2015 and 2017. This dataset was collected on lowland hay meadows (EU Habitats Directive Annex I habitat type 6510, 'grasslands') in April, June, August and September in each of the studied years. At each of the five sampling sites (Figure 1), three management treatments were compared: grassland was either burnt in late winter/early spring, mown in July or remained untreated. This approximates the spectrum of grassland management activities on GTA and is, therefore, a good representation of the site conditions. In total, 15 sampling plots of 15 × 15 m were included in the dataset. Photographs illustrating one exemplary sampling area across different phenological phases are shown in Figure 2.

Figure 2: Photographs from one of the sampling plots at location B in Figure 1. Photographs were taken in a) May, b) August and c) October 2016.

Details on the respective sampling dates of the utilised dataset are given in Table 1. A subset of the dataset was used, according to the availability of Sentinel-2 data with regard to cloud contamination. For each plot and sampling date, Riesch et al. (2019) determined standing biomass and forage quality values with the following methods: standing biomass was estimated by a double-sampling strategy using CSH measured by a rising-plate meter in combination with calibration cuts, i.e. above ground biomass cut at ground level on a 0.18 m² area.

The relationship between calibration cut biomass (standing biomass dry weight, DM) and sward height was estimated using a linear model. Vegetation samples for the analysed forage quality parameters were collected on each sampling date by a hand pluck approach, mimicking grazing animals' foraging behaviour (Riesch et al., 2019). The total nitrogen concentration in plant material was assessed according to the Dumas combustion method in a CN elemental analyser and subsequently converted to CP.

Table 1: Sampling dates of the dataset provided by Riesch et al. (2019) and corresponding satellite data acquisitions used in this study.

Number	Sampling dates	Sensor	Date	Pass
1	2015-06-30−2015-07-02	S1-A	2015-06-26	D
		S1-A	2015-06-29	A
		S2-A	2015-07-04	D
2	2015-08-25−2015-08-26	S1-A	2015-08-21	A
		S1-A	2015-08-25	D
		S2-A	2015-08-26	D
3	2016-05-24−2016-05-26	S2-A	2016-05-22	D
		S1-A	2016-05-23	A
		S1-A	2016-05-27	D
4	2016-08-23−2016-08-24	S1-A	2016-08-19	D
		S1-A	2016-08-22	A
		S2-A	2016-08-27	D
5	2016-10-17−2016-10-20	S2-A	2016-10-16	D
		S1-A	2016-10-18	D
		S1-A	2016-10-21	A
6	2017-05-16−2017-05-17	S1-B	2017-05-16	D
		S2-A	2017-05-17	D
		S1-A	2017-05-18	A
7	2017-08-28−2017-08-30	S2-A	2017-08-25	D
		S1-A	2017-08-29	A
		S1-B	2017-09-01	D
8	2017-10-23−2017-10-25	S1-B	2017-10-22	A
		S1-A	2017-10-25	D
		S2-B	2017-10-29	D

S1: Sentinel-1, S2: Sentinel-2, D: descending orbit, A: ascending orbit.

Organic acid detergent fibre (exclusive of residual ash, oADF) was determined by near-infrared spectroscopy. Figure 3 gives an overview of the forage quantity and quality parameters provided by the field dataset. The variability of all parameters increased after June, as cutting lowered the quantity of

standing biomass, decreased the fibre and increased the protein concentration in the mown plots (Riesch et al., 2019).

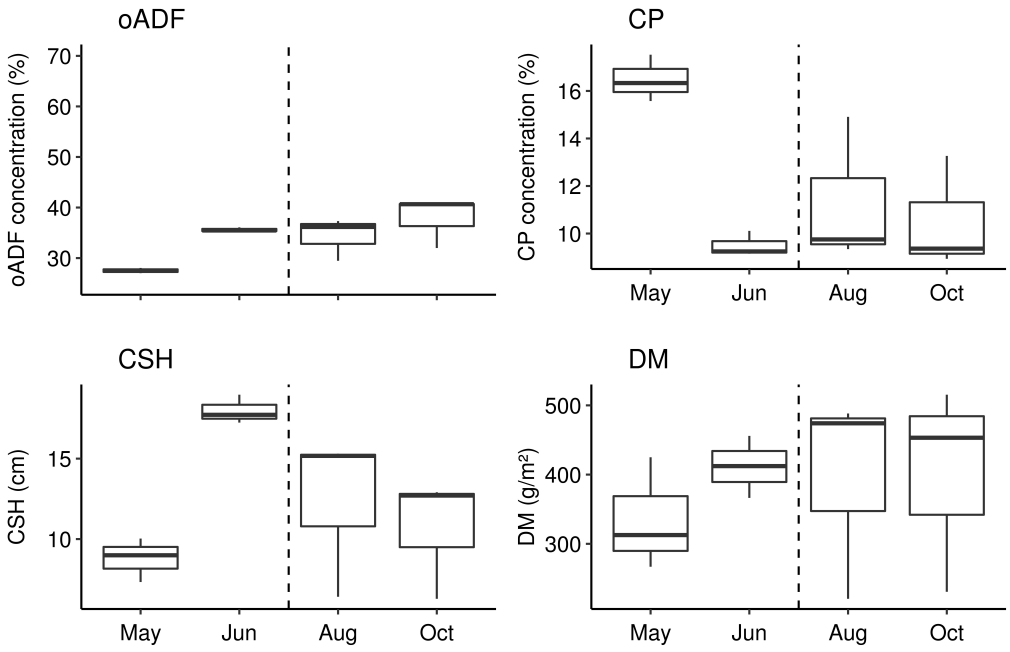

Figure 3: Grassland forage quantity and quality data used in this study (Riesch et al., 2019). The respective sampling dates are shown in Table 1. oADF = organic acid detergent fibre concentration (dry-matter-based, exclusive of residual ash), CP = crude protein concentration (dry-matter-based), CSH = compressed sward height, DM = standing biomass dry weight. The cutting events in July are indicated by the dashed line.

Satellite data and pre-processing

The study used Sentinel-1 and Sentinel-2 imagery for the estimation of semi-natural grassland forage quantity and quality. Both constellations are part of the Copernicus program, a joint initiative of the European Commission, European Space Agency and the European Union.

Sentinel-1A (launched on 3 April 2014) and Sentinel-1B (launched on 25 April 2016) satellites are equipped with a C-band synthetic-aperture

radar (SAR) with 5.6 cm wavelength (ESA, 2016a). Sentinel-1 level-1 (Ground Range Detected) data collected in the interferometric wide swath mode with dual polarisation (VV and VH) were used. This mode has a defined spatial resolution of 5 × 20 m.

Table 2: Spectral and spatial specifications of the Sentinel-2 constellation. NIR = near-infrared, SWIR = short-wave-infrared.

Band	Band name	Spatial resolution (m)	Wavelength centre (nm)	Spectral width (nm)
1	Coastal aerosol	60	443	20
2	Blue	10	490	65
3	Green	10	560	35
4	Red	10	665	30
5	Red-edge-1	20	705	15
6	Red-edge-2	20	740	15
7	Red-edge-3	20	783	20
8	NIR	10	842	115
8A	Narrow NIR	20	865	20
9	Water vapour	60	945	20
10	SWIR-cirrus	60	1375	30
11	SWIR-1	20	1610	90
12	SWIR-2	20	2190	180

Sentinel-2A (launched on 23 June 2015) and Sentinel-2B (launched on 7 March 2017) acquire data in 13 spectral wavelengths with a spatial resolution of 10, 20 and 60 m (Drusch et al., 2012). A detailed overview of the specifications is outlined in Table 2. Since the plot size of field sampling by Riesch et al. (2019) was 15 × 15 m, all analyses were continued with a spatial resolution of 10 m. In addition, all non-grassland areas were masked

according to the Copernicus High Resolution Layer: Grassland (GRA) 2015 (© European Union, Copernicus Land Monitoring Service 2018, European Environment Agency (EEA)).

Multispectral data pre-processing

All available level-1C top of atmosphere (TOA) reflectance Sentinel-2 data were acquired from https://scihub.copernicus.eu/dhus/#/home within a temporal window of seven days before and after the temporal mean of the respective sampling period of Riesch et al. (2019). All images with cloud and cloud-shadow contamination over the sampling sites were subsequently removed from the analysis. The final selection of Sentinel-2 images and the corresponding sampling dates are compiled in Table 1.

The pre-processing included atmospheric and topographic correction using Sen2Cor (Müller-Wilm et al., 2018), version 2.5.5). The Sentinel-2 data was resampled to 10 m spatial resolution using the SNAP software (ESA, 2016b) and the Sen2res resolution enhancement operator provided by Brodu (2017). For the subsequent analyses, all 60 m resolution bands were excluded, as they are mainly designed for atmospheric application purposes.

SAR data pre-processing

Sentinel-1 data were acquired from https://scihub.copernicus.eu/dhus/#/home in descending and ascending orbits as close as possible to the temporal mean of the selected sampling periods of Riesch et al. (2019) (Table 1). The data were pre-processed using

SNAP, applying the respective orbit file, geometric calibration, terrain correction, resampling to 10 m spatial resolution using bilinear interpolation and speckle filtering (Lee filter, 3×3). Finally, the data were converted to dB using a range-doppler approach.

Calculation of indices

Vegetation indices (VIs) are established as a suitable tool for the analysis of plant dynamics and ecosystem monitoring by multispectral satellite remote sensing (Pettorelli et al., 2005), including the chemical composition (Clevers and Gitelson, 2013; Frampton et al., 2013; Tong and He, 2017; Loozen et al., 2019) and quantity (Silleos et al., 2006; Ramoelo et al., 2015; Schweiger et al., 2015) of grassland biomass. Most VIs are relatively easy to compute and are able to reduce variability introduced by site-specific conditions, such as bare soil, illumination angle or the atmosphere. Thus, VIs can support the transferability of the estimation of vegetation conditions. VIs consist of a combination of different spectral bands. Simple ratios (SR) and normalised difference indices are the most commonly used, the normalised difference vegetation index (NDVI) (Rouse et al., 1973) being the most prominent. More complex VIs, such as the soil adjusted vegetation index (SAVI) (Huete, 1988) or the MERIS terrestrial chlorophyll index (MTCI) (Dash and Curran, 2004) have been successfully applied in several studies (Ullah et al., 2012; Jin et al., 2014; Loozen et al., 2019). Due to the well-covered red-edge-region of the Sentinel-2 sensors,

Frampton et al. (2013) proposed the inverted red-edge chlorophyll index (IRECI) and the Sentinel-2 red-edge position (S2REP) index for the quantitative estimation of biophysical variables in vegetation. The red-edge region describes the spectral feature between the red absorption maximum and a reflectance-peak in the near infrared, which can be linked to the chemical composition of vegetation and vegetation biomass (Clevers and Gitelson, 2013; Frampton et al., 2013). The Microwave Polarization Difference Index (MPDI) is calculated similarly to the multispectral-based NDVI (Hird et al., 2017). Calculated from vertical-vertical (VV) and vertical-horizontal polarisation (VH) data of a SAR-system, the MPDI elements were shown to be sensitive to, for example surface roughness and vegetation structure (Chauhan and Srivastava, 2016; Periasamy, 2018).

In total, 77 multispectral-based vegetation indices were included, commonly found in the literature. In addition, five biophysical products (L2B) were calculated using the biophysical processor in SNAP. These L2B products included leaf area index, fraction of absorbed photosynthetically active radiation, cover fraction, canopy water content and canopy chlorophyll content. Moreover, six SAR indices, such as simple ratios and MPDI were added to the analyses. In total, 102 predictor variables were available for the grassland forage quantity and quality random forest regression models, including 10 multispectral bands, four SAR bands from different orbits and five L2B products. All included predictor variables can be found in Table S1−S3 of the supplementary material.

Statistical analysis

The random forest (RF) regression algorithm was used to assess the relationships between grassland forage quantity and quality and remote sensing derived datasets. Several statistical analysis techniques for the estimation of forage biomass and chemical composition exist (Ali et al., 2016). They include partial least square regression or stepwise multiple linear regression (Ramoelo et al., 2012; Pellissier et al., 2015) and more advanced machine learning techniques, such as RF (Ramoelo et al., 2015) and artificial neural networks (Skidmore et al., 2010). RF can be characterised as an ensemble of decision trees. The prediction is based on a majority vote among all constructed trees. The variables used and the training samples for each respective tree are randomly sampled with replacement from the input data. So far, the RF algorithm has most commonly been used for classification (Belgiu and Drăguţ, 2016), but its robustness in a regression context has been confirmed in various studies (e.g. Mutanga et al. (2012) and Ramoelo et al. (2015)). Therefore, we will use of the RF algorithm in this study.

In a first step, three different predictor variable sets were applied to RF algorithm in order to compare the change in model performance depending on the selected input variables. These models used either predictor variables originating from Sentinel-2 data only, Sentinel-1 only or a combination of both. The analyses were initially performed with a full predictor dataset. The model performance was estimated as the root mean

square error (RMSE) using a 10-fold cross-validation. In addition, predictor variable importance was estimated using a permutation approach (Brenning, 2012; Ruß and Brenning, 2010). The least important variable was determined by excluding one variable at a time from the model and calculating the mean decrease in RMSE after 100 permutations and 100 repetitions. The variable whose exclusion caused the smallest increase in RMSE was permanently left out of the respective model. Based on an a priori decision, this process was repeated until only two variables were left in the final model.

In a second step, an optimised predictor variable combination for each response variable (oADF, CP, CSH and DM) was selected based on the lowest RMSE from all calculated models. These respective optimised final models were additionally validated using a 10-fold cross-validation procedure with 1000 repetitions. The calculation of variable importance for each optimum model was estimated with 1000 permutations per predictor variable.

All RF models were built using default settings. The number of variables randomly sampled as candidates at each split (mtry) were set to the number of input variables divided by three, constructed with 500 trees (num.trees) (Belgiu and Drăguț, 2016).

Finally, the spatial distribution of oADF, CP, CSH and DM was predicted using the best variable combination. All final maps were averaged over 100 predictions.

All analyses were carried out within the R statistical programming environment (R Core Team, 2018) using the packages *ranger* for RF regression (Wright and Ziegler, 2015), *mlr* (Bischl et al., 2016) for cross-validation and permutation, and *raster* (Hijmans, 2017) for the spatial predictions.

Results

Selection of predictor dataset and validation

A relatively weak performance was observed for models with Sentinel-1 data only, compared to models where Sentinel-2 data were included (Table 3). The lowest RMSE and highest R^2 for oADF, CP and CSH were reached using the combined Sentinel-1 and Sentinel-2 predictor dataset. For DM, the lowest RMSE was obtained by the Sentinel-2 only dataset, but the difference to the combined Sentinel-1 and Sentinel-2 predictor dataset was marginal. Therefore, all subsequent analyses were conducted with the combined Sentinel-1 and Sentinel-2 dataset.

The validation results after iteratively removing predictor variables from the combined Sentinel-1 and Sentinel-2 dataset are illustrated in Figure 4. Starting with a full set of 102 variables, removing predictor variables initially increased the R^2 value. After reaching a maximum, the R^2 rapidly decreased for oADF, CP, CSH and DM. A reverse behaviour was observed for the normalised RMSE. The normalisation is expressed between zero and one according to the observed minimum and maximum. The models with the lowest RMSE contained 8−15 predictor variables (Table 4).

Table 3: Performance of the three different predictor datasets estimated using random forest regression. Predictors were iteratively removed based on variable importance. The R^2 and RMSE testing values are means of 100 repetitions of a 10-fold cross validation. oADF = organic acid detergent fibre concentration, CP = crude protein concentration, CSH = compressed sward height, DM = standing biomass dry matter weight. S1 = Sentinel-1 predictor dataset, S2 = Sentinel-2 predictor dataset, S1+S2 = combined Sentinel-1 and Sentinel-2 predictor dataset. The lowest RMSE and highest R^2 values are highlighted in bold.

	oADF (%)			**CP (%)**			**CSH (cm)**			**DM (g/m²)**		
	S1	**S2**	**S1+S2**	**S1**	**S2**	**S1+S2**	**S1**	**S2**	**S1+S2**	**S1**	**S2**	**S1+S2**
RMSE max	5.51	2.71	2.70	3.52	2.13	2.1	4.55	3.44	3.44	127.75	111.24	111.44
RMSE min	5.32	2.37	**2.29**	3.38	1.78	**1.7**	4.11	2.79	**2.76**	120.48	**90.63**	90.82
RMSE *sd*	0.07	0.06	0.08	0.04	0.04	0.06	0.15	0.08	0.09	2.08	2.61	2.55
R^2 max	-0.02	0.78	**0.79**	-0.05	0.7	**0.73**	0.12	0.59	**0.60**	0.04	**0.45**	**0.45**
R^2 min	-0.01	0.71	0.71	-0.15	0.57	0.58	-0.08	0.36	0.36	-0.09	0.17	0.16
R^2 *sd*	0.03	0.01	0.01	0.03	0.02	0.02	0.06	0.03	0.03	0.04	0.03	0.03

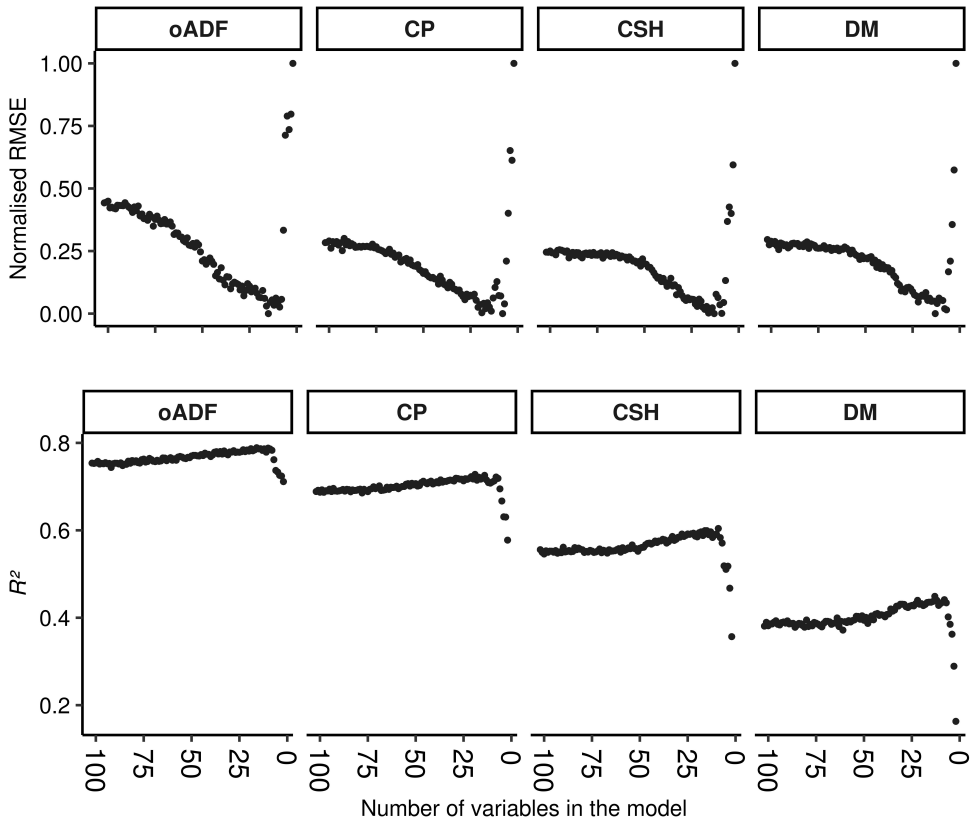

Figure 4: Changes in R^2 and normalised RMSE depending on the number of predictor variables remaining in the random forest regression model as variables are iteratively removed from the combined Sentinel-1 and Sentinel-2 predictor dataset. The R^2 and RMSE testing values are means of 100 repetitions of a 10-fold cross validation of the respective predictor and repetition. oADF = organic acid detergent fibre concentration, CP = crude protein concentration, CSH = compressed sward height, DM = standing biomass dry matter weight.

The high R^2 testing values indicated a good match between observed and predicted oADF and CP concentrations. This was supported by relatively low RMSE testing values in comparison to the range of oADF and CP concentrations measured in the field. The small R^2 and RMSE standard deviation testing values after 1000 repetitions further supported good model

performances. For CSH and DM, lower R^2 testing values were observed compared to oADF and CP. The estimated RMSE values were moderately higher, considering the respective observed range of the data. For both CSH and DM, 13 predictor variables remained in the final model.

Table 4: Statistics reporting the comparison of the selected best model for oADF = organic acid detergent fibre concentration, CP = crude protein concentration, CSH = compressed sward height, DM = standing biomass dry weight. The R^2 and RMSE values are means of 1000 repetitions of a 10-fold cross validation using random forest regression.

	oADF (%)	**CP (%)**	**CSH (cm)**	**DM (g/m²)**
Min observed	23.37	5.91	2.93	117.57
Max observed	47.97	21.33	25.55	630.07
RMSE testing	2.29	1.70	2.77	90.84
RMSE testing *sd*	0.42	0.35	0.60	17.63
RMSE training	0.99	0.75	1.20	39.18
RMSE training *sd*	0.02	0.02	0.03	0.95
R^2 testing	0.79	0.72	0.60	0.45
R^2 testing *sd*	0.13	0.15	0.17	0.23
R^2 training	0.97	0.96	0.94	0.91
R^2 training *sd*	<0.01	<0.01	<0.01	<0.01
Number of variables	15	8	13	13
Number of radar variables	2	1	2	0

To assess how the models behave when applied to test data, the RMSE and R^2 were compared for both training and testing datasets from the cross-validation procedure (see Table 4). The mean RMSE results of the training phase of all models were considerably lower than the testing results. For oADF, the RMSE testing value was 1.3% higher compared to the training result. Little variation in the model robustness was observed for the

training result across all models, indicated by low standard deviation values. For all grassland forage quantity and quality indicators, R^2 values close to 1 were observed for the training phase. However, the testing results were much lower for all models. For DM, a large difference between training (R^2 = 0.91) and testing (R^2 = 0.45) was found. For oADF and CP, the differences were less pronounced. Thus, the robustness of CSH and DM R^2 results was lower than that of forage quality indicators.

Variable importance

Permutation-based variable importance was used to identify important predictor variables for oADF, CP, CSH, and DM from the optimised combined Sentinel-1 and Sentinel-2 dataset (see Figure 5). For oADF and CP, the most important variable was the simple ratio between the narrow near-infrared (B8A) and the red-edge-3 (B7) band. Excluding this simple ratio from the model decreased the performance in terms of R^2 by 0.10 for oADF and 0.18 for CP. A similar simple ratio, narrow near-infrared divided by red-edge-2 (B6), contributed substantially to the model performance of CSH and DM. For DM, R^2 decreased by 0.22 when this particular simple ratio was excluded from the model. For CSH, the simple ratio between the short-wave-infrared-2 (B12) and the red (B4) band was found to be the most relevant variable. Single multispectral bands were in the optimised predictor dataset for oADF, CSH and DM, but their removal did not decrease R^2 by more than 0.06. The SAVI and its extensions that use

different red-edge bands instead of the red band were important for oADF, CP, CSH and DM. Other vegetation indices contributed to the model performances to smaller extents. For CP, vegetation indices were more important than for oADF, CSH and DM. Sentinel-1 variables were only selected for oADF, CP and CSH models. The general contribution of SAR-variables was low compared to simple ratios or vegetation indices. No L2B variable was selected by the variable optimisation process.

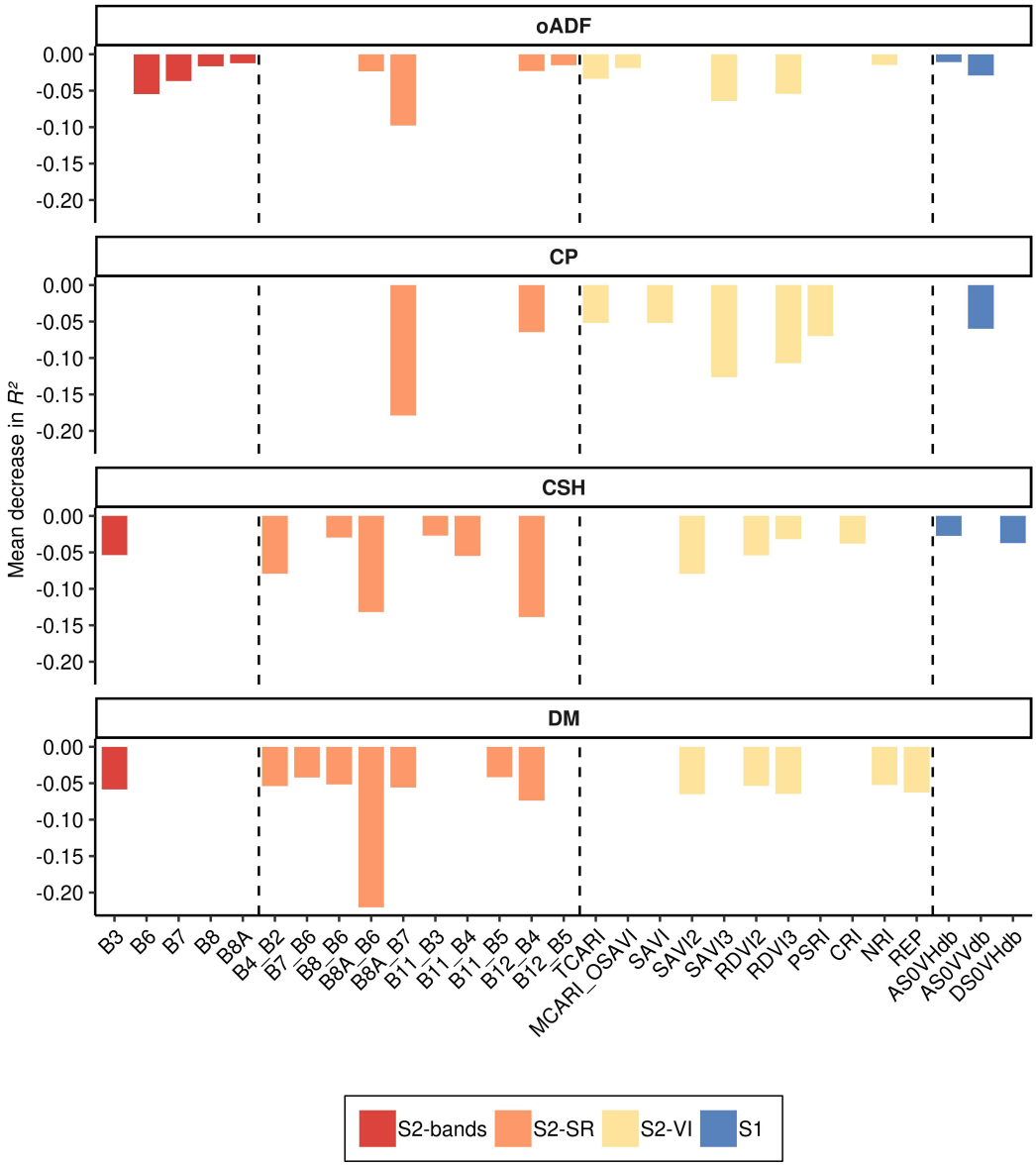

Figure 5: Permutation-based variable importance derived as an increase in RMSE caused by excluding one variable and keeping the rest in the model. Explanations to the respective x-axis labels can be found in the supplementary material (Tables S1–S3). B = band (Table 2), underscore = divided by. a) oADF = organic acid detergent fibre (exclusive of residual ash), b) oNDF = organic neutral detergent fibre (exclusive of residual ash), c) CP = crude protein, d) CSH = compressed sward height, e) DM = standing biomass dry weight.

Spatial prediction

Figure 6 displays the spatial predictions for oADF, CP, CSH and DM derived from the optimised predictor variables by applying the respective RF model. For illustration purposes, the figures and following descriptions are presented for the area surrounding the two sample locations A and B of Figure 1. Only the results for May and October 2016 are presented; spatial predictions for further sampling dates can be found in Figures S1–S3 in the supplementary material.

A relatively even distribution of oADF concentrations was observed for May 2016 (Figure 6a). In October 2016, the spatial distribution of concentrations was more differentiated, especially at the edges of the masked non-grassland areas. The mean predicted oADF concentration was about 29.3% (*sd* = 0.97%) for May and about 36.6% (*sd* = 4.52%) for October 2016, which corresponds to the observed concentrations in Figure 3.

Similar to oADF, a relatively even distribution of CP concentrations was observed for May 2016 (Figure 6b). The mean CP concentration in May 2016 was about 15.1% (*sd* = 0.98%). For October 2016, the spatial distribution of CP showed a distinct differentiation in areas with CP concentrations either above or below approximately 8%, with a mean predicted CP concentration of 10.8% (*sd* = 2.54%).

For May 2016, a mean CSH of 10.3 cm (*sd* = 1.84 cm) and for October a mean CSH of 9.9 cm (*sd* = 2.64 cm) were predicted. Similar to the

predictions of CP, CSH showed a spatial differentiation, with values either below or above 10 cm (Figure 6c). A corresponding distinction was present for the DM predictions. A mean DM of 355.0 g/m² (*sd* = 67.0 g/m²) in May and 329.9 g/m² (*sd* = 84.18 g/m²) in October was predicted. In general, a more even spatial distribution of oADF and CP concentrations in May and a more pronounced differentiation in October 2016 was observed. This was similar for CSH and DM, but with a higher degree of variance in May. Areas with high CP and low oADF concentrations in October 2016 were related to areas with low CSH and DM values, and vice versa. A similar but less pronounced pattern between the predicted vegetation characteristics was observed for the spatial predictions in May.

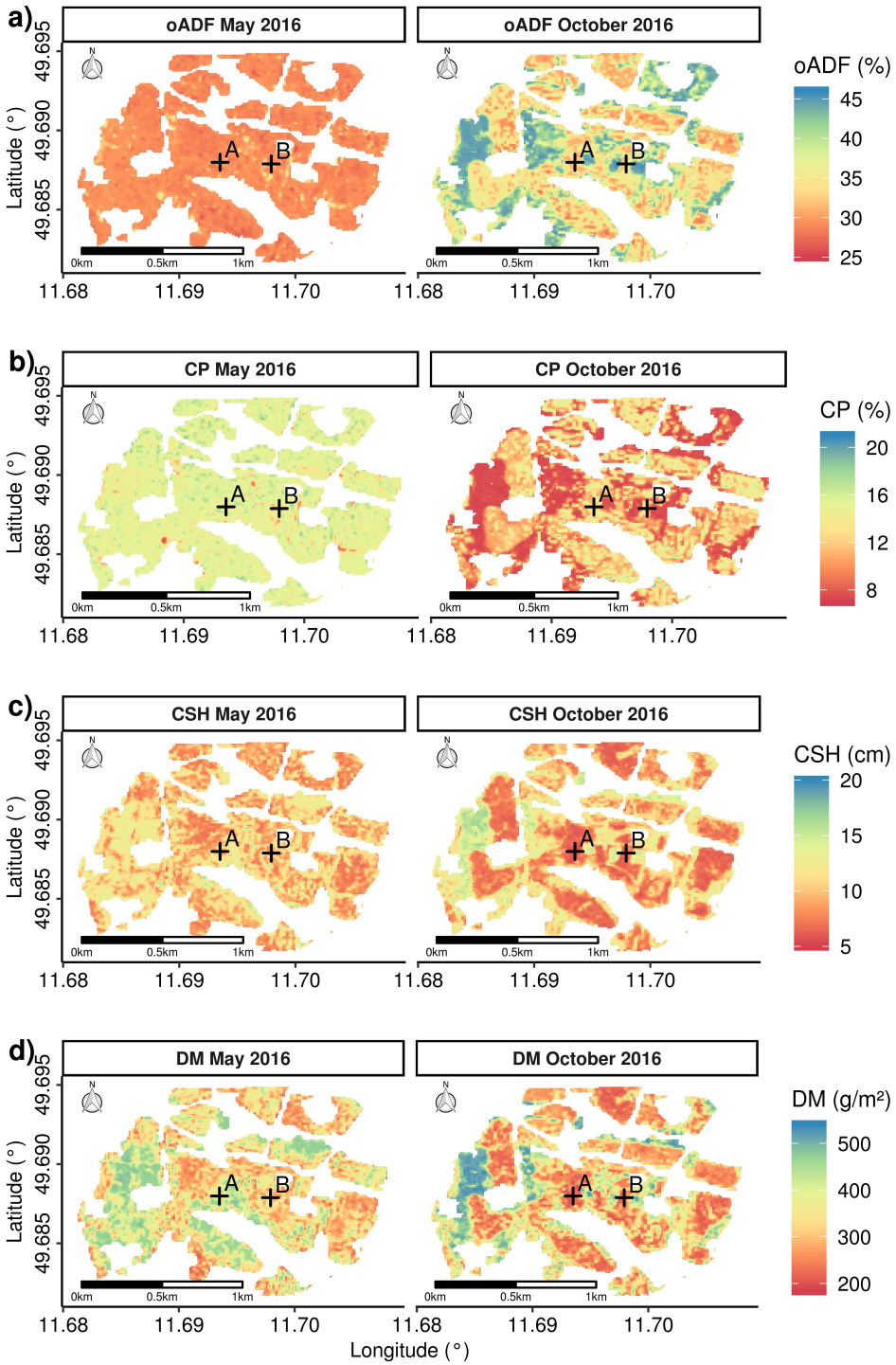

Figure 6: Spatial predictions of oADF = organic acid detergent fibre concentration, CP = crude protein concentration, CSH = compressed sward height, DM = standing biomass dry weight for May and October 2016 using random forest regression, averaged over 100 repetitions. The illustrations are presented for the area surrounding the two sampling locations A and B of Figure 1.

Discussion

This study shows that semi-natural grassland forage quality indicators can be mapped with high accuracy, as R^2 values of the regression models ranged from 0.72 (*sd* = 0.15) for CP to 0.79 (*sd* = 0.13) for oADF. For the grassland forage quantity indicators, lower R^2 values were obtained (R^2 = 0.60, *sd* = 0.17 for CSH and R^2 = 0.45, *sd* = 0.23 for DM). When analysed separately, Sentinel-1 data had a low performance for all considered indicators. When Sentinel-1 data were added to Sentinel-2 data, the RF model performance increased only marginally. In particular, the max R^2 values of all models considered in Table 3 were only higher by 0.025 for CP and about 0.012 higher for oADF and CSH for the combination of both data sources. For DM, the difference was negligible.

Sentinel-1 data for grassland forage quantity and quality prediction

Despite the generally low contribution of Sentinel-1 data to the model performance, between one and two SAR variables were among the most important variables for the prediction of oADF, CP and CSH (Figure 5). The small contribution of Sentinel-1 data to the final models might be attributed to the wavelength (5.6 cm) of the C-band sensor. Even though the amount of studies concerned with the estimation of biophysical parameters for semi-natural grasslands is limited, Zalite et al. (2016) demonstrated the potential of X-band data with a wavelength of about 3 cm to map biophysical parameters on agricultural grassland. For this purpose,

HH-polarised COSMO-SkyMed 1-day repeat-pass SAR pairs were used to inversely relate temporal interferometric coherence to vegetation height and fresh above-ground biomass. In addition, Ali et al. (2017) showed that TerraSAR-X interferometric coherence data can be used successfully to predict agricultural grassland height (R^2 = 0.55) and biomass (R^2 = 0.75) at the paddock scale. Thus, further research is required to investigate the potential contribution of X-band SAR data to predict semi-natural grassland forage quality and quantity indicators.

Optimisation of the predictor dataset

The repeated reduction of the combined Sentinel-1 and Sentinel-2 complete dataset (102 variables) provided an optimised subset of predictor variables for semi-natural grassland forage quantity and quality indicators with 8 to 15 variables. Several studies have selected important variables for the prediction of biophysical parameters of grassland from remote sensing data (Loozen et al., 2019; Mutanga et al., 2004; Tong and He, 2017). Linear-based machine learning approaches, such as lasso and ridge regression, recently showed promising results for the selection of important predictor variables (Zandler et al., 2015). However, non-linear relationships between spectrally-derived predictor variables and biophysical response variables can be present (Mutanga and Kumar, 2007; Mutanga and Skidmore, 2004; Skidmore et al., 2010). When time-series data are applied, the correlation between a predictor variable and the respective biophysical variable may

change its slope, depending on the phenological phase. In such cases, the non-linear, decision-tree-like RF regression algorithm can be superior to linear regression techniques (Beckschäfer et al., 2014; Strobl et al., 2007). Because the internal importance measure of the RF was shown to be biased (Strobl et al., 2007), and the conditional RF is very computationally intensive (Nicodemus et al., 2010), the applied permutation-based variable selection can be seen as an appropriate strategy. Thus, a subset of variables could be identified, important for the prediction of semi-natural grassland quantity and quality. However, a tendency of the RF to adapt to the training data and a decreased performance in the validation phase was observed (Table 4).

Important variables for the prediction of semi-natural grassland forage quantity and quality

The dominant source for the selected predictor for the prediction of semi-natural grassland forage quantity and quality indicators variables originated from both 10 m and 20 m spatial resolution Sentinel-2 data (Figure 5). This underlines the importance of including all 20 m spatial resolution bands, resampled to 10 m using the applied Sen2res resolution enhancement operator provided by Brodu (2017). This is contrary to the results observed by Punalekar et al. (2018) who found that the 10 m bands from *in situ* hyperspectral data resampled to Sentinel-2A were sufficient to estimate leaf area index (LAI) using a radiative transfer model (PROSAIL) on agricultural grassland. The LAI can be related to vegetation biomass (e.g.

Friedl et al. (1994) and Dusseux et al. (2015)), but radiative transfer models such as PROSAIL assume canopies to be rather homogeneous. Hence, Darvishzadeh et al. (2008) showed that the limitation of PROSAIL-based LAI predictions increased with increasing species diversity. Therefore, the presented regression approach might be more suitable for mapping forage quality and quantity on semi-natural grasslands.

In order to relate field observations of grassland forage quantity and quality to remote sensing data, a certain number of predictor variables might be required to increase the predictive power of a regression model. In the presented study, the most important groups of variables for the prediction of oADF, CP, CSH and DM were simple spectral ratios followed by spectral vegetation indices (Figure 5). For the prediction of the quality indicators oADF and CP, the simple ratio between the narrow near-infrared (band 8A, Table 2) and red-edge-3 (band 7, Table 2) band contributed most to the respective model. A similar result was observed for CSH and DM. The simple ratio between the narrow near-infrared and red-edge-2 band as well as the ratio between the short-wave-infrared-2 and red band were the two most essential variables for the model. The importance of the red-edge region to predict biophysical parameters of grassland was confirmed by several other studies (Clevers and Gitelson, 2013; Delegido et al., 2011; Duan et al., 2012; Frampton et al., 2013; Ramoelo et al., 2015b, 2012; Tong and He, 2017; Verrelst et al., 2012). The reflectance in the NIR-part can be related to leaf structure, while the red-edge region is related to chlorophyll

concentration (Sims and Gamon, 2002; Tong and He, 2017). Because of the relationship between chlorophyll and nitrogen, the red-edge reflectance may therefore be related to vegetation protein concentration. As illustrated in Figure 3, the positive relationship between vegetation quantity indicators (CSH and DM) and CP was very pronounced until mowing in July. For oADF the relationship was negative. Thus, the ratio between the narrow near-infrared band 8A and one of the red-edge bands can approximate the relationship between grassland quality and quantity. The application of this relationship by a normalisation, similar to the NDVI, might therefore facilitate the estimation and monitoring of semi-natural and agricultural grassland quantity and quality by remote sensing. This would require further research for different geographical regions and types of grassland.

Remote sensing for the conservation of semi-natural grassland

For pasture management purposes, remote sensing has been proven to be a valuable tool to predict grassland forage mass and quality indicators (Ali et al., 2016; Wachendorf et al., 2017). This can be of high importance for farmers, e.g. for rotational grazing systems, as well as for conservation (e.g. Punalekar et al. (2018) and Riesch et al. (2019)). Marginal areas, however, are often characterised by more heterogeneous land cover. In the special case of an active military training area, access restrictions challenge the management and conservation of open habitats, such as semi-natural grasslands. Under such landscape conditions, the potential of wild

herbivores as a management and conservation option has recently been acknowledged (Pausas and Bond, 2018; Schulze et al., 2018). For the GTA, Riesch et al. (2019) showed that red deer can contribute significantly to the conservation of semi-natural grassland ecosystems. In particular, it was shown that forage removal was enhanced in mown grassland, related to an increased productivity and forage quality (Riesch et al., 2019). The present study provides evidence that for semi-natural grassland ecosystems forage mass and quality indicators can be successfully predicted using freely available Sentinel data. Thus, the conservation of open landscapes could be supported by a target-oriented habitat and consequently wildlife management (Raynor et al., 2017). To what extent management activities, such as mowing, can be used to spatially direct the utilisation of semi-natural grasslands as foraging areas by wild herbivores requires further research.

Conclusion

The present study has evaluated the possibilities of combining Sentinel-1 and Sentinel-2 data for estimating semi-natural grassland quantity and quality. Predictor variables derived from the Sentinel-2 sensors were sufficient to accurately predict organic acid detergent fibre concentration, crude protein concentration, compressed sward height, and standing biomass dry weight from field observations. A repeated reduction of the predictor variable set was implemented, guided by a permutation-based variable

importance measure. Thus, a subset of important variables was identified. The simple ratios between the narrow near-infrared and red-edge region were found to be particularly important. As the spatial distribution and the activities of large herbivores are affected by the availability and quality of potential forage areas, this may help to support the future conservation of semi-natural grassland ecosystems grazed by livestock species or wildlife.

Acknowledgements

The project was supported by funds of German government's Special Purpose Fund held at Landwirtschaftliche Rentenbank (28 RZ 7007). We thank the Federal Forests Division (Bundesforst) of the German Institute for Federal Real Estate (Bundesanstalt für Immobilienaufgaben) and the Institut für Wildbiologie Göttingen und Dresden e.V. for close cooperation and support.

References

Adesogan, A.T., D.I. Givens, and E. Owen. 2000. “Measuring Chemical Composition and Nutritive Value in Forages.” In *Field and Laboratory Methods for Grassland and Animal Production Research.*(Eds L t"Mannetje, RM Jones) Pp. 263–278. CABI Publishing: Warwickshire.

Ali, I., F. Cawkwell, E. Dwyer, B. Barrett, and S. Green. 2016. "Satellite Remote Sensing of Grasslands: From Observation to Management-a Review". *Journal of Plant Ecology*.

Ali, I., B. Barrett, F. Cawkwell, S. Green, E. Dwyer, and M. Neumann. 2017. "Application of Repeat-Pass TerraSAR-X Staring Spotlight Interferometric Coherence to Monitor Pasture Biophysical Parameters: Limitations and Sensitivity Analysis". *IEEE Journal of Selected Topics in Applied Earth Observations and Remote Sensing* 10 (7): 3225–3231.

Ali, I., F. Cawkwell, E. Dwyer, and S. Green. 2017. "Modeling Managed Grassland Biomass Estimation by Using Multitemporal Remote Sensing Data–A Machine Learning Approach". *IEEE Journal of Selected Topics in Applied Earth Observations and Remote Sensing*.

Barrett, B., I. Nitze, S. Green, and F. Cawkwell. 2014. "Assessment of Multi-Temporal, Multi-Sensor Radar and Ancillary Spatial Data for Grasslands Monitoring in Ireland Using Machine Learning Approaches". *Remote Sensing of Environment* 152: 109–124.

Beckschäfer, P., L. Fehrmann, R.D. Harrison, J. Xu, and C. Kleinn. 2014. "Mapping Leaf Area Index in Subtropical Upland Ecosystems Using RapidEye Imagery and the RandomForest Algorithm". *IForest-Biogeosciences and Forestry* 7 (1): 1.

Belgiu, M., and L. Drăguţ. 2016. "Random Forest in Remote Sensing: A Review of Applications and Future Directions". *ISPRS Journal of Photogrammetry and Remote Sensing* 114: 24–31.

Bischl, B., M. Lang, L. Kotthoff, J. Schiffner, J. Richter, E. Studerus, G. Casalicchio, and Z.M. Jones. 2016. "Mlr: Machine Learning in R". *Journal of Machine Learning Research* 17 (170): 1–5.

Borer, E.T., E.W. Seabloom, D.S. Gruner, W.S. Harpole, H. Hillebrand, E.M. Lind, P.B. Adler, J. Alberti, T.M. Anderson, and J.D. Bakker. 2014. "Herbivores and Nutrients Control Grassland Plant Diversity via Light Limitation". *Nature* 508 (7497): 517.

Breiman, L. 2001. "Random Forests". *Machine Learning* 45 (1): 5–32.

Brenning, A. 2012. "Spatial Cross-Validation and Bootstrap for the Assessment of Prediction Rules in Remote Sensing: The R Package Sperrorest". In *Geoscience and Remote Sensing Symposium (IGARSS), 2012 IEEE International*, 5372–5375. IEEE.

Brodu, N. 2017. "Super-Resolving Multiresolution Images With Band-Independent Geometry of Multispectral Pixels". *IEEE Transactions on Geoscience and Remote Sensing* 55 (8): 4610–4617.

Bunzel-Drüke, M. 2008. *"Wilde Weiden": Praxisleitfaden Für Ganzjahresbeweidung in Naturschutz Und Landschaftsentwicklung*. Arbeitsgem. Biologischer Umweltschutz im Kreis Soest eV (ABU).

Catchpole, W.R., and C.J. Wheeler. 1992. "Estimating Plant Biomass: A Review of Techniques". *Australian Journal of Ecology* 17 (2): 121–131.

Catorci, A., F.M. Tardella, K. Piermarteri, R. Pennesi, L. Malatesta, M. Corazza, and P. Scocco. 2016. "Effect of Red Deer Grazing on Alpine Hay Meadows: Biodiversity and Management Implications". *Applied Ecology and Environmental Research* 14 (2): 301–318.

Chauhan, S., and H.S. Srivastava. 2016. "Comparative Evaluation of the Sensitivity of Multi-Polarized SAR and Optical Data for Various Land Cover Classes". *Int. J. Adv. Remote Sens. GIS Geogr* 4: 1–14.

Cho, M.A., and A.K. Skidmore. 2009. "Hyperspectral Predictors for Monitoring Biomass Production in Mediterranean Mountain Grasslands: Majella National Park, Italy". *International Journal of Remote Sensing* 30 (2): 499–515.

Clevers, J.GPW, and A.A. Gitelson. 2013. "Remote Estimation of Crop and Grass Chlorophyll and Nitrogen Content Using Red-Edge Bands on Sentinel-2 and-3". *International Journal of Applied Earth Observation and Geoinformation* 23: 344–351.

Dangal, S.RS, H. Tian, C. Lu, S. Pan, N. Pederson, and A. Hessl. 2016. "Synergistic Effects of Climate Change and Grazing on Net Primary Production of Mongolian Grasslands". *Ecosphere* 7 (5): e01274.

Darvishzadeh, R., A.K. Skidmore, M. Mirzaie, C. Atzberger, and M. Schlerf. 2014. "Fresh Biomass Estimation in Heterogeneous Grassland Using Hyperspectral Measurements and Multivariate Statistical Analysis". In *InAGU Fall Meeting Abstracts*. Vol. 1.

Darvishzadeh, R., A. Skidmore, M. Schlerf, and C. Atzberger. 2008. "Inversion of a Radiative Transfer Model for Estimating Vegetation LAI and Chlorophyll in a Heterogeneous Grassland". *Remote Sensing of Environment* 112 (5): 2592–2604.

Dash, J., and P.J. Curran. 2004. "The MERIS Terrestrial Chlorophyll Index". *International Journal of Remote Sensing* 25 (23): 5403–13.

Delegido, J., J. Verrelst, L. Alonso, and J. Moreno. 2011. "Evaluation of Sentinel-2 Red-Edge Bands for Empirical Estimation of Green LAI and Chlorophyll Content". *Sensors* 11 (7): 7063–7081.

Dengler, J., M. Janišová, P. Török, and C. Wellstein. 2014. "Biodiversity of Palaearctic Grasslands: A Synthesis". *Agriculture, Ecosystems & Environment* 182: 1–14.

Drusch, M., U. Del Bello, S. Carlier, O. Colin, V. Fernandez, F. Gascon, B. Hoersch, C. Isola, P. Laberinti, and P. Martimort. 2012. "Sentinel-2: ESA"s Optical High-Resolution Mission for GMES Operational Services". *Remote Sensing of Environment* 120: 25–36.

Duan, M., Q. Gao, Y. Wan, Y. Li, Y. Guo, Z. Ganzhu, Y. Liu, and X. Qin. 2012. "Biomass Estimation of Alpine Grasslands under Different Grazing Intensities Using Spectral Vegetation Indices". *Canadian Journal of Remote Sensing* 37 (4): 413–421.

Dusseux, P., T. Corpetti, L. Hubert-Moy, and S. Corgne. 2014. "Combined Use of Multi-Temporal Optical and Radar Satellite Images for Grassland Monitoring". *Remote Sensing* 6 (7): 6163–6182.

Dusseux, P., L. Hubert-Moy, T. Corpetti, and F. Vertès. 2015. "Evaluation of SPOT Imagery for the Estimation of Grassland Biomass". *International Journal of Applied Earth Observation and Geoinformation* 38: 72–77.

ESA. 2016a. *SNAP. ESA Sentinel Application Platform* (version 6.0.1).

———2016b. "User Guides - Sentinel-1 SAR - Sentinel Online". 2016. https://earth.esa.int/web/sentinel/user-guides/sentinel-1-sar.

Fløjgaard, C., M.De Barba, P. Taberlet, and R. Ejrnæs. 2017. "Body Condition, Diet and Ecosystem Function of Red Deer (Cervus Elaphus) in a Fenced Nature Reserve". *Global Ecology and Conservation* 11: 312–323.

Frampton, W.J., J. Dash, G. Watmough, and E.J. Milton. 2013. "Evaluating the Capabilities of Sentinel-2 for Quantitative Estimation of Biophysical Variables in Vegetation". *ISPRS Journal of Photogrammetry and Remote Sensing* 82: 83–92.

Friedl, M.A., D.S. Schimel, J. Michaelsen, F.W. Davis, and H. Walker. 1994. "Estimating Grassland Biomass and Leaf Area Index Using Ground and Satellite Data". *International Journal of Remote Sensing* 15 (7): 1401–1420.

Gibson, David J. 2009. *Grasses and Grassland Ecology*. Oxford University Press.

Hijmans, R.J. 2017. "Raster: Geographic Data Analysis and Modeling". *R Package Version 2.6-7*, no. 8.

Hird, J.N., E.R. DeLancey, G.J. McDermid, and J. Kariyeva. 2017. "Google Earth Engine, Open-Access Satellite Data, and Machine Learning in Support of Large-Area Probabilistic Wetland Mapping". *Remote Sensing* 9 (12): 1315.

Huete, A.R. 1988. "A Soil-Adjusted Vegetation Index (SAVI)". *Remote Sensing of Environment* 25 (3): 295–309.

Isselstein J., 2018. Protecting biodiversity in grasslands. In: Marshall, A. and Collins, R. (ed.), *Improving grassland and pasture management in temperate agriculture*. Chapter 16, Burleigh Dodds Science Publishing, Cambridge, UK. ISBN: 978 1 78676 200 9; www.bdspublishing.com.

Isselstein, J., B. Jeangros, and V. Pavlu. 2005. "Agronomic Aspects of Biodiversity Targeted Management of Temperate Grasslands in Europe–a Review". *Agronomy Research* 3 (2): 139–151.

Jin, Y., X. Yang, J. Qiu, J. Li, T. Gao, Q. Wu, F. Zhao, H. Ma, H. Yu, and B. Xu. 2014. "Remote Sensing-Based Biomass Estimation and Its Spatio-Temporal Variations in Temperate Grassland, Northern China". *Remote Sensing* 6 (2): 1496–1513.

John, R., J. Chen, V. Giannico, H. Park, J. Xiao, G. Shirkey, Z. Ouyang, C. Shao, R. Lafortezza, and J. Qi. 2018. "Grassland Canopy Cover and Aboveground Biomass in Mongolia and Inner Mongolia: Spatiotemporal Estimates and Controlling Factors". *Remote Sensing of Environment* 213: 34–48.

Kawamura, K., T. Akiyama, H. Yokota, M. Tsutsumi, T. Yasuda, O. Watanabe, G. Wang, and S. Wang. 2005. "Monitoring of Forage Conditions with MODIS Imagery in the Xilingol Steppe, Inner Mongolia". *International Journal of Remote Sensing* 26 (7): 1423–1436.

Knox, N.M., A.K. Skidmore, H. HT Prins, G.P. Asner, H.MA van der Werff, W.F. de Boer, C. van der Waal, H.J. de Knegt, E.M. Kohi, and R. Slotow. 2011. "Dry Season Mapping of Savanna Forage Quality, Using the Hyperspectral Carnegie Airborne Observatory Sensor". *Remote Sensing of Environment* 115 (6): 1478–1488.

Lamarque, P., S. Lavorel, M. Mouchet, and F. Quétier. 2014. "Plant Trait-Based Models Identify Direct and Indirect Effects of Climate Change on Bundles of Grassland Ecosystem Services". *Proceedings of the National Academy of Sciences* 111 (38): 13751–13756.

Loozen, Y., D. Karssenberg, S.M. de Jong, S. Wang, J. van Dijk, M.J. Wassen, and K.T. Rebel. 2019. "Exploring the Use of Vegetation Indices to Sense Canopy Nitrogen to Phosphorous Ratio in Grasses". *International Journal of Applied Earth Observation and Geoinformation* 75: 1–14.

Marsett, R.C., J. Qi, P. Heilman, S.H. Biedenbender, M.C. Watson, S. Amer, M. Weltz, D. Goodrich, and R. Marsett. 2006. "Remote Sensing for Grassland Management in the Arid Southwest". *Rangeland Ecology & Management* 59 (5): 530–540.

Merkle, J.A., K.L. Monteith, E.O. Aikens, M.M. Hayes, K.R. Hersey, D. Middleton, B.A. Oates, H. Sawyer, B.M. Scurlock, and M.J. Kauffman. 2016. "Large Herbivores Surf Waves of Green-up during Spring". *Proceedings of the Royal Society B: Biological Sciences* 283 (1833): 20160456.

Müller-Wilm, U., O. Devignot, and L. Pessiot. 2018. *Sen2Cor Configuration and User Manual*. France: ESA.

Mutanga, O., E. Adam, and M. Azong Cho. 2012. "High Density Biomass Estimation for Wetland Vegetation Using WorldView-2 Imagery and Random Forest Regression Algorithm". *International Journal of Applied Earth Observation and Geoinformation* 18: 399–406.

Mutanga, O., A.K. Skidmore, and H.H.T. Prins. 2004. "Predicting in Situ Pasture Quality in the Kruger National Park, South Africa, Using

Continuum-Removed Absorption Features". *Remote Sensing of Environment* 89 (3): 393–408.

Nicodemus, K.K, J.D. Malley, C. Strobl, and A. Ziegler. 2010. "The Behaviour of Random Forest Permutation-Based Variable Importance Measures under Predictor Correlation". *BMC Bioinformatics* 11 (1): 110.

Palmer, S.CF, A.J. Hester, D.A. Elston, I.J. Gordon, and S.E. Hartley. 2003. "The Perils of Having Tasty Neighbors: Grazing Impacts of Large Herbivores at Vegetation Boundaries". *Ecology* 84 (11): 2877–2890.

Pausas, J.G., and W.J. Bond. 2018. "Humboldt and the Reinvention of Nature". *Journal of Ecology*.

Peeters, A., G. Beaufoy, R.M. Canals, A. De Vliegher, C. Huyghe, J. Isselstein, J. Jones, W. Kessler, D. Kirilovsky, and A. Van Den Pol-Van Dasselaar. 2014. "Grassland Term Definitions and Classifications Adapted to the Diversity of European Grassland-Based Systems". In *Grassland Science in Europe*, 19:743–750.

Pellissier, P.A., S.V. Ollinger, L.C. Lepine, M.W. Palace, and W.H. McDowell. 2015. "Remote Sensing of Foliar Nitrogen in Cultivated Grasslands of Human Dominated Landscapes". *Remote Sensing of Environment* 167: 88–97.

Periasamy, S. 2018. "Significance of Dual Polarimetric Synthetic Aperture Radar in Biomass Retrieval: An Attempt on Sentinel-1". *Remote Sensing of Environment* 217: 537–549.

Pettorelli, N., J.O. Vik, A. Mysterud, J.-M. Gaillard, C.J. Tucker, and N.C. Stenseth. 2005. "Using the Satellite-Derived NDVI to Assess Ecological Responses to Environmental Change". *Trends in Ecology & Evolution* 20 (9): 503–10.

Punalekar, S.M., A. Verhoef, T.L. Quaife, D. Humphries, L. Bermingham, and C.K. Reynolds. 2018. "Application of Sentinel-2A Data for Pasture Biomass Monitoring Using a Physically Based Radiative Transfer Model". *Remote Sensing of Environment* 218: 207–220.

R Core Team. 2018. *R: A Language and Environment for Statistical Computing*. R Foundation for Statistical Computing. https://www.R-project.org/.

Ramoelo, A., A.K. Skidmore, M.A. Cho, M. Schlerf, R. Mathieu, and I.M.A. Heitkönig. 2012. "Regional Estimation of Savanna Grass Nitrogen Using the Red-Edge Band of the Spaceborne RapidEye Sensor". *International Journal of Applied Earth Observation and Geoinformation* 19 (Supplement C): 151–62.

Ramoelo, A., M.A. Cho, R. Mathieu, S. Madonsela, R. Van De Kerchove, Z. Kaszta, and E. Wolff. 2015. "Monitoring Grass Nutrients and Biomass as Indicators of Rangeland Quality and Quantity Using Random Forest Modelling and WorldView-2 Data". *International Journal of Applied Earth Observation and Geoinformation* 43: 43–54.

Ramoelo, A., M. Cho, R. Mathieu, and A.K. Skidmore. 2015. "Potential of Sentinel-2 Spectral Configuration to Assess Rangeland Quality". *Journal of Applied Remote Sensing* 9 (1): 094096–094096.

Raynor, E.J., A. Joern, J.B. Nippert, and J.M. Briggs. 2016. "Foraging Decisions Underlying Restricted Space Use: Effects of Fire and Forage Maturation on Large Herbivore Nutrient Uptake". *Ecology and Evolution* 6 (16): 5843–53.

Riesch, F., B. Tonn, M. Meißner, N. Balkenhol, and J. Isselstein. 2019. "Grazing by Wild Red Deer: Management Options for the Conservation of Semi-Natural Open Habitats." *Journal of Applied Ecology*.

Riesch, F., H.G. Stroh, B. Tonn, and J. Isselstein. 2018. "Soil PH and Phosphorus Drive Species Composition and Richness in Semi-Natural Heathlands and Grasslands Unaffected by Twentieth-Century Agricultural Intensification". *Plant Ecology & Diversity* 11 (2): 239–253.

Rosenthal, G., J. Schrautzer, and C. Eichberg. 2012. "Low-Intensity Grazing with Domestic Herbivores: A Tool for Maintaining and Restoring Plant Diversity in Temperate Europe". *Tuexenia*, no. 32: 167–205.

Rouse, J.W., R.H. Haas, J.A. Schell, and D.W. Deering. 1973. "Monitoring the Vernal Advancement and Retrogradation (Green Wave Effect) of Natural Vegetation. Prog. Rep. RSC 1978-1". *Remote Sensing Center, Texas A&M Univ., College Station* 93.

Ruß, G., and A. Brenning. 2010. "Spatial Variable Importance Assessment for Yield Prediction in Precision Agriculture". *Advances in Intelligent Data Analysis IX*, 184–195.

Sanderson, M.A., C. A. Rotz, S.W. Fultz, and E. B. Rayburn. 2001. "Estimating Forage Mass with a Commercial Capacitance Meter, Rising Plate Meter, and Pasture Ruler". *Agronomy Journal* 93 (6): 1281–1286.

Schulze, K.A., G. Rosenthal, and A. Peringer. 2018. "Intermediate Foraging Large Herbivores Maintain Semi-Open Habitats in Wilderness Landscape Simulations". *Ecological Modelling* 379: 10–21.

Schweiger, A.K., A.C. Risch, A. Damm, M. Kneubühler, R. Haller, M.E. Schaepman, and M. Schütz. 2015. "Using Imaging Spectroscopy to Predict Above-Ground Plant Biomass in Alpine Grasslands Grazed by Large Ungulates". *Journal of Vegetation Science* 26 (1): 175–190.

Scurlock, J.M.O., and D.O. Hall. 1998. "The Global Carbon Sink: A Grassland Perspective". *Global Change Biology* 4 (2): 229–233.

Si, Y., M. Schlerf, R. Zurita-Milla, A. Skidmore, and T. Wang. 2012. "Mapping Spatio-Temporal Variation of Grassland Quantity and Quality Using MERIS Data and the PROSAIL Model". *Remote Sensing of Environment* 121: 415–425.

Silleos, N.G., T.K. Alexandridis, I.Z. Gitas, and K. Perakis. 2006. "Vegetation Indices: Advances Made in Biomass Estimation and Vegetation

Monitoring in the Last 30 Years". *Geocarto International* 21 (4): 21–28.

Sims, D.A., and J.A. Gamon. 2002. "Relationships between Leaf Pigment Content and Spectral Reflectance across a Wide Range of Species, Leaf Structures and Developmental Stages". *Remote Sensing of Environment* 81 (2–3): 337–354.

Skidmore, A.K., J.G. Ferwerda, O. Mutanga, S.E. Van Wieren, M. Peel, R.C. Grant, H.HT Prins, F.B. Balcik, and V. Venus. 2010. "Forage Quality of Savannas—Simultaneously Mapping Foliar Protein and Polyphenols for Trees and Grass Using Hyperspectral Imagery". *Remote Sensing of Environment* 114 (1): 64–72.

Strobl, C., A.-L. Boulesteix, A. Zeileis, and T. Hothorn. 2007. "Bias in Random Forest Variable Importance Measures: Illustrations, Sources and a Solution". *BMC Bioinformatics* 8 (1): 25.

t'Mannetje, L., 2000. "Measuring Biomass of Grassland Vegetation." In *Field and Laboratory Methods for Grassland and Animal Production Research.* (Eds L't Mannetje, RM Jones) pp. 151-178. CABI Publishing: New York.

t'Mannetje, L., Jones, R.M., 2000. "Field and laboratory methods for grassland and animal production research." *CABI Publishing*.

Tamm, T., K. Zalite, K. Voormansik, and L. Talgre. 2016. "Relating Sentinel-1 Interferometric Coherence to Mowing Events on Grasslands". *Remote Sensing* 8 (10): 802.

Tong, A., and Y. He. 2017. "Estimating and Mapping Chlorophyll Content for a Heterogeneous Grassland: Comparing Prediction Power of a Suite of Vegetation Indices across Scales between Years". *ISPRS Journal of Photogrammetry and Remote Sensing* 126: 146–167.

Ullah, S., Y. Si, M. Schlerf, A.K. Skidmore, Muhammad Shafique, and Irfan Akhtar Iqbal. 2012. "Estimation of Grassland Biomass and Nitrogen Using MERIS Data". *International Journal of Applied Earth Observation and Geoinformation* 19: 196–204.

Valkó, O., S. Venn, M. Żmihorski, I. Biurrun, R. Labadessa, and J. Loos. 2018. "The Challenge of Abandonment for the Sustainable Management of Palaearctic Natural and Semi-Natural Grasslands". *Hacquetia* 17 (1): 5–16.

Van Wieren, S.E. 1995. "The Potential Role of Large Herbivores in Nature Conservation and Extensive Land Use in Europe". *Biological Journal of the Linnean Society* 56: 11–23.

Verrelst, J., J. Muñoz, L. Alonso, J. Delegido, J.P. Rivera, G. Camps-Valls, and J. Moreno. 2012. "Machine Learning Regression Algorithms for Biophysical Parameter Retrieval: Opportunities for Sentinel-2 and-3". *Remote Sensing of Environment* 118: 127–139.

Voormansik, K., T. Jagdhuber, A. Olesk, I. Hajnsek, and K.P. Papathanassiou. 2013. "Towards a Detection of Grassland Cutting Practices with Dual

Polarimetric TerraSAR-X Data". *International Journal of Remote Sensing* 34 (22): 8081–8103.

Voormansik, K., T. Jagdhuber, K. Zalite, M. Noorma, and I. Hajnsek. 2016. "Observations of Cutting Practices in Agricultural Grasslands Using Polarimetric SAR". *IEEE Journal of Selected Topics in Applied Earth Observations and Remote Sensing* 9 (4): 1382–1396.

Wachendorf, M., T. Fricke, and T. Möckel. 2017. "Remote Sensing as a Tool to Assess Botanical Composition, Structure, Quantity and Quality of Temperate Grasslands". *Grass and Forage Science*.

Warren, S.D., and R. Büttner. 2008a. "Relationship of Endangered Amphibians to Landscape Disturbance". *Journal of Wildlife Management* 72 (3): 738–44.

———2008b. "Active Military Training Areas as Refugia for Disturbance-Dependent Endangered Insects". *Journal of Insect Conservation* 12 (6): 671–76.

Warren, S.D., M. Alt, K.D. Olson, S.DH Irl, M.J. Steinbauer, and A. Jentsch. 2014. "The Relationship between the Spectral Diversity of Satellite Imagery, Habitat Heterogeneity, and Plant Species Richness". *Ecological Informatics* 24: 160–168.

Wilson, J.B., R.K. Peet, J. Dengler, and M. Pärtel. 2012. "Plant Species Richness: The World Records". *Journal of Vegetation Science* 23 (4): 796–802.

Wright, M.N., and A. Ziegler. 2015. "Ranger: A Fast Implementation of Random Forests for High Dimensional Data in C++ and R". *ArXiv Preprint ArXiv:1508.04409*.

Zalite, K., O. Antropov, J. Praks, K. Voormansik, and M. Noorma. 2016. "Monitoring of Agricultural Grasslands with Time Series of X-Band Repeat-Pass Interferometric SAR". *IEEE Journal of Selected Topics in Applied Earth Observations and Remote Sensing* 9 (8): 3687–3697.

Zandler, H., A. Brenning, and C. Samimi. 2015. "Quantifying Dwarf Shrub Biomass in an Arid Environment: Comparing Empirical Methods in a High Dimensional Setting". *Remote Sensing of Environment* 158: 140–155.

Supporting information to the paper

Raab, C., F. Riesch, B. Tonn, B. Barrett, M. Meißner, N. Balkenhol and J. Isselstein. "Combining Sentinel-1 and Sentinel-2 data for estimating semi-natural grassland forage quantity and quality in Germany to support a target-oriented habitat and wildlife management." *Remote Sensing of Environment.*

Supplementary tables

Table S1: A list of spectral predictor variables and the respective groups included in the variable selection process.

Table S2: A list of spectral biophysical predictor variables included in the variable selection process.

Table S3: A list of radar predictor variables included in the variable selection process.

Supplementary figures

Figure S1: Spatial predictions of oADF = organic acid detergent fibre (exclusive of residual ash), CP = crude protein, CSH = compressed sward height, DM = standing biomass dry weight for August 2016 and May 2017.

Figure S2: Spatial predictions of oADF = organic acid detergent fibre (exclusive of residual ash), CP = crude protein, CSH = compressed sward height, DM = standing biomass dry weight for August 2017 and October 2017.

Figure S3: Spatial predictions of oADF = organic acid detergent fibre (exclusive of residual ash), CP = crude protein, CSH = compressed sward height, DM = standing biomass dry weight for June 2015 and August 2015.

R code example

Appendix 1: A practical example.

Table S1: A list of spectral predictor variables and the respective groups included in the variable selection process. See Table 2 of the main document for band descriptions. B = band.

No	Index	Formula	Reference
1-10	Individual bands		
11-55	Simple Ratios (SR)	e.g. $\frac{B3}{B4}$	(e.g. Jordan, 1969)
56	NDVI1	$\frac{B8-B4}{B8+B4}$	
57	NDVI2	$\frac{B8A-B4}{B8A+B4}$	(Rouse, 1974)
58	NDVI3	$\frac{B7-B4}{B7+B4}$	
59	NDI45	$\frac{B5-B4}{B5+B4}$	(Delegido et al., 2011)
60	RDVI0	$\frac{(B8A-B4)}{\sqrt{(B8A+B4)}}$	
61	RDVI1	$\frac{(B8A-B5)}{\sqrt{(B8A+B5)}}$	(Roujean and Breon, 1995)
62	RDVI2	$\frac{(B8A-B6)}{\sqrt{(B8A+B6)}}$	
63	RDVI3	$\frac{(B8A-B7)}{\sqrt{(B8A+B7)}}$	
64	CRE	$\frac{B7^{-1}}{B5}$	(Gitelson et al., 2006)
65	ARI	$\frac{\frac{1}{B3}}{\frac{1}{B5}}$	(Gitelson et al., 2001)
66	NRI	$\frac{(B3-B4)}{(B3+B4)}$	(Schleicher et al., 1998)
67	GNDVI	$\frac{(B7-B3)}{(B7+B3)}$	(Gitelson et al., 1996)
68	IRECI	$\frac{(B7-B4)}{\frac{B5}{B6}}$	(Frampton et al., 2013)
69	SIPI	$\frac{(B8A-B2)}{(B8A+B2)}$	(Penuelas et al., 1995)
70	PSRI	$\frac{(B4-B2)}{(B6)}$	(Merzlyak et al., 1999)
71	CRI	$\frac{\frac{1}{B3}}{\frac{1}{B8A}}$	(Gitelson et al., 2002)
72	SAVI0	$(1+0.5)\times\frac{B8A-B4}{B8A+B4+0.5}$	
73	SAVI1	$(1+0.5)\times\frac{B8A-B5}{B8A+B5+0.5}$	(Huete, 1988)
74	SAVI2	$(1+0.5)\times\frac{B8A-B6}{B8A+B6+0.5}$	
75	SAVI3	$(1+0.5)\times\frac{B8A-B7}{B8A+B7+0.5}$	

76	OSAVI	$(1+0.16)\times\frac{B6-B5}{B6+B5+0.16}$	(Rondeaux et al., 1996; Wu et al., 2008)
77	MCARI/OSAVI	$\frac{((B6-B5)-0.2\times(B6-B3))\times\frac{B6}{B3}}{(1+0.16)\times\frac{B6-B5}{B6+B5+0.16}}$	(Wu et al., 2008)
78	EVI	$2.5\times\frac{B8A-B4}{1+B8A+6\times B4-7.5\times B2}$	(Huete et al., 1997)
79	CIre	$\frac{B7}{B5}-1$	(Gitelson et al., 2006, 2003)
80	CIg	$\frac{B7}{B3}-1$	(Gitelson et al., 2006, 2003)
81	REP	$705+\frac{35*\frac{B4+B7}{2}-B5}{(B6-B5)}$	(Guyot and Baret, 1988)
82	MTCI	$\frac{B6-B5}{B5-B4}$	(Dash and Curran, 2004)
83	MCARI	$((B5-B4)-0.2\times(B5-B3))\times\frac{B5}{B4}$	(Daughtry et al., 2000)
84	TCARI	$3\times((B6-B5)-0.2\times(B6-B3)\times\frac{B6}{B5})$	(Haboudane et al., 2002; Wu et al., 2008)
85	TCARI/OSAVI	$\frac{3\times((B6-B5)-0.2\times(B6-B3)\times\frac{B6}{B5})}{(1+0.16)\times\frac{B6-B5}{B6+B5+0.16}}$	(Wu et al., 2008)
86	NDRE1	$\frac{B6-B5}{B6+B5}$	(Gitelson and Merzlyak, 1994; Sims and Gamon, 2002)
87	NDRE2	$\frac{B7-B5}{B7+B5}$	(Barnes et al., 2000)

Table S2: A list of spectral biophysical predictor variables (L2B) included in the variable selection process.

No	Index	Definition	Reference
88	LAI	The Leaf area index is defined as the developed area of photosynthetically active elements of the vegetation per unit horizontal ground area.	(Weiss and Baret, 2016)
89	CAB	The Canopy chlorophyll content is strongly related to leaf nitrogen content.	
90	CW	Canopy water content	
91	fapar	The fapar is defined as the fraction of photosynthetically active radiation absorbed by the canopy.	
92	fCover	The fCover is defined as th gap fraction for nadir direction and used to separate vegetation and soil.	

Table S3: A list of radar predictor variables included in the variable selection process.

No	Index	Formula	Reference
93	AS0VHdb	Ascending orbit, backscatter in dB, vertical-horizintal polarisation	
94	AS0VVdb	Ascending orbit, backscatter in dB, vertical-vertical polarisation	
95	AMPDI	$\frac{AS\,0\,VHdb - AS\,0\,VVdb}{AS0\,VHdb + AS\,0\,VV\,db}$	(e.g. Hird et al., 2017)
96	DS0VVdb	Descending orbit, backscatter in dB, vertical-vertical polarisation	
97	DS0VHdb	Descending orbit, backscatter in dB, vertical-horizontal polarisation	
98	DMPDI	$\frac{DS\,0\,VHdb - DS\,0\,VVdb}{dS0\,VHdb + DS\,0\,VV\,db}$	(e.g. Hird et al., 2017)
99-101	Simple ratios (SR)	e.g. $\frac{AS0\,VHdb}{AS\,0\,VVdb}$	
102	AMPDI/DMPDI	$\frac{AMPDI}{DMPDI}$	

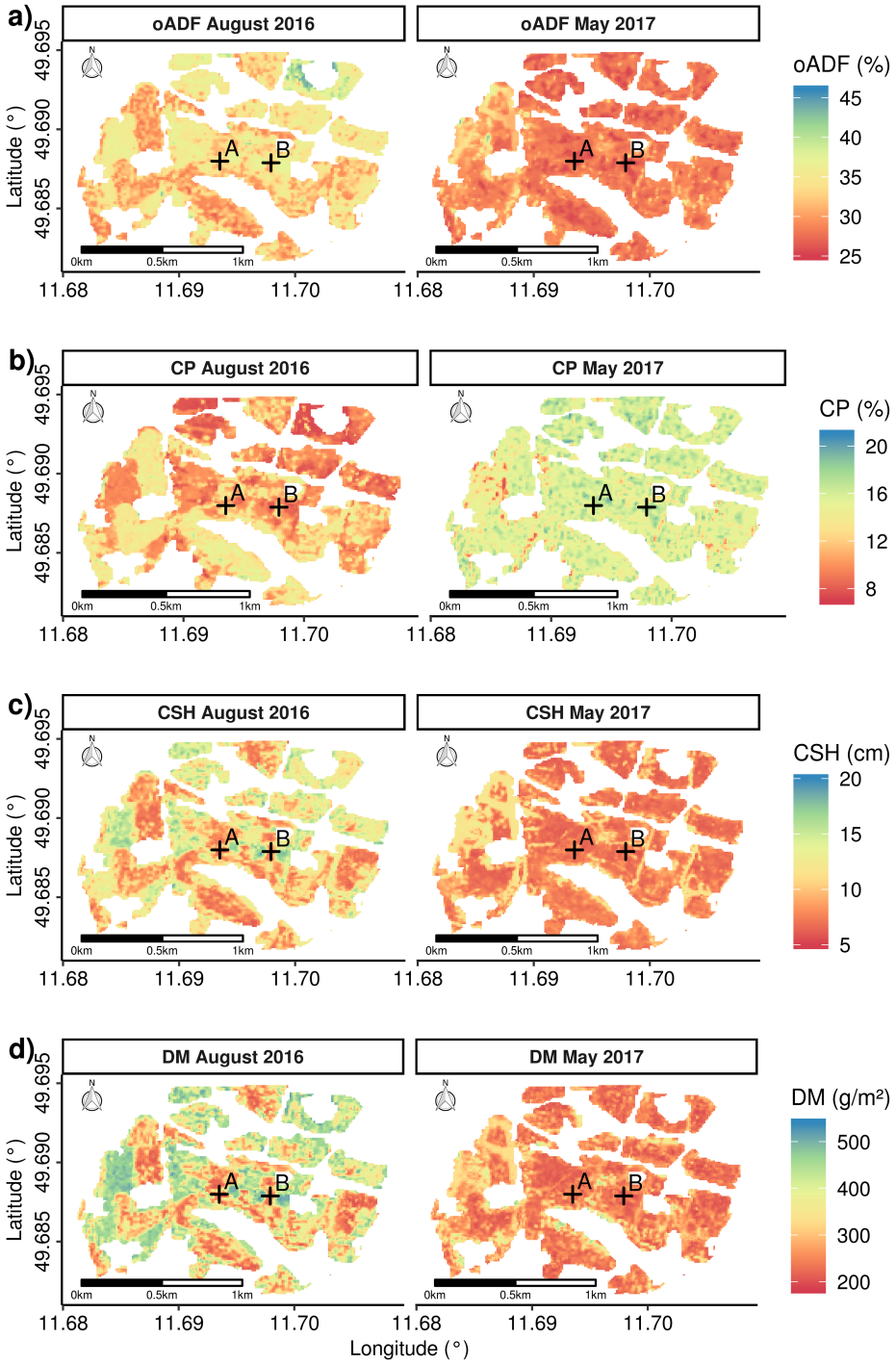

Figure S1: Spatial predictions of oADF = organic acid detergent fibre (exclusive of residual ash), CP = crude protein, CSH = compressed sward height, DM = standing biomass dry weight for August 2016 and May 2017 using random forest regression, averaged over 100 repetitions. The illustrations are presented for the area surrounding the two sampling locations A and B of Figure 1.

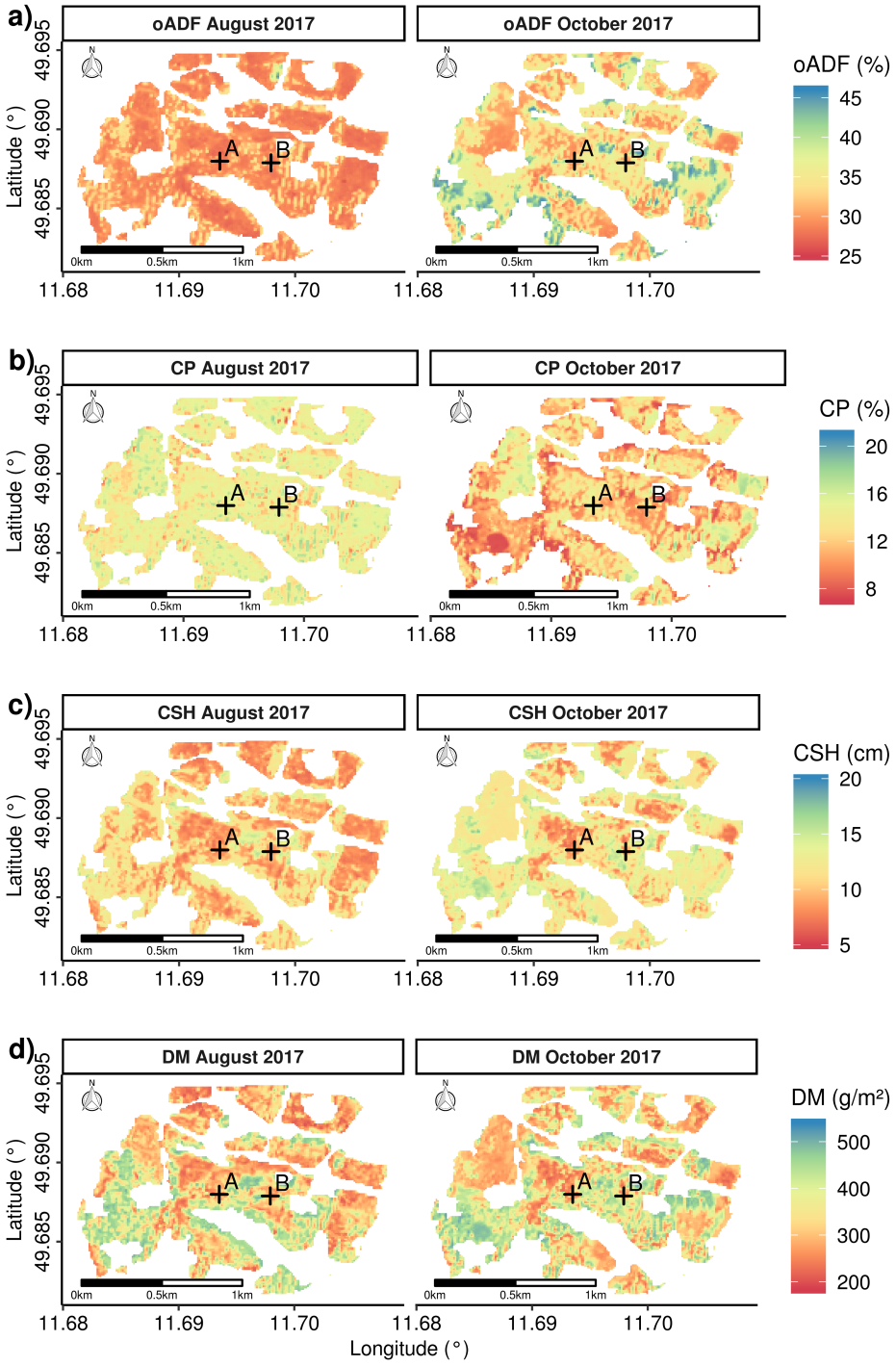

Figure S2: Spatial predictions of oADF = organic acid detergent fibre (exclusive of residual ash), CP = crude protein, CSH = compressed sward height, DM = standing biomass dry weight for August 2017 and October 2017 using random forest regression, averaged over 100 repetitions. The illustrations are presented for the area surrounding the two sampling locations A and B of Figure 1.

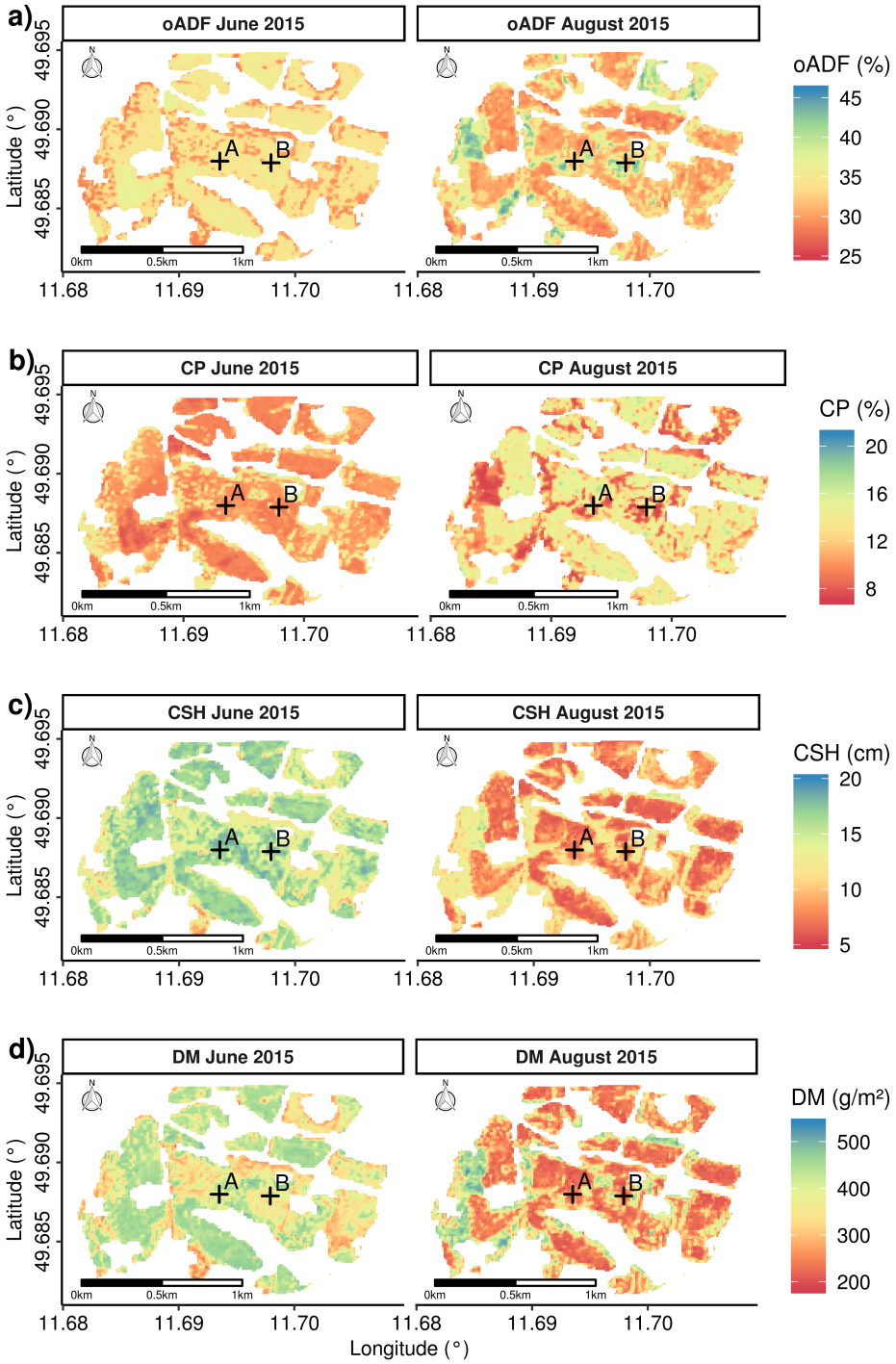

Figure S3: Spatial predictions of oADF = organic acid detergent fibre (exclusive of residual ash), CP = crude protein, CSH = compressed sward height, DM = standing biomass dry weight for June 2015 and August 2015 using random forest regression, averaged over 100 repetitions. The illustrations are presented for the area surrounding the two sampling locations A and B of Figure 1.

Appendix 1: A practical example

To illustrate how the Random Forest algorithm can be used to optimise a predictor dataset in a remote sensing regression context, we make use of a data set compilation provided by the book "Remote Sensing and GIS for Ecologists: Using Open Source Software" (Wegmann et al., 2016). The data can be accessed under the following URL:

http://book.ecosens.org/data/

Data preparation

First we load the required packages and the satellite image. In addition, we derive vegetation indices from the spectral bands of the image.

```
library(raster)
library(RStoolbox)
library(rgdal)
library(ranger)
library(mlr)

mtl <- "data_book/raster_data/LT52240632011210/LT52240632011210CUB01.xml"

lsat <- stackMeta(file=mtl, quantity = "sre", category = "image")
lsat <- lsat* 0.001

# calculate vegetation indices
lsat_vis <- spectralIndices(lsat,
                            blue = 1,
                            green = 2,
                            red = 3,
                            nir = 4,
                            swir2 = 5,
                            swir3 = 6)


# combine spectral bands and vegetation indices
lsat_imgvi <- stack(lsat,lsat_vis)
names(lsat_imgvi)
nlayers(lsat_imgvi)
```

Data sampling

```
train_points <-  readOGR("data_book/vector_data","occurrence")

train_points$occurrence <- as.numeric(train_points$occurrence)
train_points$occurrence[train_points$occurrence == 1] <-0
train_points$occurrence[train_points$occurrence == 2] <-1

#plot data
plotRGB(lsat, b=1, g=2, r=3,stretch = "lin")
pointSize <- train_points$occurrence*2+1
points(train_points, cex=pointSize,col="yellow", pch = 20)
```

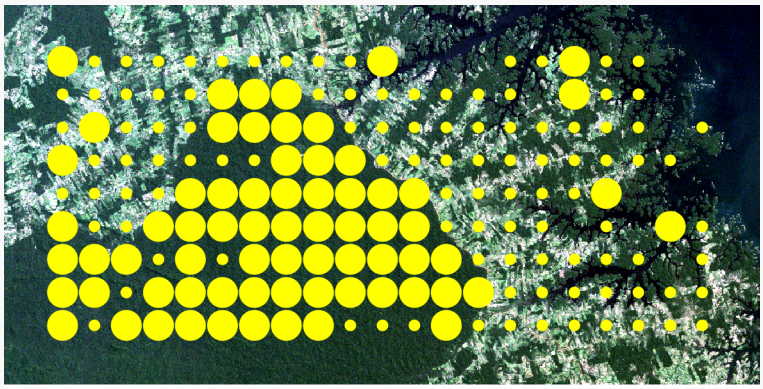

```
# extract reflectance and vegetation indices values
train_extracted <- data.frame(extract(lsat_imgvi,
                                      y=train_points,
                                      cellnumbers = TRUE,
                                      sp=TRUE))

# remove potential duplicates
train_extracted  <- train_extracted [!duplicated(train_extracted$cells),]
# remove potential NAs
train_extracted <- train_extracted[complete.cases(train_extracted),]
```

Modelling

```
library(plyr)
library(parallelMap)
set.seed(123)

train_df <- train_extracted[c(3,5:30)]
```

```
# number of trees to be constructed
num.trees <- 500
# number of folds
k <- 5
# number of repetitions
reps <- 20
# number of permutations
perm <- 20

#define repeated cross-validation
rdesc = makeResampleDesc("RepCV",
                         reps=reps,
                         folds=k,
                         predict = "test")
#predictor names of the full model
ff_start <- names(train_df)[c(2:(length(names(train_df))))]
ff <- ff_start
response <- "occurrence"

#define result lists
res_rmse_rf <- list()
res_varn_rf <- list()
leng <- length(ff)

for( x in 1:(leng-1)){
  data <- train_df[c(ff,response)]
  # define task
  nsp_task <- makeRegrTask(id = "sdm",
                           data = data,
                           target = response)

  #number of predictor variables randomly sampled as candidates at each split
  mtry <- round((length(ff)) /3)
  # define learner
  rf_learner <- setHyperPars(makeLearner("regr.ranger"),
                             par.vals = list(mtry = mtry,
                                             num.trees = num.trees))

  # validation)
  res_nsp <- mlr::resample(learner = rf_learner,
                           resampling = rdesc,
                           task = nsp_task,
                           measures = list(setAggregation(rmse, test.mean),
                                           setAggregation(rmse, test.sd),
                                           setAggregation(rsq,test.mean),
                                           setAggregation(rsq,test.sd)),
                           models = FALSE,
                           show.info = FALSE)
    # variable importance
```

```
  res_var_imp <- generateFeatureImportanceData(
    task = nsp_task,
    method = "permutation.importance",
    learner = rf_learner,
    measure = list(mlr:rmse),
    nmc = perm)$res

  res_var_imp <- data.frame(t(res_var_imp))
  res_var_imp$var <- rownames(res_var_imp)
  res_var_imp <- arrange(res_var_imp,rmse,var)
  varn <- res_var_imp$var

  res_rmse_rf[[x]] <- res_nsp$aggr
  res_varn_rf[[x]] <- res_var_imp
  ff <- varn[2:(length(varn))]
}

res_rmse_rf <- data.frame(do.call(rbind, res_rmse_rf))
res_rmse_rf$var_num <- seq(length(ff_start), 2)
res_rmse_rf$model_run <- seq(1:(length(ff_start)-1))
```

Modeling results

```
library(ggplot2)
ggplot(data=res_rmse_rf, aes(x=var_num, y=rmse.test.mean))+
  geom_point()+
  geom_smooth()+
  theme_bw()+
  labs(x = "Number of variables in the model", y = "RMSE")+
  scale_x_reverse()
```

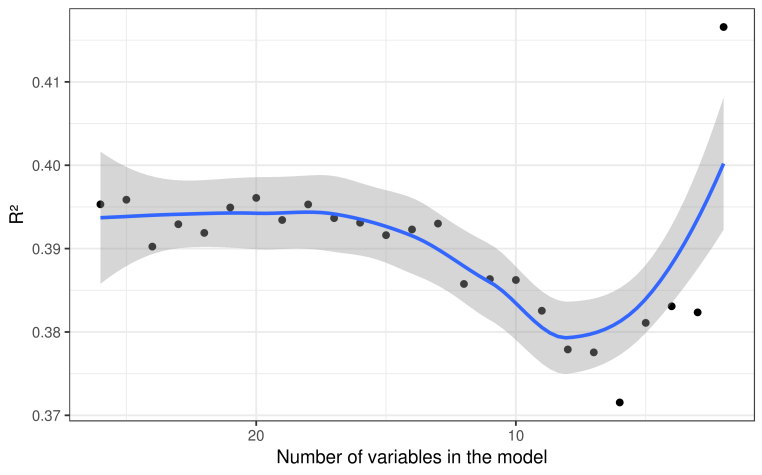

Variable importance

```
res_rmse_rf[which(res_rmse_rf$rmse.test.mean ==
min(res_rmse_rf$rmse.test.mean)),]
##    rmse.test.mean rmse.test.sd rsq.test.mean rsq.test.sd var_num model_run
## 21      0.3715429   0.03577308     0.4061821   0.1142985       6        21
m <- res_rmse_rf[which(res_rmse_rf$rmse.test.mean ==
min(res_rmse_rf$rmse.test.mean)),]$model_run
res_varn_rf[[m]]

##         rmse    var
## 1 0.08384547  MNDWI
## 2 0.08904531 B3_sre
## 3 0.09212387 B2_sre
## 4 0.09807378  GNDVI
## 5 0.10643804   NDWI
## 6 0.13396461  SATVI

ggplot(res_varn_rf[[m]], aes(x=var, y=rmse)) +
  geom_bar( stat="identity", width = 0.6)+
  theme_classic()+
  labs(x = "Variable", y = "Mean increase in RMSE")
```

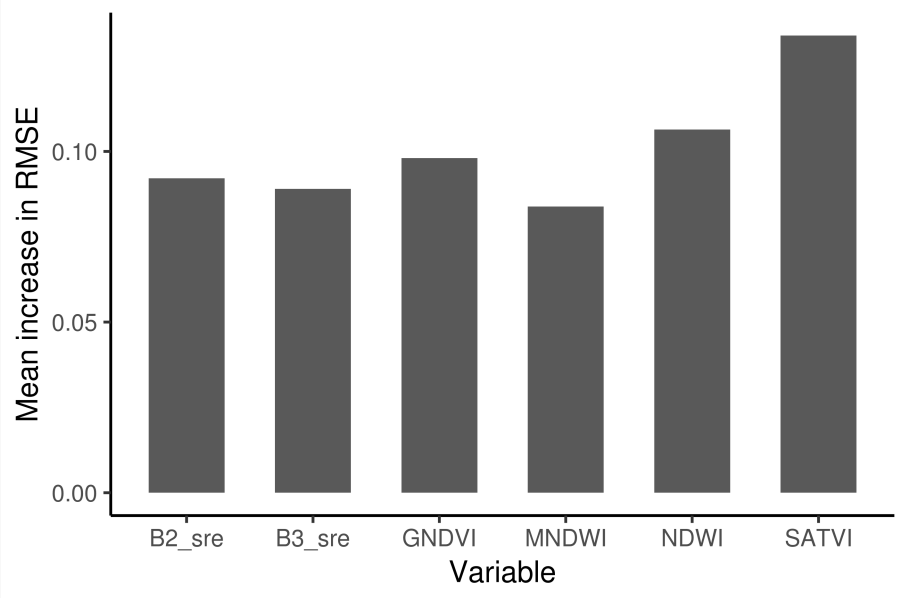

References

Barnes, E.M., T.R. Clarke, S.E. Richards, P.D. Colaizzi, J. Haberland, M. Kostrzewski, P. Waller, C. Choi, E. Riley, and T. Thompson. 2000. "Coincident Detection of Crop Water Stress, Nitrogen Status and Canopy Density Using Ground Based Multispectral Data". In *Proceedings of the Fifth International Conference on Precision Agriculture, Bloomington, MN, USA*. Vol. 1619.

Dash, J., and P.J. Curran. 2004. "The MERIS Terrestrial Chlorophyll Index". *International Journal of Remote Sensing* 25 (23): 5403–13.

Daughtry, C.S.T., C.L. Walthall, M.S. Kim, E. Brown De Colstoun, and J.E. McMurtrey. 2000. "Estimating Corn Leaf Chlorophyll Concentration from Leaf and Canopy Reflectance". *Remote Sensing of Environment* 74 (2): 229–239.

Delegido, J., J. Verrelst, L. Alonso, and J. Moreno. 2011. "Evaluation of Sentinel-2 Red-Edge Bands for Empirical Estimation of Green LAI and Chlorophyll Content". *Sensors* 11 (7): 7063–7081.

Frampton, W.J., J. Dash, G. Watmough, and E.J. Milton. 2013. "Evaluating the Capabilities of Sentinel-2 for Quantitative Estimation of Biophysical Variables in Vegetation". *ISPRS Journal of Photogrammetry and Remote Sensing* 82: 83–92.

Gitelson, A.A., Y. Gritz, and M.N. Merzlyak. 2003. "Relationships between Leaf Chlorophyll Content and Spectral Reflectance and Algorithms for Non-Destructive Chlorophyll Assessment in Higher Plant Leaves". *Journal of Plant Physiology* 160 (3): 271–82.

Gitelson, A. A., and M. N. Merzlyak. 1994. "Quantitative Estimation of Chlorophyll-a Using Reflectance Spectra: Experiments with Autumn Chestnut and Maple Leaves". *Journal of Photochemistry and Photobiology B: Biology* 22 (3): 247–252.

Gitelson, A.A., Y.J. Kaufman, and M.N. Merzlyak. 1996. "Use of a Green Channel in Remote Sensing of Global Vegetation from EOS-MODIS". *Remote Sensing of Environment* 58 (3): 289–98.

Gitelson, A.A., G.P. Keydan, and M.N. Merzlyak. 2006. "Three-Band Model for Noninvasive Estimation of Chlorophyll, Carotenoids, and Anthocyanin Contents in Higher Plant Leaves". *Geophysical Research Letters* 33 (11).

Gitelson, A.A., M.N. Merzlyak, Y. Zur, R. Stark, and U. Gritz. 2001. "Non-Destructive and Remote Sensing Techniques for Estimation of Vegetation Status".

Gitelson, A.A., Y. Zur, O.B. Chivkunova, and M.N. Merzlyak. 2002. "Assessing Carotenoid Content in Plant Leaves with Reflectance Spectroscopy¶". *Photochemistry and Photobiology* 75 (3): 272–81.

Guyot, G., and F. Baret. 1988. "Utilisation de La Haute Resolution Spectrale Pour Suivre l"etat Des Couverts Vegetaux". In *Spectral Signatures of Objects in Remote Sensing*, 287:279.

Haboudane, D., J.R. Miller, N. Tremblay, P.J. Zarco-Tejada, and L. Dextraze. 2002. "Integrated Narrow-Band Vegetation Indices for Prediction of Crop Chlorophyll Content for Application to Precision Agriculture". *Remote Sensing of Environment* 81 (2): 416–426.

Hird, J.N., E.R. DeLancey, G.J. McDermid, and J. Kariyeva. 2017. "Google Earth Engine, Open-Access Satellite Data, and Machine Learning in Support of Large-Area Probabilistic Wetland Mapping". *Remote Sensing* 9 (12): 1315.

Huete, A.R. 1988. "A Soil-Adjusted Vegetation Index (SAVI)". *Remote Sensing of Environment* 25 (3): 295–309.

Huete, A.R., H.Q. Liu, Kv Batchily, and WJDA Van Leeuwen. 1997. "A Comparison of Vegetation Indices over a Global Set of TM Images for EOS-MODIS". *Remote Sensing of Environment* 59 (3): 440–451.

Jordan, C.F. 1969. "Derivation of Leaf-Area Index from Quality of Light on the Forest Floor". *Ecology* 50 (4): 663–666.

Merzlyak, M.N., A.A. Gitelson, O.B. Chivkunova, and V.Y.U. Rakitin. 1999. "Non-Destructive Optical Detection of Pigment Changes during Leaf Senescence and Fruit Ripening". *Physiologia Plantarum* 106 (1): 135–141.

Penuelas, J., I. Filella, and J.A. Gamon. 1995. "Assessment of Photosynthetic Radiation-Use Efficiency with Spectral Reflectance". *New Phytologist* 131 (3): 291–296.

Rondeaux, G., M. Steven, and F. Baret. 1996. "Optimization of Soil-Adjusted Vegetation Indices". *Remote Sensing of Environment* 55 (2): 95–107.

Roujean, J.-L., and F.-M. Breon. 1995. "Estimating PAR Absorbed by Vegetation from Bidirectional Reflectance Measurements". *Remote Sensing of Environment* 51 (3): 375–384.

Rouse, J.W. 1974. "Monitoring the Vernal Advancement and Retrogradation (Green Wave Effect) of Natural Vegetation".

Schleicher, T.D., W.C. Bausch, J.A. Delgado, and P.D. Ayers. 1998. "Evaluation and Refinement of the Nitrogen Reflectance Index (NRI) for Site-Specific Fertilizer Management". In *2001 ASAE Annual Meeting*, 1. American Society of Agricultural and Biological Engineers.

Sims, D.A., and J.A. Gamon. 2002. "Relationships between Leaf Pigment Content and Spectral Reflectance across a Wide Range of Species, Leaf Structures and Developmental Stages". *Remote Sensing of Environment* 81 (2–3): 337–354.

Wegmann, M., B. Leutner, S. Dech. 2016. “Remote Sensing and GIS for Ecologists: Using Open Source Software.” *Pelagic Publishing Ltd.*

Weiss, M., and F. Baret. 2016. *S2ToolBox Level 2 Products: LAI, FAPAR, FCOVER* (version 1.1).

Wu, C., Z. Niu, Q. Tang, and W. Huang. 2008. "Estimating Chlorophyll Content from Hyperspectral Vegetation Indices: Modeling and Validation". *Agricultural and Forest Meteorology* 148 (8–9): 1230–1241.

5

CHAPTER 5 – GENERAL DISCUSSION

The overall aim of this thesis was to evaluate different satellite remote sensing sources to characterise the heterogeneous landscape of the GTA. A particular focus was on semi-natural grassland as there is an urgent need for conservation activities for these habitats across Europe. In this context, the final part of this thesis discusses the main findings of the presented chapters and provides an outlook on future contributions of remote sensing to the conservation of semi-natural grassland.

Remote sensing land cover classification

RapidEye remote sensing data can be used to accurately derive land cover information of a heterogeneous landscape, such as the GTA. The RapidEye earth observation constellation consists of five identical satellites, which provided a dense inter-annual time series at a spatial resolution of 5 m. The applied Tasselled Cap Transformation can be seen as an effective data compression measure, which can decrease the data intensity for multi-temporal land cover applications.

Object- or segmentation-based land cover mapping could be an alternative approach to the pixel-based classification presented in **Chapter 2**. In particular, for high-resolution images, object- or segmentation-based land cover classification provides higher accuracies compared to pixel-based maps (Förster et al., 2010; Laliberte et al., 2007). This can be attributed to the aggregation of spectrally homogeneous pixels into objects and the reduced mixed-pixel effect. Most image segmentation algorithms require adequate parameter settings by the user, which often have to be defined manually (Stefanski et al., 2013). Thus, the segmentation result can be subjective. In addition, the aggregation of pixels into objects comes with the trade-off of losing information, as small features are integrated into bigger objects (Schmidtlein and Sassin, 2004; Liu and Xia, 2010; Schmidt et al., 2017). This could potentially impact the analysis of grazing behaviour of red deer, for example by, GPS (Global Positioning System) telemetry data, because movement decisions might be made at fine scales (Wallace et al.,

1995; Langvatn and Hanley, 1993). Hence, a pixel-based land cover classification can be considered as a valid mapping approach in order to characterise a heterogeneous landscape. A coarser spatial resolution of 10 m provided for example by the Sentinel-2 (10 – 60 m spatial resolution) tandem satellite constellation could, however, be sufficient for the analysis of movement data, as location uncertainties can be introduced by the GPS-signal (Lewis et al., 2007).

Remote-sensing-based mapping of semi-natural grassland

Semi-natural grassland ecosystems are characterised by continuous transitions between botanical communities associated with environmental gradients, such as soil fertility or moisture availability (Riesch et al., 2018). The composition of grassland communities can further be influenced by large herbivores, e.g. by grazing, trampling and seed dispersal (Catorci et al., 2016). This structural and botanical heterogeneity at small scales is a particular challenge for field-based as well as remote-sensing-based mapping and monitoring efforts.

Typically, training data or field observations are used to relate spectral remote sensing data to a respective class or botanical community. Classification algorithms assign each pixel to the most probable community, e.g. by using maximum likelihood. This forces the continuous transitions between different communities into sharp boundaries (Rocchini et al., 2013). Alternatively, classification algorithms such as the Random Forest can

provide a discrete map along with information about the associated uncertainty (Barrett et al., 2016). As shown in **Chapter 3**, this uncertainty or probability of a pixel belonging to a class can be used to better represent gradual transitions between semi-natural grassland communities. The recently presented fuzzy logic mapping approach for semi-natural grassland by Rapinel et al. (2018) and the results shown in **Chapter 4** both offer promising perspectives to meet management requirements, e.g. under Article 17 of the EU Habitats Directive. In this context, major challenges are related to the definition of vegetation classes or communities as well as to a spatial mismatch between the scale of field observation and the image resolution of remote sensing data (Rocchini et al., 2013). The use of very high resolution remote sensing data, such as WorldView-3 (0.31 – 3.7 m spatial resolution) would decrease the scale mismatch between field and remote sensing observations, but would introduce a high noise fraction e.g. by shading effects (Rocchini et al., 2013).

Future applications could focus on satellite remote sensing data sources which facilitate a repeated inventory and monitoring of large areas. From an operational perspective for the reporting obligations under Article 17 of the EU Habitats Directive, Sentinel-2 data could be the preferred choice as they are freely available. For this, further research is required to support the conservation of semi-natural grassland habitats in Europe.

Remote sensing of semi-natural grassland biophysical properties

The recent advances of the Sentinel program by the European commission offer new possibilities for the prediction of semi-natural grassland biophysical properties. As illustrated in **Chapter 4**, simple ratio indices based on red-edge and near-infrared bands were particularly useful for the prediction of grassland forage quality and quantity indicators. In order to ensure a good agreement between collected field samples and remote sensing image acquisitions, the time difference between both data acquisitions should be as small as possible. Due to the high temporal resolution of the Sentinel-2 satellites of five days, a sufficient number of cloud free image acquisitions is possible. Even higher frequencies could be expected by the harmonised Landsat 8 Sentinel-2 data (HLS) (Claverie et al., 2018). The HLS dataset provides surface reflectance data, harmonized between both satellite systems. Thus, higher temporal frequencies at a spatial resolution of 30 m can be realized (Li and Roy 2017). Since no reflectance data are recorded in the red-edge region by the optical Landsat 8 sensor, a reduction of the predictive power could be a consequence compared to Sentinel-2 data. Hyperspectral remote sensing data provide much more spectral information compared to multi-spectral sensors and are a promising data source for the prediction of grassland biophysical properties (Mutanga et al., 2004; Cho and Skidmore, 2009; Skidmore et al., 2010; Knox et al., 2011; Darvishzadeh et al., 2014; Pellissier et al., 2015). However, hyperspectral remote sensing data are usually not freely available

and often cover only small regions. With the upcoming Environmental Mapping and Analysis Program mission (EnMAP) the hyperspectral data availability will increase (Guanter et al., 2015). In comparison to hyperspectral approaches, unmanned-aerial-vehicle-based (UAV) RGB images are a useful alternative to predict grassland biophysical properties (Bareth and Schellberg, 2018; Michez et al., 2019). The battery charge, however, limits the application of UAV-based approaches to smaller areas. For larger geographical regions, a coupled climate- and multi-spectral remote-sensing-based modelling approach could facilitate the understanding of grazing patterns of large herbivores, and thus the conservation of semi-natural grassland with regard to environmental changes (Raynor et al., 2017).

Outlook

Remote sensing has proven to be a powerful application to characterise semi-natural grassland ecosystems (**Chapters 2–4**). Promising research perspectives towards the conservation of grassland habitats include the assessment of grassland use intensity (Franke et al., 2012; Giménez et al., 2017), the detection of mowing events (Tamm et al., 2016; Kolecka et al., 2018) and the estimation of habitat quality of protected dry grasslands (Weber et al., 2018).

Cooperation between different disciplines, such as grassland science, wildlife science and remote sensing are more necessary than ever to advance

conservation activities (Clark et al., 2017). Climate change and habitat loss and fragmentation are major threats to biodiversity and food security (Bellard et al., 2012; Haddad et al., 2015; O'Connor et al., 2015). This thesis presented applications of remote sensing with a spatial focus on the Grafenwoehr military training area. However, the bounsaries of the study area are artificial. The open Landsat archive provides spectral information dating back to the 1970s and the recently launched Sentinel program will continue to deliver remotely sensed data at very high temporal and spectral resolution (Belward and Skøien, 2015). Future research should therefore make use of the unprecedented amount of data available to the public to date and take larger geographical and temporal scales into consideration (Pasquarella et al., 2016). For this, open and reproducible research is of pivotal importance (Rocchini and Neteler, 2012; Turner et al., 2015).

References

Bareth, G., and J. Schellberg. 2018. "Replacing Manual Rising Plate Meter Measurements with Low-Cost UAV-Derived Sward Height Data in Grasslands for Spatial Monitoring." *PFG–Journal of Photogrammetry, Remote Sensing and Geoinformation Science*, 1–12.

Barrett, B., Raab, C., Cawkwell, F., Green, S., 2016. Upland vegetation mapping using Random Forests with optical and radar satellite data. Remote Sensing in Ecology and Conservation 2, 212–231.

Bellard, C., C. Bertelsmeier, P. Leadley, W. Thuiller, and F. Courchamp. 2012. "Impacts of Climate Change on the Future of Biodiversity". *Ecology Letters* 15 (4): 365–377.

Belward, A.S., and J.O. Skøien. 2015. "Who Launched What, When and Why; Trends in Global Land-Cover Observation Capacity from Civilian Earth Observation Satellites." *ISPRS Journal of Photogrammetry and Remote Sensing* 103: 115–128.

Catorci, A., F.M. Tardella, K. Piermarteri, R. Pennesi, L. Malatesta, M. Corazza, and P. Scocco. 2016. "Effect of Red Deer Grazing on Alpine Hay Meadows: Biodiversity and Management Implications." *Applied Ecology and Environmental Research* 14 (2): 301–318.

Cho, M.A., and A.K. Skidmore. 2009. "Hyperspectral Predictors for Monitoring Biomass Production in Mediterranean Mountain Grasslands: Majella National Park, Italy." *International Journal of Remote Sensing* 30 (2): 499–515.

Clark, B.L., M. Bevanda, E. Aspillaga, and N.H. Jørgensen. 2017. "Bridging Disciplines with Training in Remote Sensing for Animal Movement: An Attendee Perspective." *Remote Sensing in Ecology and Conservation* 3 (1): 30–37.

Claverie, M., J. Ju, J.G. Masek, J.L. Dungan, E.F. Vermote, J.-C. Roger, Sergii V. Skakun, and C. Justice. 2018. "The Harmonized Landsat and Sentinel-2 Surface Reflectance Data Set." *Remote Sensing of Environment* 219: 145–161.

Darvishzadeh, R., A.K. Skidmore, M. Mirzaie, C. Atzberger, and M. Schlerf. 2014. "Fresh Biomass Estimation in Heterogeneous Grassland Using Hyperspectral Measurements and Multivariate Statistical Analysis." In *InAGU Fall Meeting Abstracts*. Vol. 1.

Förster, M., A. Frick, C. Schuster, and B. Kleinschmit. 2010. "Object-Based Change Detection Analysis for the Monitoring of Habitats in the Framework of the NATURA 2000 Directive with Multi-Temporal Satellite Data." *The International Archives of the Photogrammetry, Remote Sensing and Spatial Information Sciences* 38: 4.

Franke, J., V. Keuck, and F. Siegert. 2012. "Assessment of Grassland Use Intensity by Remote Sensing to Support Conservation Schemes." *Journal for Nature Conservation* 20 (3): 125–134.

Giménez, M.G., R. de Jong, R.D Peruta, A. Keller, and M.E. Schaepman. 2017. "Determination of Grassland Use Intensity Based on Multi-Temporal Remote Sensing Data and Ecological Indicators." *Remote Sensing of Environment* 198: 126–139.

Guanter, L., H. Kaufmann, K. Segl, S. Foerster, C. Rogass, S. Chabrillat, T. Kuester, A. Hollstein, G. Rossner, and C. Chlebek. 2015. "The EnMAP Spaceborne Imaging Spectroscopy Mission for Earth Observation." *Remote Sensing* 7 (7): 8830–8857.

Haddad, N.M., L.A. Brudvig, J. Clobert, K.F. Davies, A. Gonzalez, R.D. Holt, T.E. Lovejoy, J.O. Sexton, M.P. Austin, and C.D. Collins. 2015. "Habitat Fragmentation and Its Lasting Impact on Earth's Ecosystems". *Science Advances* 1 (2): e1500052.

Knox, N.M., A.K. Skidmore, H. HT Prins, G.P. Asner, H. MA van der Werff, W.F. de Boer, C. van der Waal, H.J. de Knegt, E.M. Kohi, and R. Slotow. 2011. "Dry Season Mapping of Savanna Forage Quality, Using the Hyperspectral Carnegie Airborne Observatory Sensor." *Remote Sensing of Environment* 115 (6): 1478–1488.

Kolecka, N., C. Ginzler, R. Pazur, B. Price, and P. Verburg. 2018. "Regional Scale Mapping of Grassland Mowing Frequency with Sentinel-2 Time Series." *Remote Sensing* 10 (8): 1221.

Laliberte, A.S., Ed L. Fredrickson, and A. Rango. 2007. "Combining Decision Trees with Hierarchical Object-Oriented Image Analysis for Mapping Arid Rangelands." *Photogrammetric Engineering & Remote Sensing* 73 (2): 197–207.

Langvatn, R., and T.A. Hanley. 1993. "Feeding-Patch Choice by Red Deer in Relation to Foraging Efficiency." *Oecologia* 95 (2): 164–170.

Lewis, J.S., J.L. Rachlow, E.O. Garton, L.A. Vierling. 2007. "Effects of habitat on GPS collar performance: using data screening to reduce location error." *Journal of applied ecology* 44, 663–671.

Li, J., and D. Roy. 2017. 'A Global Analysis of Sentinel-2A, Sentinel-2B and Landsat-8 Data Revisit Intervals and Implications for Terrestrial Monitoring'. *Remote Sensing* 9 (9): 902.

Liu, D., and F. Xia. 2010. "Assessing Object-Based Classification: Advantages and Limitations." *Remote Sensing Letters* 1 (4): 187–194.

Michez, A., P. Lejeune, S. Bauwens, A.A.L. Herinaina, Y. Blaise, E.C. Muñoz, F. Lebeau, and J. Bindelle. 2019. "Mapping and Monitoring of Biomass and Grazing in Pasture with an Unmanned Aerial System." *Remote Sensing* 11 (5): 473.

Mutanga, O., A.K. Skidmore, and H.H.T. Prins. 2004. "Predicting in Situ Pasture Quality in the Kruger National Park, South Africa, Using Continuum-Removed Absorption Features." *Remote Sensing of Environment* 89 (3): 393–408.

O'Connor, B., C. Secades, J. Penner, R. Sonnenschein, A.K. Skidmore, N.D. Burgess, and J.M. Hutton. 2015. "Earth Observation as a Tool for

Tracking Progress towards the Aichi Biodiversity Targets." *Remote Sensing in Ecology and Conservation* 1 (1): 19–28.

Pasquarella, V.J., C.E. Holden, L. Kaufman, and C.E. Woodcock. 2016. "From Imagery to Ecology: Leveraging Time Series of All Available Landsat Observations to Map and Monitor Ecosystem State and Dynamics." *Remote Sensing in Ecology and Conservation* 2 (3): 152–170.

Pellissier, P.A., S.V. Ollinger, L.C. Lepine, M.W. Palace, and W.H. McDowell. 2015. "Remote Sensing of Foliar Nitrogen in Cultivated Grasslands of Human Dominated Landscapes." *Remote Sensing of Environment* 167: 88–97.

Rapinel, S., N. Rossignol, L. Hubert-Moy, J.-B. Bouzillé, and A. Bonis. 2018. "Mapping Grassland Plant Communities Using a Fuzzy Approach to Address Floristic and Spectral Uncertainty." *Applied Vegetation Science*.

Raynor, E.J., H.L. Beyer, J.M. Briggs, and A.Joern. 2017. "Complex Variation in Habitat Selection Strategies among Individuals Driven by Extrinsic Factors." *Ecology and Evolution* 7 (6): 1802–1822.

Riesch, F., H.G. Stroh, B. Tonn, and J. Isselstein. 2018. "Soil PH and Phosphorus Drive Species Composition and Richness in Semi-Natural Heathlands and Grasslands Unaffected by Twentieth-Century Agricultural Intensification." *Plant Ecology & Diversity* 11 (2): 239–253.

Rocchini, D., G.M. Foody, H. Nagendra, C. Ricotta, M. Anand, K.S. He, V. Amici, B. Kleinschmit, M. Förster, and S. Schmidtlein. 2013. "Uncertainty in Ecosystem Mapping by Remote Sensing." *Computers & Geosciences* 50: 128–135.

Rocchini, D., and M. Neteler. 2012. "Let the Four Freedoms Paradigm Apply to Ecology." *Trends in Ecology & Evolution* 27 (6): 310–311.

Schmidt, J., F.E. Fassnacht, M. Förster, and S. Schmidtlein. 2017. "Synergetic Use of Sentinel-1 and Sentinel-2 for Assessments of Heathland Conservation Status." *Remote Sensing in Ecology and Conservation*.

Schmidtlein, S., and J. Sassin. 2004. "Mapping of Continuous Floristic Gradients in Grasslands Using Hyperspectral Imagery." *Remote Sensing of Environment* 92 (1): 126–138.

Skidmore, A.K., J.G. Ferwerda, O. Mutanga, S.E. Van Wieren, M. Peel, R. C. Grant, H. HT Prins, F.B. Balcik, and V. Venus. 2010. "Forage Quality of Savannas—Simultaneously Mapping Foliar Protein and Polyphenols for Trees and Grass Using Hyperspectral Imagery." *Remote Sensing of Environment* 114 (1): 64–72.

Stefanski, J., B. Mack, and B. Waske. 2013. "Optimization of Object-Based Image Analysis with Random Forests for Land Cover Mapping." *IEEE Journal of Selected Topics in Applied Earth Observations and Remote Sensing* 6 (6): 2492–2504.

Tamm, T., K. Zalite, K. Voormansik, and L. Talgre. 2016. “Relating Sentinel-1 Interferometric Coherence to Mowing Events on Grasslands.” *Remote Sensing* 8 (10): 802.

Turner, W. C. Rondinini, N. Pettorelli, B. Mora, A.K. Leidner, Z. Szantoi, G. Buchanan, S. Dech, J. Dwyer, and M. Herold. 2015. “Free and Open-Access Satellite Data Are Key to Biodiversity Conservation.” *Biological Conservation* 182: 173–176.

Wallace, L.L., M.G. Turner, W.H. Romme, R.V. O’Neill, and Y. Wu. 1995. “Scale of Heterogeneity of Forage Production and Winter Foraging by Elk and Bison.” *Landscape Ecology* 10 (2): 75–83.

Weber, D., G. Schaepman-Strub, and K. Ecker. 2018. “Predicting Habitat Quality of Protected Dry Grasslands Using Landsat NDVI Phenology.” *Ecological Indicators* 91: 447–460.

Acknowledgements

The project was supported by funds of German government's Special Purpose Fund held at Landwirtschaftliche Rentenbank (28 RZ 7007). I thank the Federal Forests Division (Bundesforst) of the German Institute for Federal Real Estate (Bundesanstalt für Immobilienaufgaben) and the Institut für Wildbiologie Göttingen und Dresden e.V. for close cooperation and support. Special thanks goes to the DLR for the delivery of RapidEye images as part of the RapidEye Science Archive (proposal 00226).

This thesis would not have been possible without the continuous support, discussions, guidance, ideas of many other people. Especially, I would like to thank:

- Prof. Dr. Johannes Isselstein for the opportunity to become a member of the Grassland Science group and a very supportive and encouraging supervision and for giving me the freedom to explore new perspectives on scientific challenges.
- Prof. Dr. Niko Balkenhol for the opportunity to become a part of the Wildlife Sciences group and his support, discussions and ideas during many project meetings. It was wonderful to work at two departments – special thanks to the Wildlife Sciences Department for all the support and productive workathons.
- Special thanks to Dr. Bettina Tonn for showing me new perspectives on how to address scientific problems, supervising this thesis, endless discussions and for challenging me always in the right moment. I learned a lot from you!
- Prof. Dr. Hannes Feilhauer – for kindly serving as a co-referee.
- Special thanks to Marcus Meißner for the coordination of the project and support.
- Special thanks to Horst Reinecke for great discussions and his wonderful attribute of helping me to shift my perspective on scientific challenges.
- Dr. Johannes Signer for his inspiring dedication to R, statistics and science. Thank you very much for your support and discussions.
- Nina Rohwer for her tiredless support of the project.

- Special thanks to the Federal Forest Division Grafenwöhr, especially to the forestry district leaders Ulrich Schomann und Andreas Irle. Without their support in the field this work would not have been possible.
- All members of the Department of Grassland Science and the Department of Wildlife Sciences Göttingen for wonderful working environments and inspiring coffee breaks.
- Dr. Brian Barrett for his inspiring dedication to remote sensing and kind support of parts of this thesis.
- Special thanks to my PhD colleagues Friederike Riesch and Laura Richter – for your support in the field, critical minds and helping me to dive into new scientific fields.
- Barbara Hohlmann for her wonderful supporting attitude regarding laboratory work. Thank you very much for your help at the right moments of this thesis!
- R core Team for R and GRASS Development Team for GRASS GIS.
- Everyone who I forgot to mentioned here, but who contributed to this thesis in some way or other.
- Finally, I would like to thank my parents, family (Friedrich for his kind support during field work) and friends (Flo for proof reading) for their constant support and encouragement, without which this thesis would not have been possible.
- The biggest thank you goes to my partner Sandra – thank you for your love, your critical mind, your support and always being there for me to listen about how fantastic remote sensing is.

Thesis Declaration

I hereby confirm that I have written this doctoral thesis independently, that I have not used other sources or facilities other than the ones mentioned, that I have not used unauthorized assistance and that I have not submitted this thesis previously in any form for another degree at any university or institution.

Christoph Raab

Göttingen, 09. May 2019